AN IN SITU INVESTIGATION OF THE PHYSICAL PROPERTIES OF ROCK SALT WITH SPECIAL REFERENCE TO UNDERGROUND GAS STORAGE

A THESIS

submitted for the Degree of Doctor of Philosophy

in the

University of Newcastle upon Tyne

by

E. DACK, B.Sc., (Hons)., Newcastle

UNIVERSITY OF NEWCASTLE UPON TYNE

UNIVERSITY LIBRARY

In depositing this copy of my thesis in the University Library, I wish to arrange conditions of access as indicated below (subject to the provisions of Library Regulation IV 25.)

~~a) Normal access subject to the provisions of copyright and general control~~

b) No access without my permission on each occasion

Signed ..... E. Dack.

Date ..... 12 December 1973

Department ..... Mining Engineering

Supervisor's name ..... Prof. E.L.J. Potts

Supervisor's Department ..... Mining Engineering

Notes

1. Consultation without the author's permission is possible

   a) At all times for the supervisor of the thesis and the Head of the Department concerned.

   b) For theses deposited before August 1st 1973 - after ten years

      For theses deposited after July 31st 1973 - after three years

2. Each consultation must be recorded in the thesis volume.

3. The thesis may not leave the University Library, or any library to which it has been sent on inter-library loan.

4. The University has agreed to take part in the British Library's plan for the microfilming of theses. Any theses so treated will be subject to the normal copyright conditions.

5. The copyright remains at all times with the author.

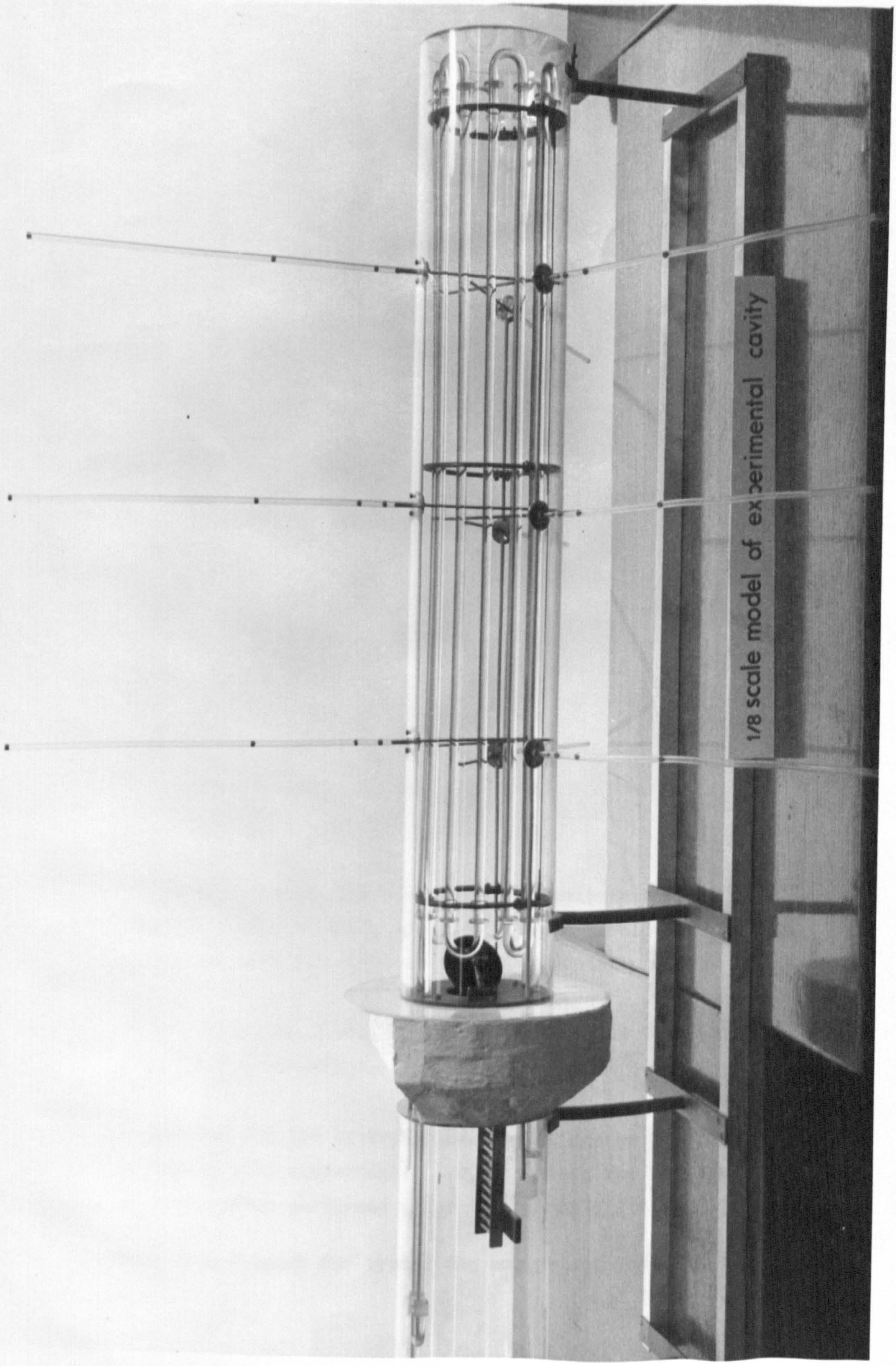

A MODEL OF THE EXPERIMENTAL CAVITY

ACKNOWLEDGEMENTS

The investigation into the rock mechanics aspects of underground gas storage in brined cavities has taken the form of a long term research project initiated some five years ago. The project was sponsored by Imperial Chemical Industries Limited, (Mond Division), and the author would like to thank the staff of the Holford Brinefields, the Meadowbank Mine and the Divisional Engineering Department for their assistance and co-operation.

A number of investigaters have worked on this project over the years and consequently must be thanked for their contributions:

Professor E.L.J. Potts, M.Sc., F.I.Min.E., F.R.I.C.S., Milburn Professor of Mining, for the opportunity and facilities to do this work, and also for his constant guidance and supervision.

T.W. Thompson, B.Sc., for his assistance, advice and co-operation throughout the three years we have worked together.

A.C. Talbott, M.Sc., C.Eng., M.I.Mech.E., for the design and administrative work he undertook during the early years of the project.

M. Thompson, M.A., for his advice and help on mathematical aspects of the project, and also for his invaluable assistance on the in situ installation and experimental programme.

E.K.S. Passaris, M.Sc., for his assistance on the in situ experimental programme.

T. Pollock for his contributions to the design and installation of the in situ experiment; also, his staff for the high standard of work, often performed under trying and difficult conditions.

Mrs. Joan Peacock for typing the script quickly and efficiently.

CONTENTS

LIST OF ILLUSTRATIONS

LIST OF TABLES

CHAPTER 1

CHAPTER 1

1. INTRODUCTION

The rate of production of any consumable, whether it be raw materials or a finished product, rarely equals the rate of its consumption. Manufacturing industries cannot produce at a rate equalling the peak consumption rate without over-capitalisation of plant. The disparity between production and consumption rates necessitates the creation of a buffer which will enable the manufacturer to produce at an economical rate and yet provide the consumer with an uninterupted supply at peak demand.

The problems of varying production and consumption rates are experienced in the energy supply industries. Solid fuels, oil and gas are all stockpiled at many links in the chain from producer to consumer. The storage of fuel is necessary to accommodate the diurnal and seasonal variation in demand occasioned by the working hours of industry and commerce and the domestic habits of householders. Solid fuels and oils are normally subject to only seasonal variations in demand but gas and electricity suffer from high diurnal variations in demand from both industrial and domestic consumers.

In its early days gas was chiefly used as an illuminant and the demand was low in summer and in daylight hours. Towards the end of the nineteenth century other uses for gas were developed, making the demands more even. A sharp return to the former annual cycle has now arisen as a result of the tremendous success of gas space heating, and it can be but a few years before the seasonal ratio midwinter: midsummer reaches the proportion 5:1 (1,2)

The gas industry can meet this challenge in two possible ways; additional gas production plant for winter use only or by increasing gas storage facilities. As both of these solutions result in under-employment of capital, the gas industry has been investigating over the last twenty years various gas storage techniques which do not sterilise as much capital as the conventional low-pressure holder. High-pressure gas storage, when allied to high pressure distribution times can effect several economics in this field.

1.1 Present trends in high-pressure gas storage.

High pressure holders have been used throughout the world for many years, but construction problems have limited capacity to about 600 mscf and pressures to 100 psi in the cylindrical type, and 1 mmscf capacity and 60 psi in spheres. It seems unlikely that either of these types can compete with the pipe-type unit as these can be pressurised to 70 atmospheres or more, holding a large quantity of gas in a relatively small installation area.

The design of the pipe type unit, whether it be a collection of vertical pipes or pipes burried horizontally, involves a row of four or five pipes connected to a header which caters for four or five similar rows. Several of these headers are connected to one or more master headers which in turn are connected to the distribution grid. The connection takes the form of a governing station for discharging and a pumping station for pressurisation. However, such storage units represent a large capital investment and maintenance costs are high.

Over the last fifteen years more and more attention has been paid to the development of underground gas storage techniques as a means of reducing the capital invested in storage facilities. Underground gas storage may take two general forms; the utilisation of a geological structure or the utilisation of an artificial subterranean cavity.

Useful geological structures include exhausted oil or natural gas fields, anticlines, faulted areas in dipping strata, and areas surrounding a salt dome. In all cases the storage medium is a porous and permeable rock capped by an unbroken bed of impermeable rock. Huge quantities of gas may be stored in such structures; the Herschor Domo, an anticline near Chicago, has a capacity of 150 x 10^9 scf with a plan area of 6000 acres (3, 4)

The most serious disadvantages of gas storage in natural structures are the restrictions of locations and the considerable amount of surface works required. For a structure to deliver gas in a quantity sufficient to meet peak demand several wells may be necessary, the number depending upon the permeability of the storage rock. The valve assemblies at the well-heads, together with the gathering lines, pumping and treatment plant, can occupy large areas of ground.

Artificial underground storage structures are usually confined to specially designed and prepared chambers; disused mines have seldom been found to be gas tight. Excavated cavities may be constructed in almost any geological formation, but if situated in permeable or unstable ground, some type of lining may be necessary.

1.2 Excavated underground gas storage units

Underground units designed for high pressure storage may be catagorised as follows:-

i) Mined caverns
ii) Salt cavities
iii) Pressure tunnels
iv) Reinforced or prestressed concrete tanks.

An economic and engineering appraisal of underground storage systems is given by Evans (5), who suggests that salt cavity storage may be up to ten times cheaper than pressure tunnel storage, the most expensive system. Although gas storage in salt cavities would appear to be an attractive proposition, its use is limited by geological conditions to the areas around the North East Coast, the Cheshire basin, Mersey Estuary and the Humber Estuary. All the other storage systems, with the exception of mined caverns in the Thames Estuary and Southampton Water areas, may be applied throughout the country.

The emergence of the North Sea gas and oil fields, together with the economics of underground storage, has resulted in renewed interest in the use of salt cavities for gas storage on the eastern seaboard. Although salt cavities have been in use for some years now (6), and the technical problems associated with the purely gas engineering aspects of the system have been largely resolved, there is a lack of relevant data concerning operational parameters and long term stability.

A salt cavity is produced by the well-established method of solution mining and when salt extraction terminates the cavity is left full of brine at hydrostatic pressure to minimise subsidence. Cavity size and shape may be controlled reasonably accurately by the introduction of a gas or an immiscible liquid (7). A typical salt cavity, excavated in the Permian middle evaporite group below Teesside, is shown in Fig. 1.

1.3 Salt cavity storage problems

A spherical gas storage cavity in salt may be designed for either wet or dry storage. Dry storage cavities are designed to be self supporting when empty but empty wet storage cavities are supported by brine at hydrostatic pressure. In a wet storage cavity, gas pressure is never less than the hydrostatic brine pressure and never exceeds overburden pressure. One of the problems encountered in wet storage is the brine storage tanks required for such an operation. Volumes as great as 350,000 cu.ft. may have to be catered for, and at brine storage costs of between £30 and £225/1,000 cu.ft., this can represent a large capital investment, (5, 6). Compressed gas may be used to support the cavity instead of brine, i.e., cavity pressure never drops below the hydrostatic pressure of brine, but this technique sterilises large volumes of gas.

The gas engineering problems associated with salt storage cavities are either well known or quite predictable. However, there is an almost complete lack of data on the mechanical behaviour of salt under these conditions. Pressurisation of a storage cavity implies an adiabatic compression of the gas, resulting in a rise in temperature of the stored gas and surrounding salt. Similarly, the adiabatic expansion of the gas during depressurisation causes temperature decreases in the storage unit. A theoretical study of the stresses imposed by gravitational forces, internal gas pressure and thermal loading must be based on many assumptions. It is not only the physical parameters of the storage medium that must be assumed, but also the mathematical model which uses the physical parameters to predict stress distribution.

Budavari (8) has suggested that the only practical method of predicting the stress distribution is to conduct a large scale in situ experiment. The experiment must be designed with the following objectives in mind:-

i) To determine the material parameters characterising the in situ behaviour of the rock mass
ii) To provide data for the development or testing of a mathematical model capable of predicting the behaviour of a gas storage cavity in salt.

This thesis describes the design, development and operation of such an experiment and concludes with a discussion of the results obtained from initial tests and gives a preliminary appraisal of long term cavity stability.

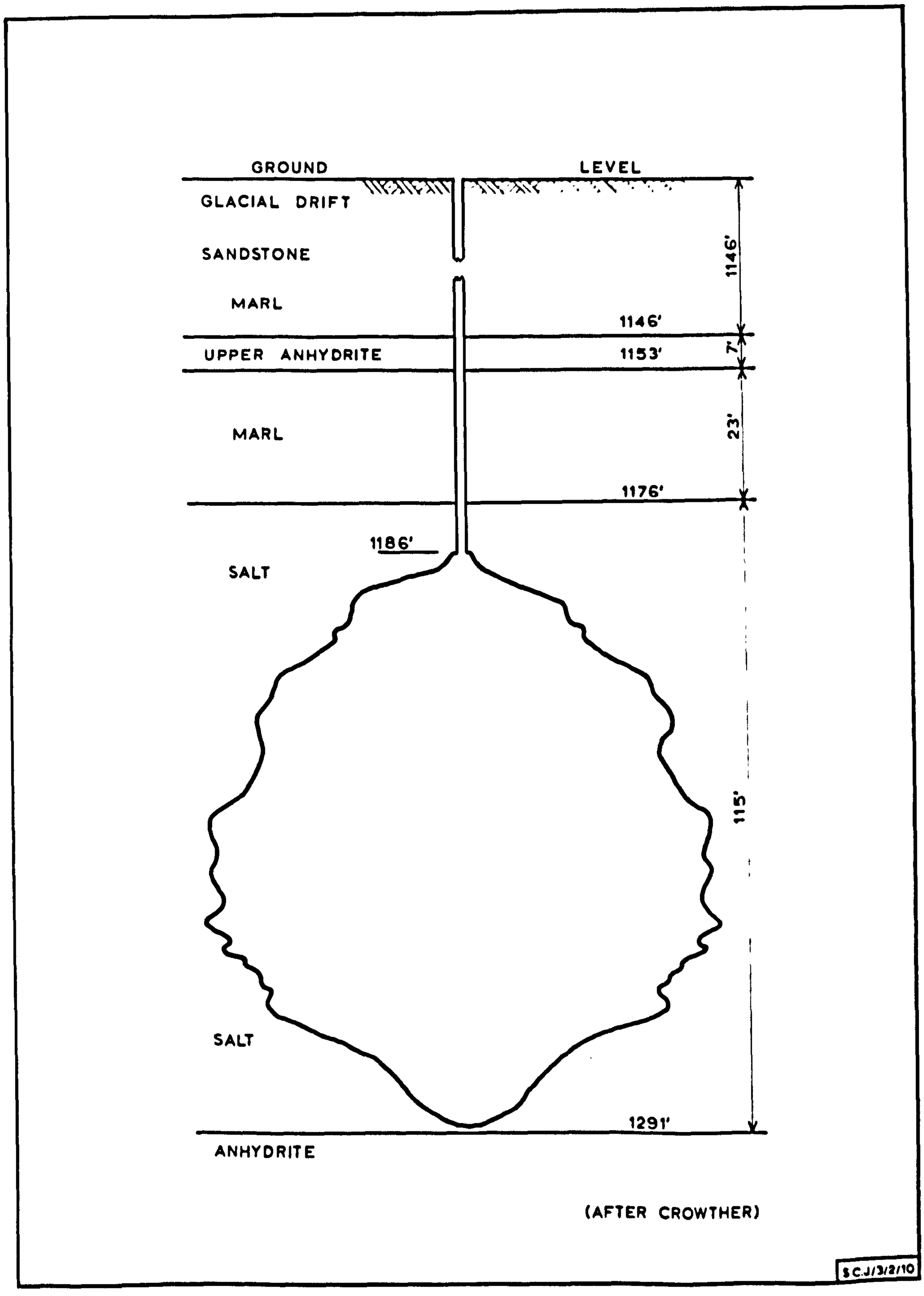

FIG. 1 SECTION THROUGH A BRINED CAVITY EXCAVATED IN THE PERIAN MIDDLE EVAPORITE GROUP BELOW TEESSIDE

CHAPTER 2

DEVELOPMENT OF A MATHEMATICAL MODEL FOR THE DETERMINATION OF THE STABILITY OF A GAS STORAGE CAVITY IN SALT

CHAPTER 2

2. DEVELOPMENT OF A MATHEMATICAL MODEL FOR THE DETERMINATION OF THE STABILITY OF A GAS STORAGE CAVITY IN SALT

2.1 Stresses around a storage cavity in salt

The stresses imposed on an operational storage cavity are the resultant of three separate stress fields:-

i) Stress components due to coverload.
ii) Stress components due to the internal hydrostatic pressure on the cavity surface.
iii) Thermal stress components due to temperature gradients in the salt mass.

The mechanical loading due to the superincumbent strata imposes a three-dimensional stress field on the cavity. This stress field can be expressed as:-

$$\sigma_z = -H\gamma = \frac{(1-\upsilon)}{\upsilon}\sigma_x = \frac{(1-\upsilon)}{\upsilon}\sigma_y \qquad (1)$$

where σ_z = vertical components
σ_x, σ_y = horizontal components
H = vertical distance from the surface
γ = average rock density
υ = Poisson's ratio

The variation of the stress components in any radial direction in the salt mass, induced by an internal gas pressure P on the surface of a spherical cavity, is described by the equations:

$$\sigma_r = -P\frac{R^3}{r^3} \qquad (2)$$

$$\sigma_\theta = \sigma_\phi = \frac{P R^3}{2 r^3} \qquad (3)$$

where σ_r = radial stress

$\sigma_\theta, \sigma_\phi$ = tangential stress components (at the cavity both σ_θ and σ_ϕ are horizontal; at the equator σ_θ is directed vertically and σ_ϕ horizontally. (See Fig. 2)

R = cavity radius

r = radial variable

These equations are derived from Lame's solution of the spherical container under uniform internal or external pressure, described by Timoskenko (9). It can be seen from Equations (2, 3) that these stress components reach their maximum values at the surface of the cavity. The radial stress component is compressive and the tangential components are tensile everywhere around the cavity.

In the derivation of the equations for the stress components due to a temperature gradient within the rock, it is assumed that the strata is free from thermal stresses before the introduction or withdrawal of the gas. The stationary temperature distribution around a spherical cavity, when the cavity surface is kept at a constant temperature, is given by (10):-

$$T = T_o \frac{R}{r} \qquad (4)$$

where T = temperature at radial distance from the cavity centre.

To = cavity surface temperature.

R = cavity radius

If the cavity surface temperature is raised, then the induced thermal stresses will be due to the temperature difference T, between the cavity surface temperature and the temperature of a point at a great distance from the cavity. Using T instead of T and T to replace To, Equation (4) can be re-written in the form :-

$$T_r = \Delta T \frac{R}{r} \qquad (5)$$

Assuming the material to be thermoelastic, the magnitudes of the three principal stresses at any point in the solid can be given by:-

$$\sigma_r = -\frac{E \alpha \Delta T}{1-\nu}\left(\frac{R}{r} - \frac{R^3}{r^3}\right) \qquad (6)$$

$$\sigma_\theta = \sigma_\phi = -\frac{E \alpha \Delta T}{2(1-\nu)}\left(\frac{R}{r} + \frac{R^3}{r^3}\right) \qquad (7)$$

In these equations, derived from the principles of thermoelasticity described by Timoskenko (9), T is taken to be positive for temperature increases and denotes the coefficient of linear thermal expansion. The stresses are compressive for a temperature increase and tensile for a temperature decrease; at a great distance from the cavity the stresses are zero and reach a maximum at the cavity surface.

2.1.1 Application of the elastic model

It is assumed that the idealised material representing the salt is homogeneous, isotropic and linearally elastic. It is also assumed that the parameters characterising the materials behaviour, namely the Young's modulus and Poisson's ratio are the same in tension as in compression. Although this is not usually so for rock materials, the assumption is made superfluous due to the low tensile strength of rock salt.

It can be shown that the most relevant stresses occur at the poles and at the equator of the cavity. Therefore, the variation of the stress components is investigated only along the radial lines through the poles and the equator. Applying the principle of super position, the mathematical expressions for the resultant stress components in the vicinity of the pole and equator can be obtained. Since the largest stresses are set up at the cavity surface, the resultant stress components for r = R are given below as:-

i) Resultant stress components at the pole

$$\sigma_r = -P \tag{8}$$

$$\sigma_\theta = \sigma_\phi = 3H\gamma\frac{(1-5\nu)(1+\nu)}{2(7-5\nu)(1-\nu)} + \frac{P}{2} - \frac{E\alpha\Delta T}{1-\nu} \tag{9}$$

ii) Resultant stress components at the equator

$$\sigma_r = -P \tag{10}$$

$$\sigma_\theta = 3H\gamma\frac{(9-16\nu+5\nu^2)}{2(7-5\nu)(1-\nu)} + \frac{P}{2} - \frac{E\alpha\Delta T}{1-\nu} \tag{11}$$

$$\sigma_\phi = 3H\gamma\frac{(1-14\nu+15\nu^2)}{2(7-5\nu)(1-\nu)} + \frac{P}{2} - \frac{E\alpha\Delta T}{1-\nu} \tag{12}$$

A numerical evaluation of the resultant stress components may be obtained by substituting known and assumed values into Equations (8-12). The Young's modulus of rock salt, tested in the laboratory under uniaxial compression, may be taken as 3×10^6 p.s.i. (20.685×10^6 kN/m^2). The stresses around a storage cavity may be obtained from Fig. 3 by substituting the values for the physical parameters and selecting values for depth, internal pressure and Poisson's ratio. (16).

The selection of a suitable criterion of cavity failure must be closely limited to the compressive and tensile strengths of rock salt. Laboratory investigations indicate a very low tensile strength of 240 psi, and this is clearly a key factor in cavity stability. The tensile strength is so low that a zero stress condition can be assumed to precipitate cavity failure. This criterion has the advantage of eliminating the assumption that the physical parameters in tension are the same as in compression.

An indication of the stability of a storage cavity 1000 feet below ground is given by Fig. 4. This graph illustrates the effects of internal pressure and temperature on the stresses around cavity using the assumed values of 3×10^6 psi for Young's modulus and 40×10^{-6} for the coefficient of linear thermal expansion. Conditions applicable for values of Poisson's ratio of 0.3 and 0.5 are plotted, with a broken line representing an assumed tensile strength of 250 psi and the solid line zero stress conditions. (16).

2.1.2 Application of the elasto-plastic model

If an internal and external hydrostatic pressure (Pi and Po respectively) is applied to a spherical cavity located in an infinite elasto-plastic medium, then plastic deformation will take place. The plastic flow originates from the cavity surface and extends into the solid to a distance denoted by C. Beyond this zone the deformation is elastic.

It can be shown (11) that the stress components may be written as:-

When $R \leq r \leq C$

$$\sigma_r'' = -2\sigma_\gamma \log \frac{r}{R} - P_i \qquad (13)$$

$$\sigma_t'' = -\sigma_\gamma (1 + 2\log \frac{r}{R}) - P_i \qquad (14)$$

When $C \leq r$

$$\sigma_r' = -P_o + \frac{2}{3}\sigma_\gamma \cdot \frac{R^3}{r^3} e^{\left(\frac{3(P_o - P_i) - 2\sigma_\gamma}{2\sigma_\gamma}\right)} \qquad (15)$$

$$\sigma_t' = -P_o - \frac{\sigma_\gamma}{3} \frac{R^3}{r^3} e^{\left(\frac{3(P_o - P_i) - 2\sigma_\gamma}{2\sigma_\gamma}\right)} \qquad (16)$$

where $\sigma_\gamma = \sigma_r'' - \sigma_t''$

and $C = R\, e^{\left(\frac{3(P_o - P_i) - 2\sigma_\gamma}{6\sigma_\gamma}\right)}$

The radial stress component is zero at the cavity surface and rises to Po at a great distance from the cavity. The tangential stress rises from some value at the cavity surface to a maximum at the boundary between the plastic and elastic zones, and decreases to Po at a great distance from the cavity.

2.1.3 Application of the visco-elastic model

A spherical cavity is located in an infinite visco-elastic medium and placed under internal and external hydrostatic pressures Pi and Po. The solution to this problem must describe the distribution of the stress components around the cavity and evaluate the strain rates around the opening. Investigations in the Department of Mining Engineering, University of Newcastle upon Tyne (12, 13, 14) have shown that the nature of time-dependent creep deformation of rock salt is predominantly permanent. Consequently only the permanent strain components as a result of creep deformation are considered here (8):-

$$\sigma_r = (P_o - P_i)\left(\frac{R}{r}\right)^{\frac{3}{n}} - P_o \qquad (17)$$

$$\sigma_\theta = (P_o - P_i)\left(\frac{R}{r}\right)^{\frac{3}{n}}\left(1 - \frac{3}{2n}\right) - P_o \qquad (18)$$

$$\dot{\varepsilon}_r = -B\left(\frac{R}{r}\right)^3\left[\frac{-3}{2n}(P_o - P_i)\right]^n \qquad (19)$$

$$\dot{\varepsilon}_\theta = -\frac{\dot{\varepsilon}}{2}$$

B and n are parameters derived from an experimental analysis of the creep properties of rock salt. The equation is of the general form:-

$$\dot{\varepsilon}_K = B\,\sigma_K^n \qquad (20)$$

2.2 Comparison and evaluation of mathematical models used in defining the behaviour of rock salt.

Many rocks are known to exhibit linear stress-strain relationships, especially at low stress levels, thus satisfying the principal requirements of elasticity. Furthermore, other strata reactions to stress, e.g. visco-elasticity, elasto-plasticity, can be regarded as modifications to the elastic solution. Hence the elastic solution can be considered as a first approximation.

Although the elastic model discussed in 2.11 has the tremendous advantage of mathematical simplicity, there are several inherent drawbacks, some of which are common to all mathematical models. It is assumed that the elastic constants have the same value in both compression and in tension, and that their values, obtained by the laboratory testing of rock samples, closely represents the in situ value. It is by no means certain that these assumptions are correct and only an in situ materials test will provide the answer.

The thermal stresses expressed in Equations (9), (11) and (12) are based on a stationary temperature distribution around a spherical cavity, and do not take into account the steeper temperature gradient encountered near the surface during the early stages of the introduction of a temperature difference. In addition to this, the magnitudes of the thermal stresses are again dependent upon the values of the in situ Young's modules and Poisson's ratio. Although the elastic model will provide an approximate solution, it can be clearly seen that it is unsatisfactory for an accurate analysis of the problem.

An evaluation of the linear elasto-plastic model reveals that the main problem lies in including the influence of thermal stresses upon cavity stability. This inclusion has not been attempted due to the mathematical difficulties involved. Although the thermal stresses are only set up in the elastic zone, their chief influence would be to increase or decrease the radius of the plastic zone. The evaluation of the stresses in the elastic zone suffers from the same disadvantages inherent in the elastic model.

The application of the linear visco-elastic model suffers from similar disadvantages in that the predicted behaviour of the idealised material described by the model differs significantly from in situ observations. In addition, it is most probable that the two parameters B and n will vary with temperature.

Investigations have revealed that the non-linear visco-elastic model best describes the laboratory behaviour of rock salt, but the mathematical difficulties involved in applying it to the complex loading system may prove insuperable. It is apparent when deriving expressions for the distribution of stress and strain around a storage cavity that great dependence is placed on the values used for the material parameters, which can be quite critical especially when considering thermal stresses.

A more detailed treatment of mathematical model development is given by Thompson (16) who discusses both linear and non-linear visco-elastic models. Thompson concludes that the most critical conditions will occur during temperature decreases caused by cavity depressurisation and points out that further difficulties could arise in a deep cavity at low internal pressures.

It is quite clear from the problems discussed that none of the models give an accurate mathematical description of the behaviour of rock salt. If a mathematical model is to be used in the analysis of this problem then data provided by an in situ experiment is needed in order to modify and expand a suitable model. Furthermore, the in situ experiment must provide information on the creation and development of temperature gradients induced in rock salt by the application of a temperature difference.

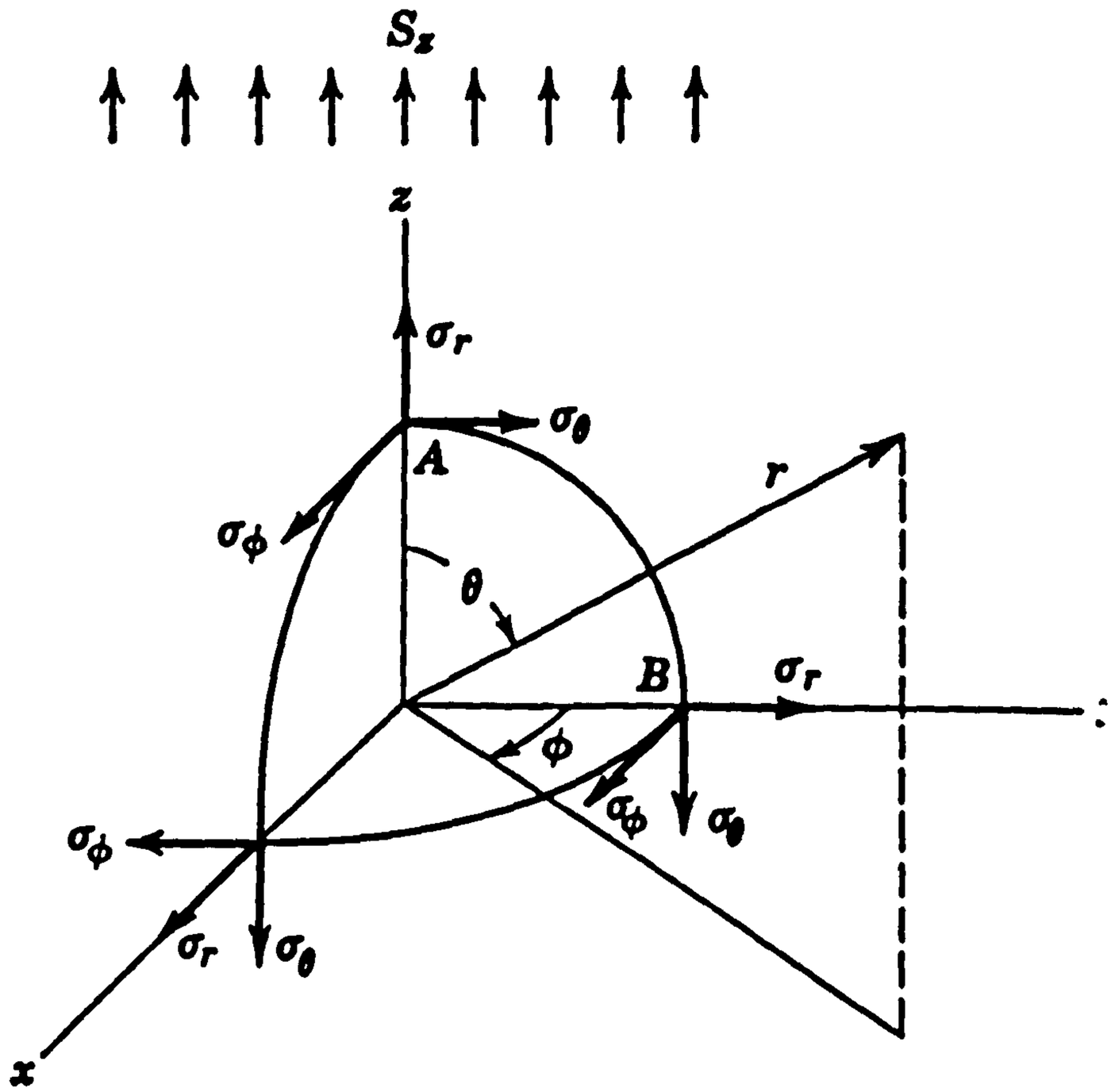

Spherical coordinates and stresses.

FIG. 2 SPHERICAL COORDINATE SYSTEM

FIG. 3 STRESSES AROUND A STORAGE CAVITY

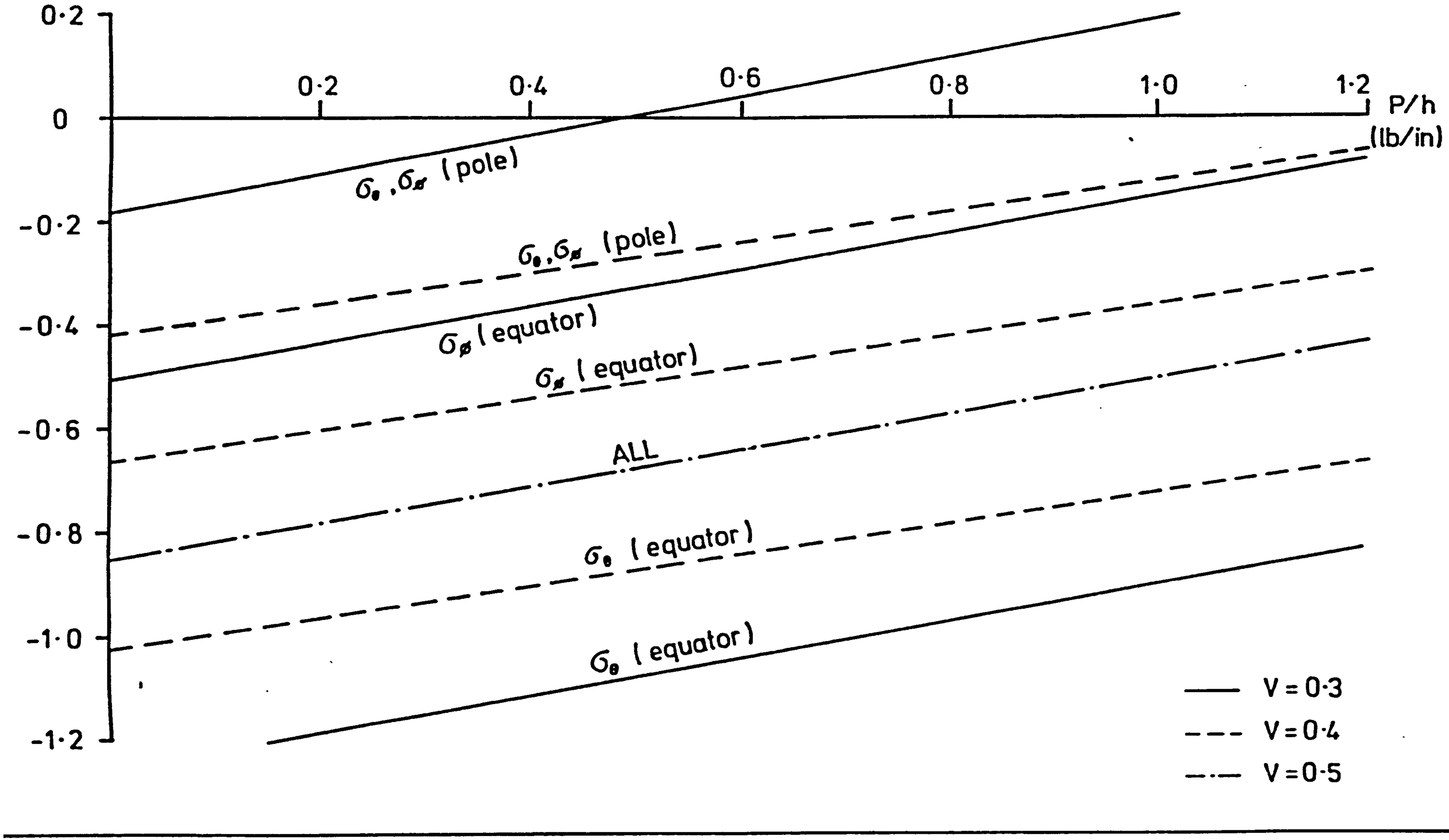

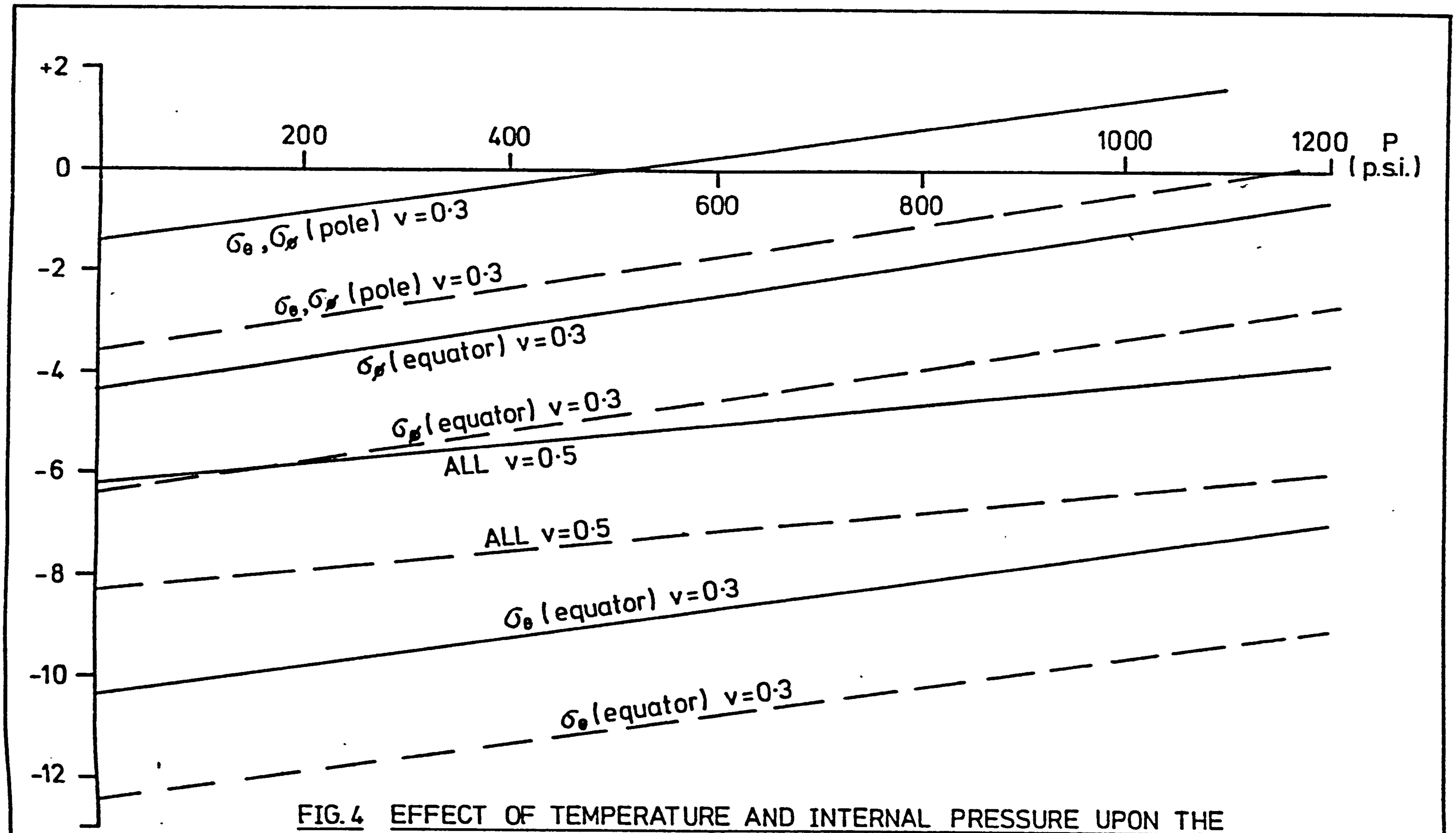

FIG. 4 EFFECT OF TEMPERATURE AND INTERNAL PRESSURE UPON THE STRESSES AROUND A STORAGE CAVITY

CHAPTER 3

THE DESIGN OF AN IN SITU EXPERIMENT FOR MATHEMATICAL MODEL EVALUATION

CHAPTER 3

3. THE DESIGN OF AN IN SITU EXPERIMENT FOR MATHEMATICAL MODEL EVALUATION

3.1 Fundamental design considerations

The in situ experiment must be capable of exerting a set of stress fields on the rock salt similar to that experienced by the rock surrounding an operational gas storage cavity. The behaviour patterns of the rock under these stresses will provide data applicable to the analysis of the forces at work during gas storage operations. From the discussion in 2.1 it is clear that the experiment should involve an underground opening in solid rock. This opening should be capable of accepting an internal pressure and be of such a form that a temperature difference can be applied to its surface. Various shapes were considered for the experimental cavity, but the advantages of mathematical simplicity and ease of construction limited the choice to the cylinder.

An approximate analysis of the stress distribution around a horizontal cylindrical cavity may be made by assuming linear elasticity. If an infinite elastic medium containing a cylindrical opening is subjected, at infinity, to a biaxial stress field then, assuming a condition of plane strain, the stress distribution around the opening may be given by (11) :-

$$\sigma_r = -\left(\frac{S_h+S_v}{2}\right)\left(1-\frac{R^2}{r^2}\right)-\left(\frac{S_h-S_v}{2}\right)\left(1+\frac{3R^4}{r^4}-\frac{4R^2}{r^2}\right)\cos 2\theta \quad (21)$$

$$\sigma_\theta = -\left(\frac{S_h+S_v}{2}\right)\left(1+\frac{R^2}{r^2}\right)+\left(\frac{S_h-S_v}{2}\right)\left(1+\frac{3R^4}{r^4}\right)\cos 2\theta \quad (22)$$

$$\tau_{r\theta} = +\left(\frac{S_h-S_v}{2}\right)\left(1-\frac{3R^4}{r^4}-\frac{2R^2}{r^2}\right)\sin 2\theta \quad (23)$$

where σ_r, σ_θ = radial and tangential stress respectively

$\tau_{r\theta}$ = shear stress

S_h, S_v = horizontal and vertical stress respectively
R = cavity radius
r, θ = radial and angular variables respectively

If the axial strain is zero, i.e., a condition of plane strain is assumed, then the axial stress can be expressed as:-

$$\sigma_z = \nu(\sigma_r + \sigma_\theta) \qquad (24)$$

The critical stress values will occur at the cavity surface and the zones of particular interest are the top, bottom and sides of the cavity. By making the necessary substitutions in Equations (21), (22) and (24), the stress distribution at the cavity surface may be written as:-

<u>At the sides, $\theta = 0^\circ, 180^\circ$</u>

$$\sigma_r = 0 \qquad (25)$$

$$\sigma_\theta = S_h - 3S_v \qquad (26)$$

$$\sigma_z = \nu(S_h - 3S_v) \qquad (27)$$

<u>At top and bottom $\theta = 90^\circ, 270^\circ$</u>

$$\sigma_r = 0 \qquad (28)$$

$$\sigma_\theta = S_v - 3S_h \qquad (29)$$

$$\sigma_z = \nu(S_v - 3S_h) \qquad (30)$$

In the evaluation of the thermal stress components it is assumed that the experimental cabity is an opening of circular cross-section in a cylinder of elastic material. It is also assumed that the cavity surface is held at a temperature difference T above the temperature of rock mass at a distance nR from the cavity, when n is some number and R the cavity radius. For mathematical simplicity the temperature gradient around the cavity is considered to be stationary for the whole of the time considered. Finally, it is assumed that the radial stress components are zero at the cavity surface and at a distance nR from the cavity axis. The thermal stresses may be given by (15):-

$$\sigma_r = \frac{\alpha E \Delta T}{2(1-\nu)\log n}\left[-\log\left(\frac{nR}{r}\right) - \frac{\log n}{n^2-1}\left(1-\frac{n^2R^2}{r^2}\right)\right] \qquad (31)$$

$$\sigma_\theta = \frac{\alpha E \Delta T}{2(1-\nu)\log n}\left[1-\log\left(\frac{nR}{r}\right) - \frac{\log n}{n^2-1}\left(1+\frac{n^2R^2}{r^2}\right)\right] \qquad (32)$$

$$\sigma_z = \frac{\alpha E \Delta T}{2(1-\nu)\log n}\left[1-2\log\left(\frac{nR}{r}\right) - \frac{2\log n}{n^2-1}\right] . \qquad (33)$$

Substituting the appropriate values in these equations will give the thermal stress components symmetrically distributed around the cavity surface:-

$$\sigma_r = 0 \qquad (34)$$

$$\sigma_\theta = \frac{\alpha E \Delta T}{2(1-\nu)\log n}\left[1-\frac{2n^2\log n}{n^2-1}\right] \qquad (35)$$

$$\sigma_z = \frac{\alpha E \Delta T}{2(1-\nu)\log n}\left[1-\frac{2n^2\log n}{n^2-1}\right] \qquad (36)$$

It may be shown (9) that if a thick-walled hollow cylinder of elastic material has an inner radius of R and an outer radius of ∞, then an internal pressure P will set up the following stresses at a radial distance r from the axis:-

$$\sigma_r = -P\frac{R^2}{r^2} \tag{37}$$

$$\sigma_\theta = +P\frac{R^2}{r^2} \tag{38}$$

$$\sigma_z = 0 \tag{39}$$

The maximum stress components occur at the cavity surface where their values are given by:-

$$\sigma_r = -P \tag{40}$$

$$\sigma_\theta = +P \tag{41}$$

$$\sigma_z = 0 \tag{42}$$

The expressions for the resultant stress components may be obtained by applying the principle of superposition. The stress components at the sides and top of the cavity surface may be expressed as:-

<u>At the sides, $\theta = 0^\circ$</u>

$$\sigma_r = -P \tag{43}$$

$$\sigma_\theta = S_h - 3S_v + \frac{\alpha E \Delta T}{2(1-\nu)\log n}\left[1 - \frac{2n^2}{n^2-1}\log n\right] + P \tag{44}$$

$$\sigma_z = \nu(S_h - 3S_v) + \frac{\alpha E \Delta T}{2(1-\nu)\log n}\left[1 - \frac{2n^2 \log n}{n^2-1}\right] \quad (45)$$

<u>At the top, $\theta = 90^\circ$</u>

$$\sigma_r = -P \quad (46)$$

$$\sigma_\theta = S_v - 3S_h + \frac{\alpha E \Delta T}{2(1-\nu)\log n}\left[1 - \frac{2n^2 \log n}{n^2-1}\right] + P \quad (47)$$

$$\sigma_z = \nu(S_v - 3S_h) + \frac{\alpha E \Delta T}{2(1-\nu)\log n}\left[1 - \frac{2n^2 \log n}{n^2-1}\right] \quad (48)$$

The elastic mathematical model can be used, together with engineering considerations, in the design of an experimental cavity. Although the basic design suggests a horizontal cylindrical chamber, data provided by an approximate mathematical model is needed to design a deformation and temperature measurement system.

3.2 Design of a deformation measurement scheme in the experimental cavity

3.2.1 Longitudinal deformation

All of the mathematical models discussed in 2.1 assume a condition of plane strain when applied to the experimental cavity. To verify that no strain takes place in the axial direction it is necessary to measure axial deformation. A review of the techniques available would indicate that this may best be done by means of deformation transducers, preferably with a gauge length of several feet.

The siting of these transducers must be such that any axial strain within the cavity will be detected. Therefore the measurements must be made at several points along the length of the cavity and at several points around the circumference. The transducers must be capable of measuring small amounts of axial strain; therefore, the longer the transducer, up to a practical limit, the less is the need for accuracy. A four foot long transducer capable of accurately measuring to $\pm 1 \times 10^{-4}$ in. can detect strains as small as 2×10^{-6}, and this strain detection accuracy would be adequate for the purposes of this experiment.

3.2.2 Diametral deformation

It can be shown (9), (11) that the radial displacement of the cavity surface, Ur , due to a temperature decrease ΔT and an internal pressure P may be given by :-

$$U_r = \frac{(1+\nu)PR}{E} + \frac{(1+\nu)\alpha E \Delta T R}{2\log n}\left(\frac{1}{2} - \frac{\log n}{n^2-1}\right) \quad (49)$$

If the following values are assumed :-

E	=	1×10^6 psi	$\alpha = 37 \times 10^{-6}$ in/in /°C
ν	=	0.4	T = -15°C
P	=	200 psi	n = 10
R	=	2 ft	

This set of values represents the maximum stress attainable according to the theory of elasticity without involving the experiment in troublesome technical difficulties. The resulting radial displacement would be:-

$$Ur = 8.875 \times 10^{-3} \text{ in.}$$

Although the maximum theoretical diametrical displacement should be less than 2×10^{-2} in., it would seem advisable to employ transducers with a maximum extension of ± 0.5 in. to take into account any unpredicted deformation. The measurements should be made with the greatest degree of accuracy that is consistent with manageable technical problems.

The siting and angular positioning of the diametral deformation transducers must be chosen with the greatest of care. The angular positioning of the transducers must be such that the movements in any direction perpendicular to the cavity axis can be detected or calculated. The most efficient method of attaining this objective is an array of three transducers at any one measurement station, with one transducer aligned vertically and the other two each displaced by 120°.

To avoid the influence of stress concentrations at the ends of the cavity, the measurement stations must be sited at least $1\frac{1}{2}$ times the cavity diameter from the ends of the cavity. Therefore the location of the measurement stations is dependent upon cavity diameter. After much thought it was decided that a cavity diameter of four feet would provide a good compromise between the minimum working area necessary for these investigations and the technical difficulties of boring large diameter chambers. It was consequently decided that a pressure chamber 24 feet long and four feet in diameter would be ideal. This would allow the installation of three measurement stations, separated from each other and the cavity ends by six feet or $1\frac{1}{2}$ times the cavity diameter.

3.2.3 Measurement of deformation in the rock mass surrounding the cavity

An extension of the measurements proposed in the preceding section may be made by the installation of deformation transducers in boreholes radiating from the cavity surface. It can be proved, using elastic theory, that the deformation should be symmetrical about the cavity axis, and it should therefore be sufficient to measure these deformations in one direction only. However, a greater degree of confidence in the results of these measurements would be assured if the boreholes were aligned in a pattern similar to that of the diametral deformation transducers. The additional advantage of a comprehensive picture of deformation in one plane would be gained if the boreholes were placed in the same directions as the diametral transducers.

The radial strain in the rock mass due to the imposed experimental conditions will be at a maximum at the cavity surface and diminish to zero at some distance into the rock mass. An analysis of the rock movements using the elastic model indicates that a point twelve feet from the cavity axis would experience no displacement. On the basis of this analysis it was decided to employ ten foot long instrument boreholes, making displacement measurements between the cavity surface and four points along the borehole. These points would be nine inches, two feet, four feet and ten feet from the cavity surface. This measurement scheme allows all radial and diametrical deformation measurements to be related to a stable point ten feet into solid rock.

3.2.4 Summary of deformation measurements

The preceding three sections describe the deformation measurements made in the in situ experiment. The longitudinal transducers, measuring axial strain, (if any), are located in two arrays, one each between the radial deformation stations. Each array includes three transducers, one along the roof of the cavity and the other two displaced by 120°. The radial deformation is measured at three stations, the deformation at each station being monitored by three diametral transducers and twelve borehole transducers. Thus the complete scheme is :-

	No. of Measuring Stations	Transducers at each Station.	Total
Longitudinal measurements	2	3	6
Diametrical measurements	3	3	9
Radial measurements	3	12	36
		Grand Total	51

A diagramatical representation of this measurement scheme may be seen in Fig. 5 and Fig. 6.

3.3. Measurement of thermal gradients

Section 2.1 indicates that a knowledge of the temperature gradient is required to calculate the thermal stresses in the rock mass. This temperature distribution is symmetrical about the cavity axis due to the geometry of the cavity. Therefore it was necessary to measure temperature at the cavity surface and for a radial distance into the rock mass. It was though advisable to measure this radial temperature distribution by utilising the transducer boreholes. This was done by equipping the transducer instrumentation with temperature sensing devices and thermally isolating the borehole mouth from the temperature difference applied to the cavity surface. Such a scheme would provide data on nine radial temperature distributions, each distribution being defined by temperature at five points; surface, nine inches, two feet, four feet and ten feet into the rock.

However,this scheme would not provide data on the steep temperature gradient found near the rock surface. Therefore it was necessary to introduce a second scheme for investigating the cavity skin temperature. The most serious problem to be overcome was the insertion of temperature probes to indicate a rock temperature uninfluenced by the physical presence of the probe itself. This in essence was the old problem of the observer affecting the result of an experiment.

This problem was overcome by constructing a probe in rock salt and mounting the temperature sensors within these probes. The two skin temperature measurement stations were located midway between the radial deformation measurement stations, the angular alignment taking the usual pattern with one probe inserted vertically and the other two displaced by 120°. A diagram of the temperature measurement scheme is shown in Fig. 5 and Fig. 6.

3.4 Experimental plant

A detailed description of the compressed air and heat transfer equipment used to impose the desired conditions of pressure and temperature on the rock mass may be found in Chapter 7. This chapter also describes other ancilliary equipment used in this experiment.

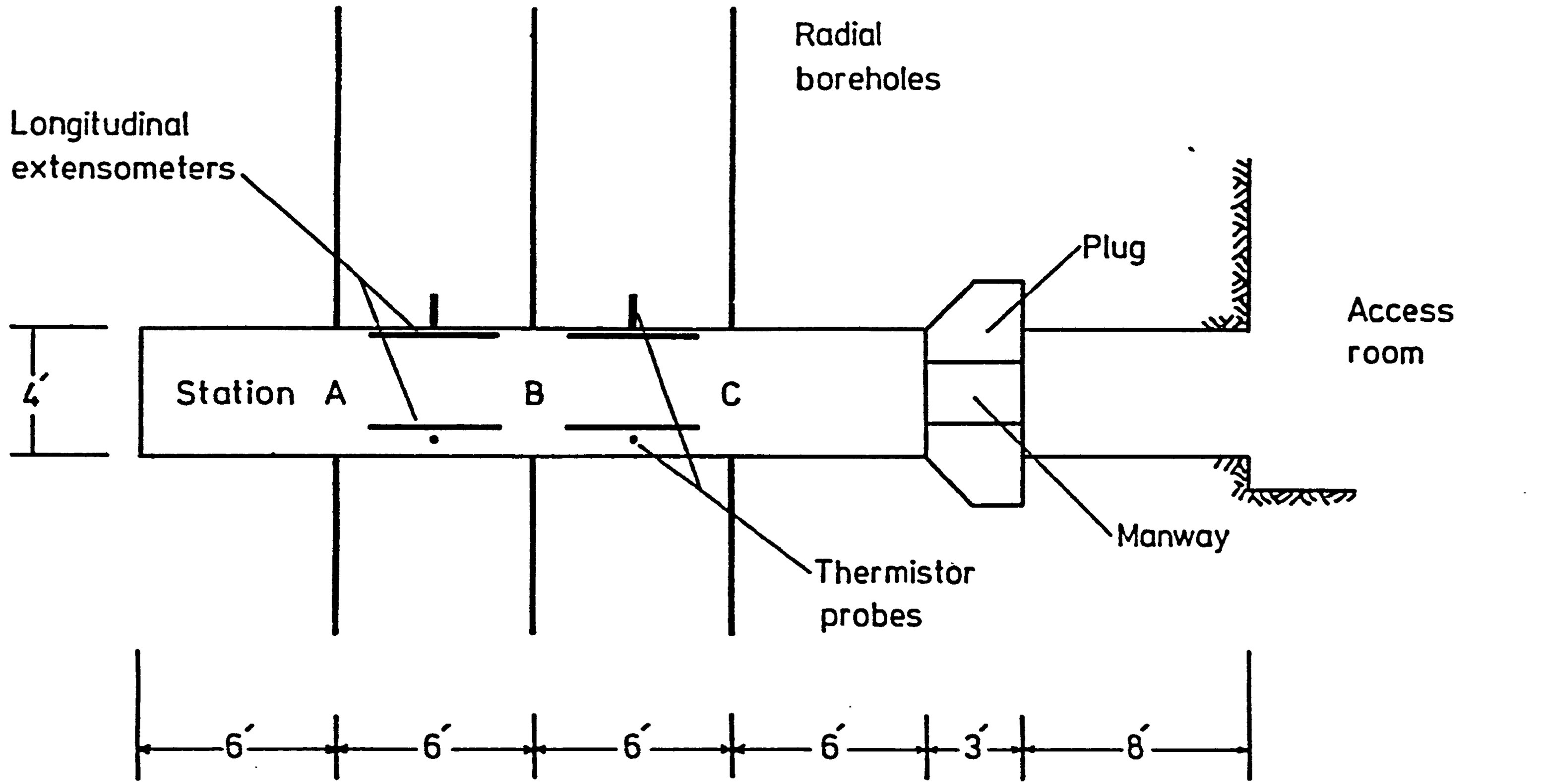

FIG. 5 THE INSTRUMENTATION SCHEME

T_a = Air temperature measurement

T_r = Rock temperature measurement

Anchor No. 1
(10 ft.)

T_a

T_r

Radial deformation measurements

Anchor No. 2
(4 ft.)

Anchor No. 3
(2 ft.)

Anchor No. 4
(9 in.)

Transducer assembly

Borehole V

vertical

left

right

Borehole L

Borehole R

Diametral deformation measurements at Stations A, B & C

surface

1/4" 1" 4"

1/2" 2" 6"

Thermistor probe

FIG. 6 DETAILS OF INSTRUMENTATION SCHEME

CHAPTER 4

DESIGN AND CONSTRUCTION OF THE UNDERGROUND INSTALLATION

CHAPTER 4

4. DESIGN AND CONSTRUCTION OF THE UNDERGROUND INSTALLATION

4.1 Site design and construction

4.1.1 Basic considerations of access room design

The proposed experiment involved the pressurising of a horizontal cylindical cavity excavated in the rock salt mass 450 feet below ground at the Meadowbank Rock Salt Mine. Although such a cavity could be designed with a high factor of safety, there existed a remote possibility that the pressure retaining plug or the surrounding salt mass could fail. In such an eventuality, the design and layout of the experimental area must be of such a form as to minimise or eliminate risk of damage to mine personnel and equipment.

A cost analysis of site construction revealed that much of the total cost could be attributed to access room construction and transportation of the hydraulic auger used to excavate the experimental cavity. The excavation of a second cavity on the same site would introduce relatively little extra cost and at the same time provide the experiment with a stand-by cavity. This second cavity could be used in the event of an unexpected failure of the first and could also be used to extend the scope of the experiment.

The final design of the site layout proposed a T-shaped access room excavated in a remote part of the mine. To facilitate ease of handling of the large construction equipment, the T-shaped room was driven at an angle of approximately 45° to the main roadway. The two horizontal large diameter holes would be bored with one on each arm of the T in such a location that the debris from a plug failure would impact on the opposite rock face. A plan of the final access room design is shown in Fig. 7.

4.1.2 Access room construction

The initial plan was to construct the access room at a location known as 'B' Tunnel, quite close to all the shafts, but remote from any current mining operations. Unfortunately, when the access room off 'B' Tunnel was almost completed, a seepage of brine was encountered. This occurrence was viewed with the utmost gravity by the mine management; in 1969 an unchartered borehole, connecting the salt beds to the brine at the wet rock-head, was intercepted by the mine workings and could have resulted in the loss of the mine. Consequently the site at 'B' Tunnel was abandoned and the seepage of brine sealed by grouting.

A new site for the access room was established on the north-west corner of Moulton No. 2 Panel. The new site was not in such a convenient position as the original choice, but satisfied the requirements of remoteness and service facilities. This site was located in mine workings which followed the base of the salt bed. Consequently it was necessary to construct a ramp enabling the access room to be mined at a height of twelve to fifteen feet above the base of the salt, thus allowing the instrument boreholes, radiating from the cavity, to be located entirely within rock salt.

The ramp was constructed so that a flat area at the top of the rise could be used to site the compressor and heater/chiller equipment. The access room, the ramp top and one half of the ramp were laid with saltcrete to provide good access and a firm level foundation for the transportation and installation of heavy equipment. The new site was eventually supplied with compressed air (80 - 90 psi), electricity and suitable ventilation.

4.2 The cavity pilot holes

4.2.1 The downhole

The Jason Auger used to bore out the cavities has a working centreline three feet above ground level, and consequently the pilot hole centrelines should be ideally at the same height. However, before the pilot holes could be drilled it was necessary to check that there was a sufficient depth of salt beneath the access room floor. An insufficient depth of salt could be dealt with by either packing up the auger to the desired height or laying an extra bed of saltcrete on the access room floor.

The downhole was bored by a Boyles BBS10 Swivelhead drill approximately on the access room centreline and nine feet from the working face. The base of the salt bed was intersected 13' $4\frac{3}{4}$" below floor level, the underlying rock being a red-brown marl.

4.2.2 The pilot holes

The two cavity pilot holes were located 31 feet apart and drilled perpendicular to the working face three feet above floor level. A diesel driven Boyles BBS110 Swivelhead drill fitted with compressed air flush was used for this work. The drill string was made up of two and five feet lengths of NW ($2\frac{5}{8}$" O.D.) drill rod fitted with stabilisers every five to ten feet. The cutting tool was a two foot long core barrel producing $5\frac{3}{8}$" diameter cores out of a six inch diameter hole.

It was extremely important that the pilot holes be drilled as accurately as possible as they determined the final position and alignment of the two horizontal cavities. Consequently it was decided to drill through a bearing frame to ensure maximum drill string stability. The bearing frame was bolted to the ground and was so constructed that the levels of each corner could be adjusted, allowing the frame to be accurately manoeuvred into a horizontal position. Lateral alignment was defind by centrelines laid down by I.C.I. surveyors.

When drilling commenced, a wooden steady was bolted to the front of the bearing frame to allow the core barrel to be accurately sumped in. The steady, constructed in two halves to allow easy assembly around the core barrel, was removed after the first foot of the hole had been drilled. As the work proceeded stabilisers were fitted to the drill string every five to ten feet. The stabilisers were made up of short cylinders of steel connected to a central boss by means of vanes, and the boss clamped to the drill rods.

As completion of the holes was neared, the work became rather tedious as every two feet the drill string had to be removed from the hole to extract the core. Core extraction was achieved using a hemicylindrical scoop attached to extension rods. The core was broken off the solid by a wedge welded to the scoop bottom, and when broken off, the core dropped into the scoop and was pulled out of the hole. Withdrawing the rods every two feet was made slightly easier by the design of the bearing frame. The upper half of the frame could be unbolted on one side and swung clear of the hole by means of hinges fitted at the other side. This meant that drill rods could be removed in ten foot lengths instead of unscrewing each individual five foot length.

The holes were identified as the right or left hand hole when facing the drilled cavities. Each piece of recovered core was marked with a letter L or R (left or right hand hole) followed by a number corresponding to the order in which the pieces of core were removed. To aid further identification each piece of core was marked with a distance mark and a letter F to denote the end of the core nearest the rock face of the access room. In many cases, especially in Hole R, cores were broken either during drilling or core recovery.

The access room was ventilated using an auxiliary fan. Diesel fumes from the drill were fed into the fan ducting by an arrangement of tubes and flexible pipes converted from an industrial vacuum cleaner.

The final depth of Hole R was 42' 1" from which 41' 2" of core was recovered. Hole L was drilled to a depth of 42' 5" and all of the core recovered.

4.3 An engineering appraisal of the pilot holes and recovered core

4.3.1 Pilot hole pressure testing

Although the last few feet of the front face of the access room had been excavated by only light blasting, it was still possible that this had induced some fracturing of the rock mass. Core recovery had indicated that there was no sign of severe fracturing, but further proof was needed before excavation of the two cavities could commence.

It was decided that the best way to investigate the possibility of fracturing was to subject the two pilot holes to a pressure test using the equipment shown in Fig. 8. The boreholes were divided into two foot lengths and each length was isolated in turn by means of the two pressurised sealing rings. The section of borehole under test was then subjected to approximately 80 - 90 psi (585 kN/m^2) and held there for a few minutes to determine that it was air tight. The procedure was repeated at other sections to give a complete pressure test of the two boreholes. The back of the hole was vented to atmosphere to prevent the rapid ejection of the equipment in the event of a leak.

It was found that the entire lengths of the two pilot boreholes were completely airtight at pressures up to 80 - 90 psi.

4.3.2 Survey of the two pilot holes

The holes were surveyed by means of a downhole target, tape measure and a mining type theodolite and target. The downhole target, shown in Fig. 9, was designed specially for this survey, and consists of a shaft supported at each end by a trolley. An illuminated perspex target and reflector was mounted at the front end of the shaft and the dry battery

supply to the target illuminator was strapped onto the middle of the shaft. The target was traversed along the hole by means of rigid extension rods connected to a bracket on the underside of the target shaft.

This instrument had a bulls'-eye type target graduated in quarters of an inch. Each hole was surveyed by pushing the target to the back of the hole and sighting the theodolite cross-hairs onto the centre of the target. The angle and elevation of the theodolite was noted and the target withdrawn a certain distance from the back of the hole. Without moving the theodolite the target was sited again and the apparent horizontal and vertical movement recorded. It was possible to estimate this movement to an accuracy of $\pm$1/32 inch. Using this technique, and measuring angles and distances between the survey stations at the mouth of each hole, it was possible to build up an accurate plot of hole inclination and alignment.

The elevations of Holes L and R may be seen in Fig. 10 and Fig. 11, respectively. The first hole to be drilled was Hole R and it can be seen that this dropped a total of 6.9 in. at the back of the pilot hole. This inaccuracy was due to two factors:-

i) Both the bearing frame and the Boyles drill were anchored to the floor by means of expansion bolts. But either weakness of the salterete floor (caused by an insufficient curing period being allowed before commencement of drilling operations), or the use of expansion bolts of too small a diameter, created difficulties in bolting the equipment to the access room floor. If the gradual and persistent loosening of the foundation bolts went unnoticed, a small amount of drill string movement took place, possibly introducing errors in borehole inclination.

ii) When the bearing frame had been accurately aligned prior to drilling, it was found difficult to maintain it in a level position whilst it was being tightened down onto the expansion bolts. With time and patience it was possible to effect a compromise between setting up time and the degree of accuracy achieved.

Hole L, using larger diameter foundation bolts, experienced none of the problems encountered in drilling Hole R. The centreline of Hole L began three feet above floor level but dropped a total of 2.4 in. at the back of the hole. The alignment of the two holes can be seen in Fig. 12. It can be seen that Hole R was driven at an angle of 18' 03" to the access room centreline; Hole L was parallel to the access room centreline, but 3/16 in. closer to it than intended.

Cavity L and Cavity R, formed by over boring these holes, were bored to depths of 36 and 35 feet respectively. Consequently the backs of Cavities L and R were 2 in. and 6 in. respectively below the intended three feet high centreline.

4.3.3 Physical properties of the recovered core

The core recovered from the two pilot holes was subjected to a series of tests to ascertain the physical properties of the rock mass surrounding the experimental cavities.

i) Compressive strength

Twenty specimens of diameter $5\frac{3}{8}$ in. and height $10\frac{3}{4}$ in. were tested in uniaxial compression. The results of these tests indicated that there was no definite pattern of strength or weakness along the length of the cavities; the strength of the salt appeared to be dependent on the presence or absence of the randomly distributed marl content of the specimens.

TABLE 1

	p.s.i.	kN/m^2
Mean compressive strength	4,174	28,779
Standard deviation	649	4,475 (15.5%)
Minimum compressive strength	3,080	21,236
Maximum compressive strength	5,390	37,163

ii) Tensile strength

Forty-one specimens, 2 11/16 in. long by $5\frac{3}{8}$ in. in diameter were cut from the two cores and subjected to the Brazilian disc test to ascertain a representative value for the tensile strength of the rock mass surrounding the cavities. Once again, there was no definite pattern of rock strength along the lengths of the cavities. When considering the results of this test, it should be borne in mind that the tensile strength given by the Brazilian disc method, an indirect test, is slightly higher than the tensile strength indicated by a direct tensile test.

TABLE 2

	p.s.i.	kN/m^2
Mean tensile strength	240.0	1655
Standard deviation	35.4	244.2 (14.75%)
Minimum tensile strength	169.3	1167
Maximum tensile strength	326.2	2249

iii) Shear strength

When a cavity is pressurised the rock mass surrounding the plug is subjected to shear stresses. Consequently it became necessary to establish the shear strength of rock salt, the value of which could be used in plug design calculations. Five samples, all taken from the first eleven feet of the two cores were cut into specimens $5\frac{7}{8}$ in. long by $2\ ^{15}/16$ in. in diameter and put under load in a triaxial cell with the following results:-

TABLE 3

Specimen No.	Confining Pressure		Axial pressure at failure	
	p.s.i.	kN/m^2	p.s.i.	kN/m^2
R1	200	1379	7950	54,815
L7A	400	2758	8160	56,263
L6	600	4137	9100	62,745
R8	800	5516	10,900	75,155
R5	1000	6895	did not	fail

These results, shown graphically in Fig. 13, indicate a shear strength of approximately 450 p.s.i.

iv) Modulus of elasticity

Fifteen specimens, $5\frac{3}{8}$ in. in diameter by $10\frac{3}{4}$ in. long, were twice preloaded to 1000 p.s.i. and then subjected to three loading and unloading cycles in uniaxial compression. Ten specimens were instrumented by means of dial gauges and the remaining five with electrical resistance strain gauges. The mean values of the secant modulus for each cycle, taken from the most linear section of the loading cycle, 400 to 900 p.s.i., are given below:-

TABLE 4

	Mean decent modulus X10^6 psi		
	1st cycle	2nd cycle	3rd cycle
Dial gauged speciments	2.099	2.336	2.356
Strain gauged specimens	3.359	3.640	3.690

It can be seen from the results of these tests that the strain gauged specimens gave a higher value than the dial gauged specimens. This was probably due to the steel platens bending during the tests and the resulting deformation being recorded along with the deformation of the specimen. The results obtained from the dial gauged specimens can be regarded as being more realistic than those obtained from the dial gauged specimens.

v) Poisson's ratio

The five specimens used to determine the modulus of elasticity with strain gauges were fitted with circumferential strain gauges. The values of circumferential deformation were recorded during the elastic moduli tests, and from these results values of Poisson's ratio were calculated.

	2nd cycle	3rd cycle
Mean value of Poisson's ratio	0.299	0.237

Values obtained during the first cycles were unacceptably high due to the non-linear behaviour of the material during consolidation. Consequently, values for only the second and third cycles were recorded.

vi) Summary of physical properties

TABLE 5

	p.s.i.	kN/m^2
Mean compressive strength	4,174 (±15.5%)	28,779
Mean tensile strength	240.0 (±14.75%)	1,655
Estimated shear strength	450	3,103
Mean secant modulus in range 400–900 psi	3.69×10^6	25.4×10^6
Mean value of Poisson's ratio	0.237	-

4.4 Excavation of the cavities

4.4.1 Introduction

The contract for this work was awarded to Tube Headings Ltd., a subsidary of Cementation Company Ltd. It was agreed that this company would excavate two cavities four feet in diameter by thirty five feet long using a Jason Auger. The cavities were to be bored to an accuracy of ±1" on diameter and to have a finish consistant with that achieved by machine tools on rock.

The drill string was to consist of a cutter head and a series scrolls to remove the excavated rock. As this company did not have a suitable cutter head, it was agreed that they would design and construct one at their workshops. Subsequent events proved that the company had neither the expertise or the necessary experience in this field to design an efficient cutting head. Consequently the cutter head was designed and made by the Department, a front view of which is shown in Fig. 14. The cutter head probe was designed to slide along the pilot hole and remain stationary whilst the pick-bearing arms rotated under power from the auger.

The maximum size of hole normally bored by Tube Headings Ltd. was three foot six inches in diameter, so it was necessary to provide some form of stabilisation for this size of scroll working in a four foot diameter hole. The company decided to prefabricate one length of scroll four foot in diameter to be used just behind the cutter head, and to fit the remaining lengths of scroll with outrigger-type stabilisers. These stabilisers consisted of a mushroom head attached to the apex of a short triangular plate which was in turn bolted to the periphery of the scroll every 120°. A sketch of these stabilisers is shown in Fig. 16a.

4.4.2 Excavation of Cavity R

The Jason Auger was transported to the top of No. 4 shaft, and dismantled to allow passage down the shaft. The auger was carried by low loader to the experiment site and re-assembled in the access room by means of lifting gear coupled to rock bolts set in the roof and sides of the room. A photograph of the auger at work is shown in Fig. 15.

An inspection of the site on the day after boring commenced revealed the following points:-

i) The thrust washer between the cutter head and first length of scroll was missing. It was pointed out to the machine operators that if work continued without the thrust washer, the square-section socket on the scroll would bear against a radius on the cutter head and a burst socket would result.

ii) One pick, close to the probe, was missing and should have been replaced.

iii) The auger had not been correctly set up. Although the front of the auger was at the correct height, the rear was four inches below the three foot high centreline line marked on the back wall of the access room.

iv) The stabilisers attached to the undersized scrolls appeared to be of a poor design. It was thought that the mushroom heads would become choked with cuttings and cause the scroll to bind in the hole.

v) A poor rate of advance was being achieved due to the low torque produced by the hydraulic motor drive. The debris size was very small, (mostly powder, indicating inefficient cutting), but any increase in thrust caused the machine to stall.

vi) The four foot diameter scroll was binding in the cavity and rubbing on projections in the guiding structure. It was arranged for the scroll to be ground down to its correct size and the projections on the guide to be removed.

At the completion of Cavity R the site was revisited to survey the cavity and check upon the efficiency of the drilling operations. It transpired that Tube Headings had neither fitted the thrust washer or modified the design of the stabilisers, and these omissions had led to damage of both the cavity and the drilling equipment.

The leading flight of scroll had its square section socket burst outwards due to the absence of the thrust washer. This meant that the forward thrust of the machine would be taken by a $\frac{3}{4}$ in. diameter pin designed to hold the cutter head in place during drill string withdrawal. The pin, not being designed to transmit the forward thrust, had bent almost double and allowed the scroll socket to bear against a radius which burst it outwards.

The mushroom type of stabiliser proved to be unworkable. The stabilisers tended to trap the debris being scrolled out of the hole, between the mushroom head and the cavity wall. This caused the drill string to jam solid and produce two distinct types of damage to the scrolls. The first type of damage involved individual stablisers being wrenched out of the scroll vanes. A more serious type of damage occurred when several stabilisers on a length of scroll jammed; this resulted in the scroll being held fast whilst the central shaft continued to turn, causing the vanes of the scroll to unwind from the shaft.

Tube Headings Ltd. lost so much time and drilling equipment through these problems that they decided to remove the stabilisers completely. This removal took place after approximately twenty-five feet of cavity had been bored; however, this led to even greater difficulties.

The removal of the stabilisers allowed the scrolls to whip up and down within the cavity, causing damage to the cavity bottom. This resulted in the finished cavity being almost elliptical in parts. This double radius may be seen in Fig. 17 which shows a four feet diameter disc in the supposedly four feet diameter cavity. The upper radius of two feet was created by the cutter head boring out the cavity; the lower radius, of one foot nine inches, was the damage resulting from the unstabilised scroll. Table 6 gives the results of a survey of the completed Cavity R.

Tube Headings Ltd. put forward the suggestion that the damage to the cavity was caused by a steeply dipping pilot hole. Reference to Table 6 indicates that this was not so; the worst damage occurred at a point twenty-four feet from the back of the cavity, not at the mouth of the hole as would be expected for a steeply dipping hole. The point of worst damage approximately coincides with the centre of a complete drill string: thirty-five feet up the hole with eight to ten feet between the mouth and the machine. This would seem to indicate that the damage was indeed caused by an unstabilised drill string.

TABLE 6

A survey of the completed cavities

Distance from the back of the cavity in feet	CAVITY L		CAVITY R	
	Length of cavity = 36' 0"		Length of cavity = 35' 0"	
	Diameter (± 1/16 inch)			
	Vertical	Horizontal	Vertical	Horizontal
0	47 3/4	47 3/4	47 7/8	47 7/8
2	47 7/8	47 3/4	48 1/4	48
4	47 3/4	47 3/4	48 3/8	48
6	47 7/8	47 7/8	48 1/2	48
8	48 1/8	48	48 3/4	47 7/8
10	48 1/4	48 1/8	48 7/8	48
12	48	48 1/8	49	48
14	48 1/4	47 7/8	49 3/8	48
16	48	48	50	48
18	48	48	50 3/8	48
20	47 7/8	47 3/4	50 3/8	48
22	47 7/8	47 3/4	52 1/4	48
24	47 7/8	47 3/4	52 7/8	48
26	47 7/8	47 3/4	52 3/4	48 1/8
28	48	47 3/4	51 7/8	48 1/4
30	48	47 7/8	51	48 1/4
32	48	48	50 3/8	48 3/8
34	48 3/8	48 1/4	50	48 1/4
36	48	48		

Nominal diameter specified = 48" ± 1"

Consultations with Tube Headings Ltd. revealed that they could put forward no suggestions for design improvements which would ensure the accurate excavation of the second cavity. Consquently it was suggested to them that they should, using their undersize scrolls, bore through their standard 3' 6" diameter borehole liners which could be fitted with centralising spacers. This arrangement, shown in Fig. 16b, has the advantage of not only supporting and stabilising the scrolls, but also protects the surface of the cavity from damage.

4.4.3 Excavation of Cavity L

Cavity L was excavated using the method of drill string stabilisation shown in Fig. 16b: When the completed cavity was inspected the accuracy and general condition was found to be quite good. The tolerance of $\pm$ 1 inch on the diameter was not exceeded, and in the pressure chamber section of the cavity, the maximum deviation from 48" was $\frac{1}{4}$". The surface of the cavity was scored in a helical pattern, but not severely; the worst damage in the pressure chamber section was score marks $\frac{1}{4}$" deep every one to two inches extending from a point nine feet to a point twelve feet from the back of the cavity. The detailed results of the survey are included in Table 6.

It was decided, from the results of these surveys, to utilise Cavity L as the primary experimental cavity, and maintain Cavity R as a reserve.

4.5 The pressure retaining plugs

4.5.1 General design considerations

The pressure retaining plug must be capable of containing a pressure of 200 psi without excessive leakage. It was decided that a semi-conical reinforced concrete plug would prove to be the most effective design, giving both strength and the ability for the self-sealing of leaks. A drawing of the plug showings its location and dimensions is given in Fig. 18. The plug position and dimensions were arrived at by considering the physical properties of concrete and rock salt.

There are five possible modes of failure of the concrete plug and surrounding salt mass, and using the following assumed data, an estimate of the factor of safety of the plug design may be calculated.

Assumed data:-

	Rock Salt (psi)	Concrete (1:1½:3) (psi)
Compressive strength	3000	3000
Tensile strength	150	300
Shear strength	350	360

i) Shear failure of the concrete plug. (A - A)

Surface area of failure plane = $2\pi ra$

Load on plug at 200 psi = $\pi r^2 P$

Shear stress on failure plane = $\frac{rP}{2a}$

= $\frac{2 \times 200}{2 \times 3}$

= 66.7 psi

Factor of safety = 360/66.7 = 5.4

In view of the serious damage to the experiment that would result from a plug failure, this factor of safety is apparently quite low. However, as the concrete is under a state of triaxial compression the actual shear strength of the concrete under these conditions is likely to be much higher than that quoted in the table of assumed data. Consequently, the safety factor of 5.4 can be regarded as a conservative estimate.

ii) Shear failure of the rock salt. (B - B)

The worst case is assumed, that where the compressed air has access to the whole of the inside face of the plug:-

Surface area of failure plane = $2\pi R1$

Load on plug at 200 psi = $\pi R^2 P$

Shear stress on failure plane = $\frac{R\ P}{2l}$

$= \frac{3.5 \times 200}{2 \times 9.5}$

= 36.9 psi

Factor of safety = 350/36.9 = 9.5

iii) <u>Tensile failure on cone-shaped failure surface.</u> (C - C)

Surface area of the trimcated cone = $2\pi(R + 1/2 \text{ ton } \theta)1/\cos \theta$

If the tensile stress on the cone = σt

Then:-

Tensile load perpendicular to the conical surface

$= 2\pi\ \sigma t\ (R + 1/2 \text{ ton } \theta)\ 1\ \frac{\sin \theta}{\cos \theta}$

$\therefore \quad \pi R^2 P = 2\pi\sigma t\ (R + 1/\text{ton } \theta)\ 1 \text{ ton } \theta$

$\therefore \quad \sigma t = \frac{PR^2}{2(R+1/2 \text{ ton } \theta)\ 1 \text{ ton } \theta}$

$= \frac{200 \times 3.5^2}{2\ (3.5 + 4.75 \text{ ton } \theta).\ 9.5 \text{ ton } \theta}$

For $\theta = 45^\circ$

<u>$\sigma t = 15.65$ psi</u>

Factor of safety = 150/15.65 = 9.6

iv) <u>Shear failure on the cone shaped failure surface</u> (C - C)

Surface area of the failure plane = $2\pi(E + 1/2.\ \text{ton } \theta)1/\cos \theta$

Shear force on the failure plane = $P\pi R^2 \cos \theta$

$$\therefore \quad \tau = \frac{P \; R^2 \cos \theta}{2 \quad (R + 1/2.\tan \theta) \; 1/\cos \theta}$$

$$= \frac{PR^2 \cos^2 \theta}{2 \; 1 \; (R + 1/2. \tan \theta}$$

$$= \frac{200 \times 3.5^2 \times \cos^2 \theta}{2 \times 9.5 \; (3.5 + 4.75 \tan \theta}$$

When $\theta = 45^\circ$:-

$$\underline{\tau = 4.075 \text{ psi}}$$

Factor of safety = 350/4.075 = 86

v) Compressive failure of the rock salt

$$\text{Axial bearing pressure} = \frac{\pi R^2 P}{\pi(R^2 - R^2)}$$

$$= \frac{200 \times 3.5^2}{3.5^2 - 2^2}$$

$$\therefore \quad \underline{\sigma_c = 300 \text{ psi}}$$

However assuming a state of hydrostatic stress in the surrounding salt mass, this axial compressive stress will act in opposition to the horizontal component of the over burden stress, 450 psi, the resultant being 150 psi.

It can be seen that the minimum factor of safety for the five cases considered has a value of 5.4. These calculations have not taken into account the creep phenomena of rock salt, but it was felt that at these low stress levels, the effects would be non-constant.

4.5.2 The plug reinforcing cage

The plug reinforcing cage performs the double function of reinforcing the concrete and providing a solid support for the passage of the compressed air pipe, the heater/chiller pipes, man-way and the cable glands through the plug. A side view of the cage prior to installation is shown in Fig. 19, whilst Fig. 43 gives an indication of the external location of the compressed air and heater/chiller pipework.

Since such high pressures are applied to the interior of the cavity it was necessary to use glands to pass instrument and power cables through the plug. A drawing of the gland is shown in Fig. 20, whilst Fig. 21 shows a photograph of part of the assembly procedure.

The reinforcing cage has a two foot diameter tunnel through the centre to allow access to the cavity, the inner end of which is fitted with an air-tight door. This door is hung from double hinges and can be screwed down tight onto a rubber sealing ring.

The plug was constructed by excavating an annulus of the required shape and dimensions by means of compressed air picks. The reinforcing cage was, with difficulty, manoeuvred into position manually using lifting tackle attached to an anchor installed in the remaining few feet of pilot hole at the back of the cavity. Concrete was then pumped into the annulus through the wedge-shaped excavation shown in Fig. 22 and vibrated to expedite compaction.

4.5.3 Grouting of the plug and surrounding rock mass

Prior to the plug installation, eight equally spaced grout injection holes were drilled on a 6'-6" diameter circle through to the annulus from the access room. The holes were fitted with four feet long stand pipes set approximately three feet into the rock. On completion of the concreting of the plug, the grout holes were drilled through to connect with both the back and front faces of the plug. Four weeks after the

plug concrete had been placed, grout was injected, working from the bottom stand pipe upwards. The grout mix consisted of 112 lbs of portland cement to five gallons of saturated brine and injected at a pressure not greater than 200 psi.

4.6 The radial boreholes

The discussion of the proposed instrumentation scheme in Chapter Three described the radial deformation measurements which would be achieved by anchors, push rods and transducers installed in radially orientated boreholes. The instrumentation scheme proposed three measuring stations equally spaced along the cavity, each station consisting of three 11 ft. long radial boreholes. These holes, 1 15/16 in. in diameter, were offset 1½ in. from each other to allow diametral extensometers to be installed from the coverplate of each borehole.

The boreholes were drilled by means of a small compressed air powered drill with a manual ratchet rack and pinion feed. The drill was mounted on a specially designed frame which was fitted with an extending pad allowing the drill stand to be firmly anchored in position. Once the drill stand was in position, the drill could be moved longitudinally along the cavity on a supporting shaft projecting from the frame, thus allowing each hole to be offset from its neighbour without having to move the heavy drill stand. Fig. 23 illustrates the drilling of these holes. After each hole was sunk the mouth was temporarily plugged with a wooden bung.

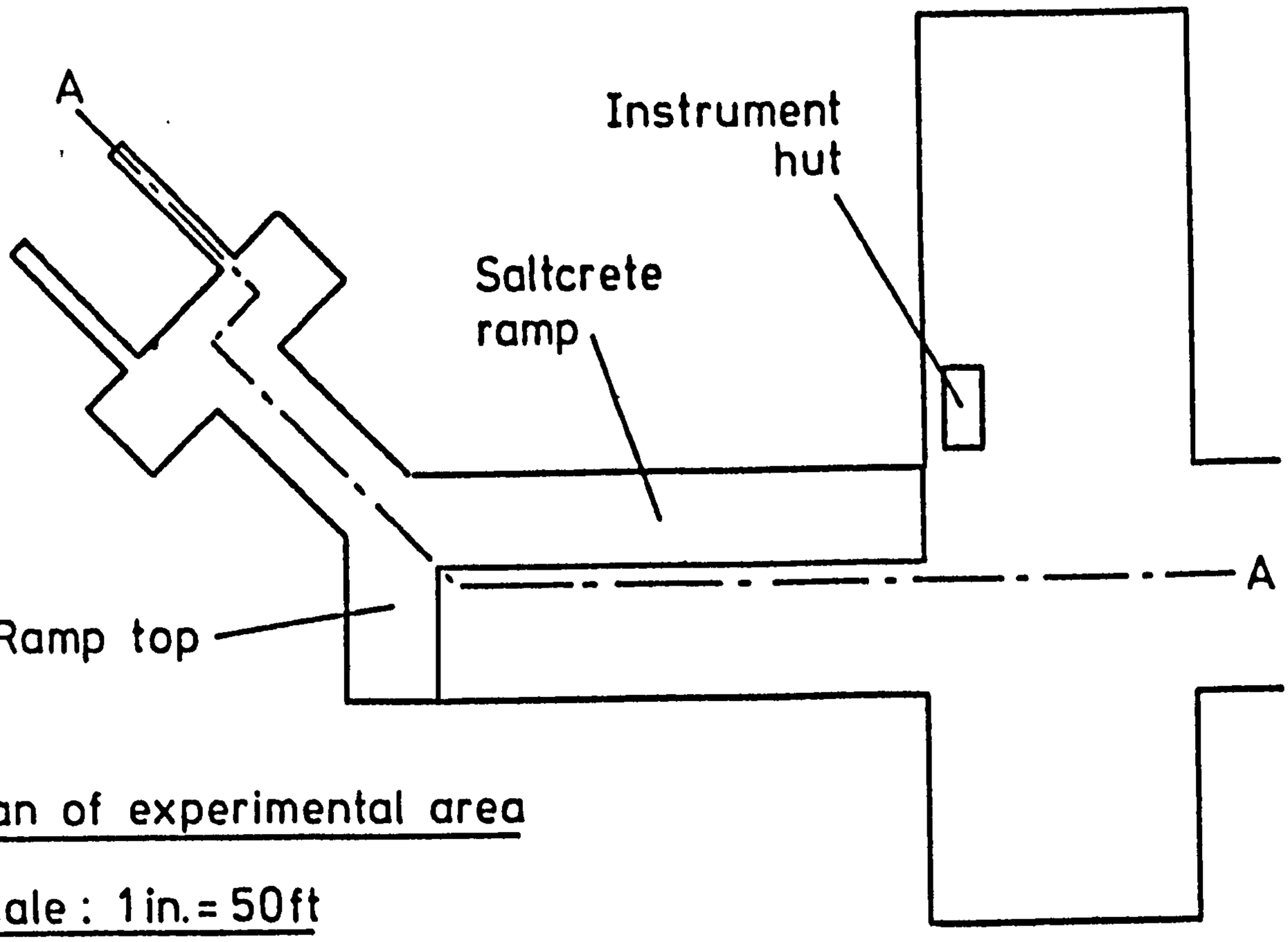

Plan of experimental area

Scale : 1 in. = 50 ft

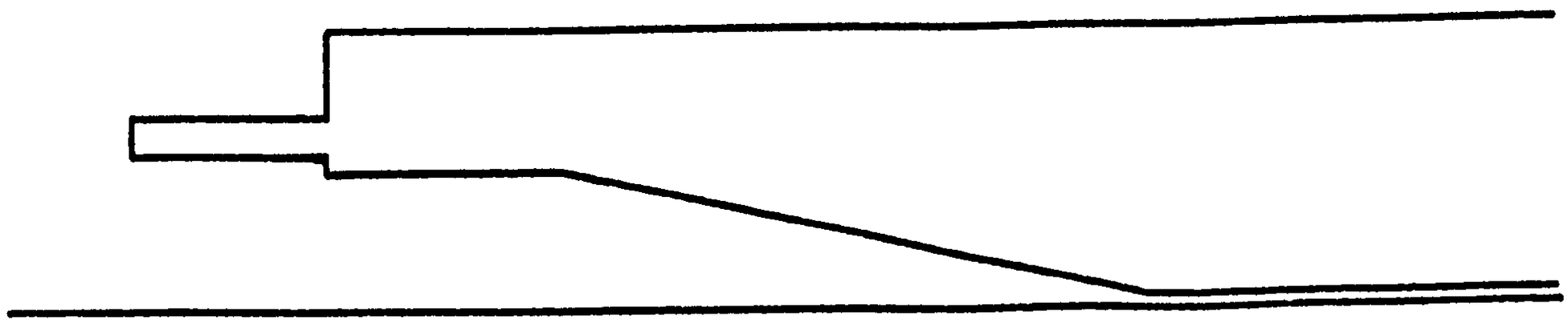

Section A—A

Vertical scale : 1 in. = 25 ft.

Horizontal scale : 1 in. = 50 ft.

FIG 7 THE SITE OF THE EXPERIMENT

FIG. 8 BOREHOLE PRESSURE TESTING EQUIPMENT

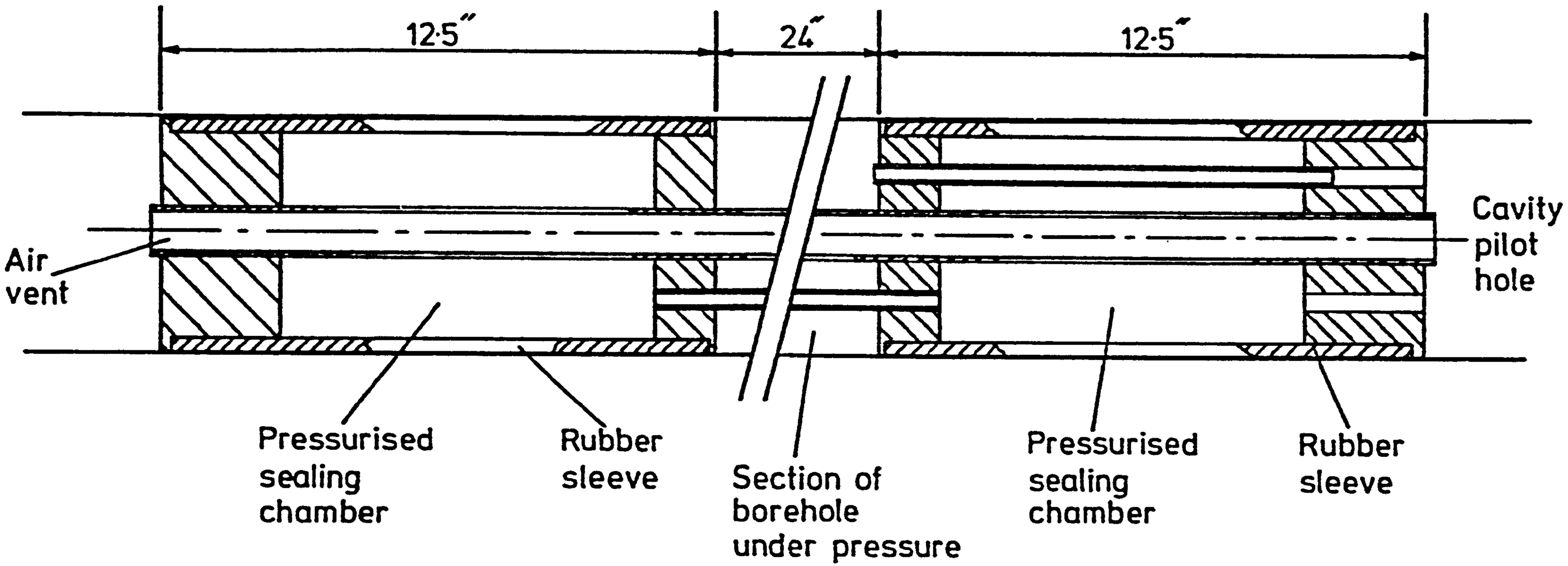

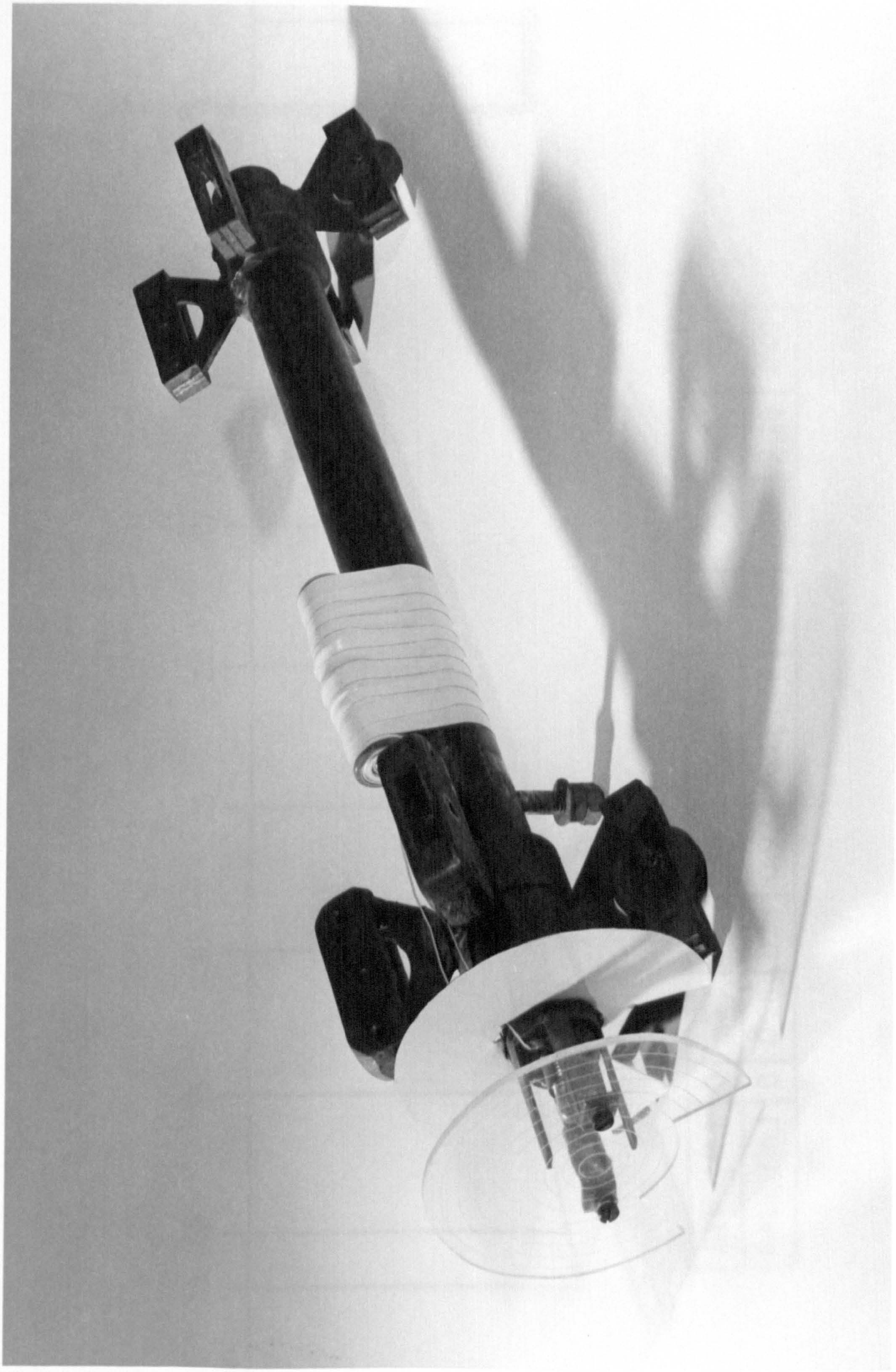

FIG. 9 DOWNHOLE SURVEYING TARGET

FIG.10 SIDE ELEVATION OF HOLE L

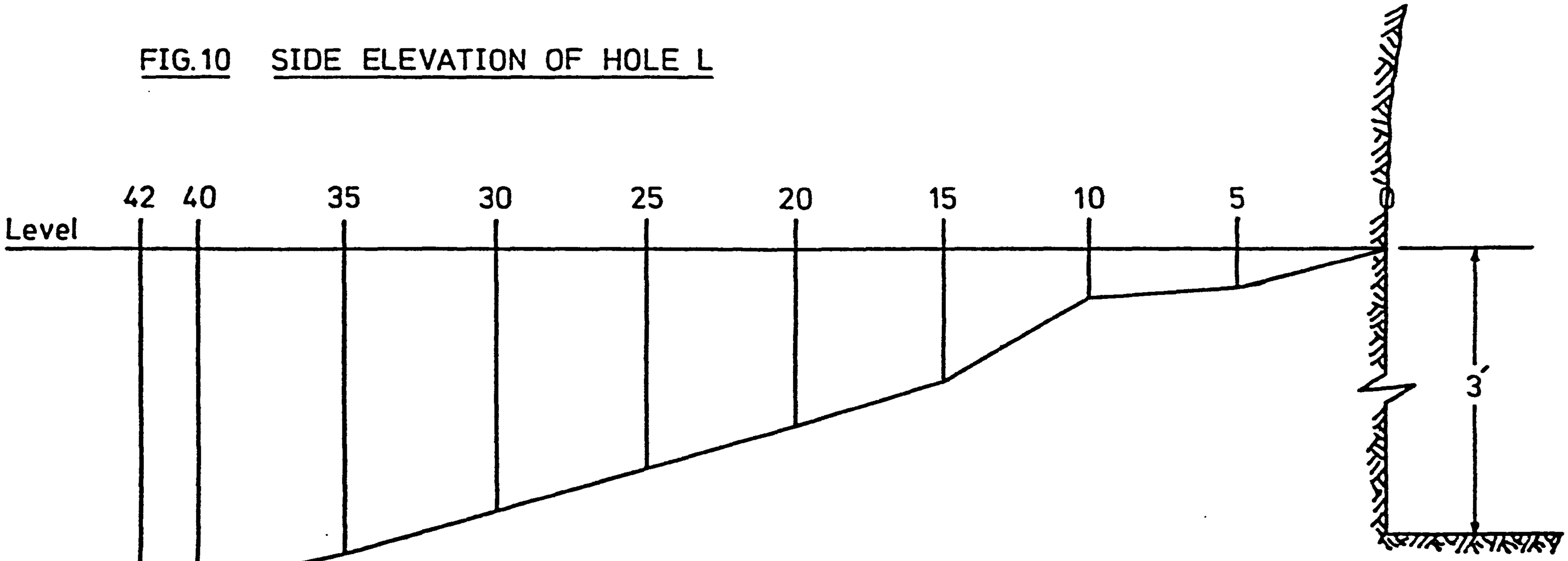

STN. (ft.)	0	5	10	15	20	25	30	35	40	42
FALL (in.)	0	0·26	0·35	0·92	1·21	1·49	1·79	2·07	2·29	2·40

FIG. 11 SIDE ELEVATION OF HOLE R

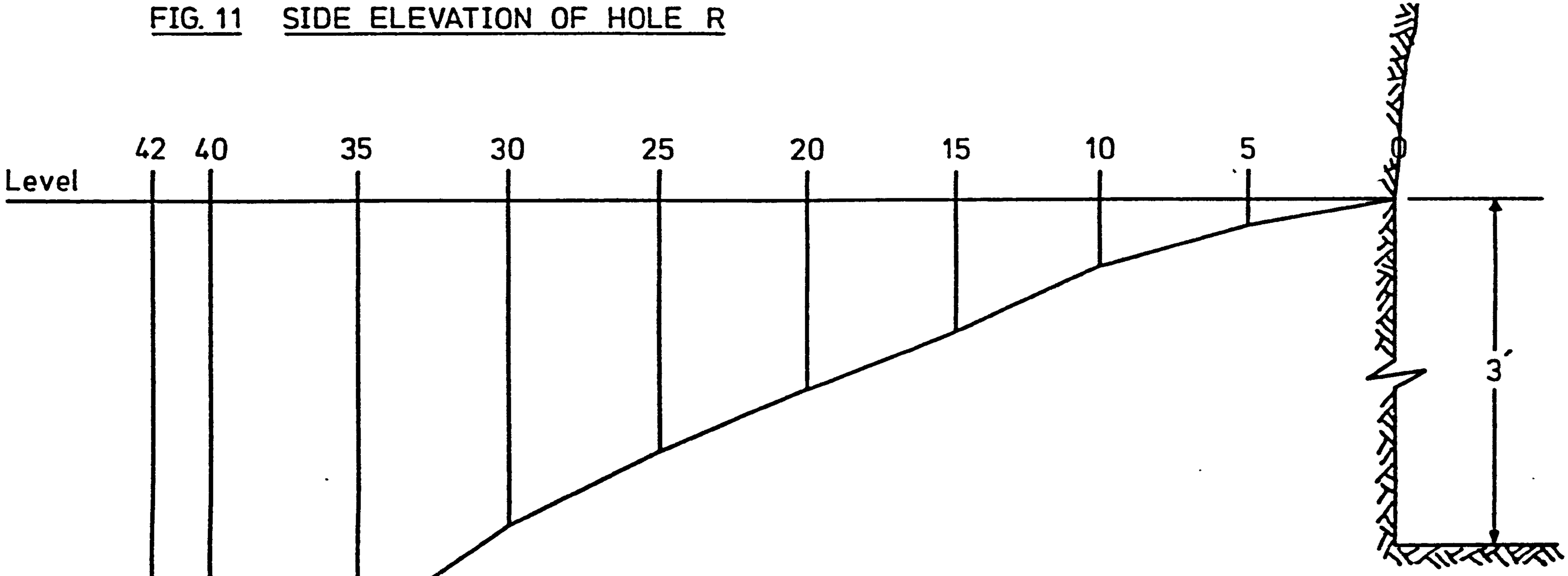

STN. (ft.)	0	5	10	15	20	25	30	35	40	42
FALL (in.)	0	0·36	0·92	1·84	2·64	3·44	4·51	5·84	6·79	6·90

FIG. 12

PLAN OF THE CENTRE LINES OF THE PILOT HOLES

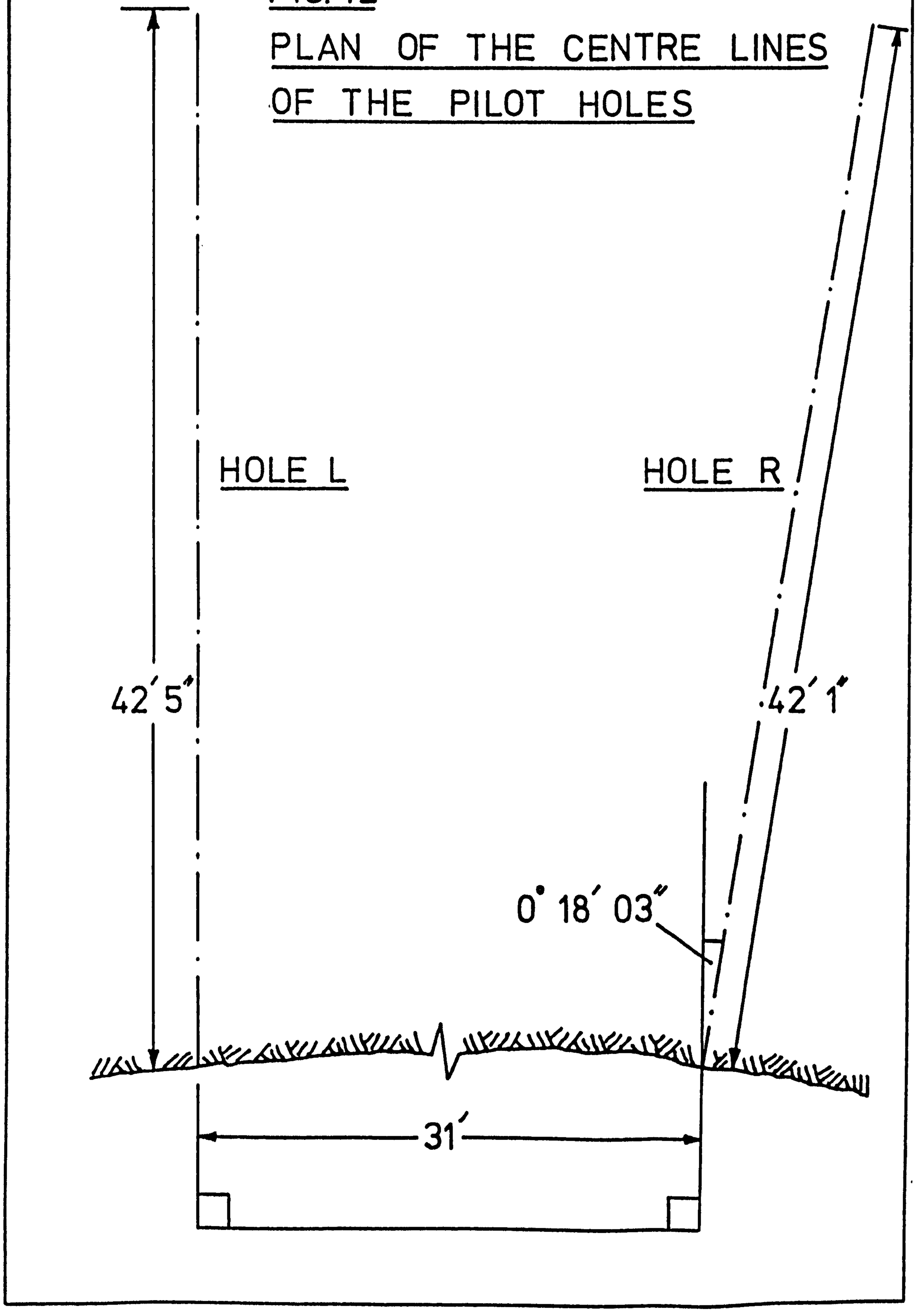

FIG.13 MOHR'S ENVELOPE

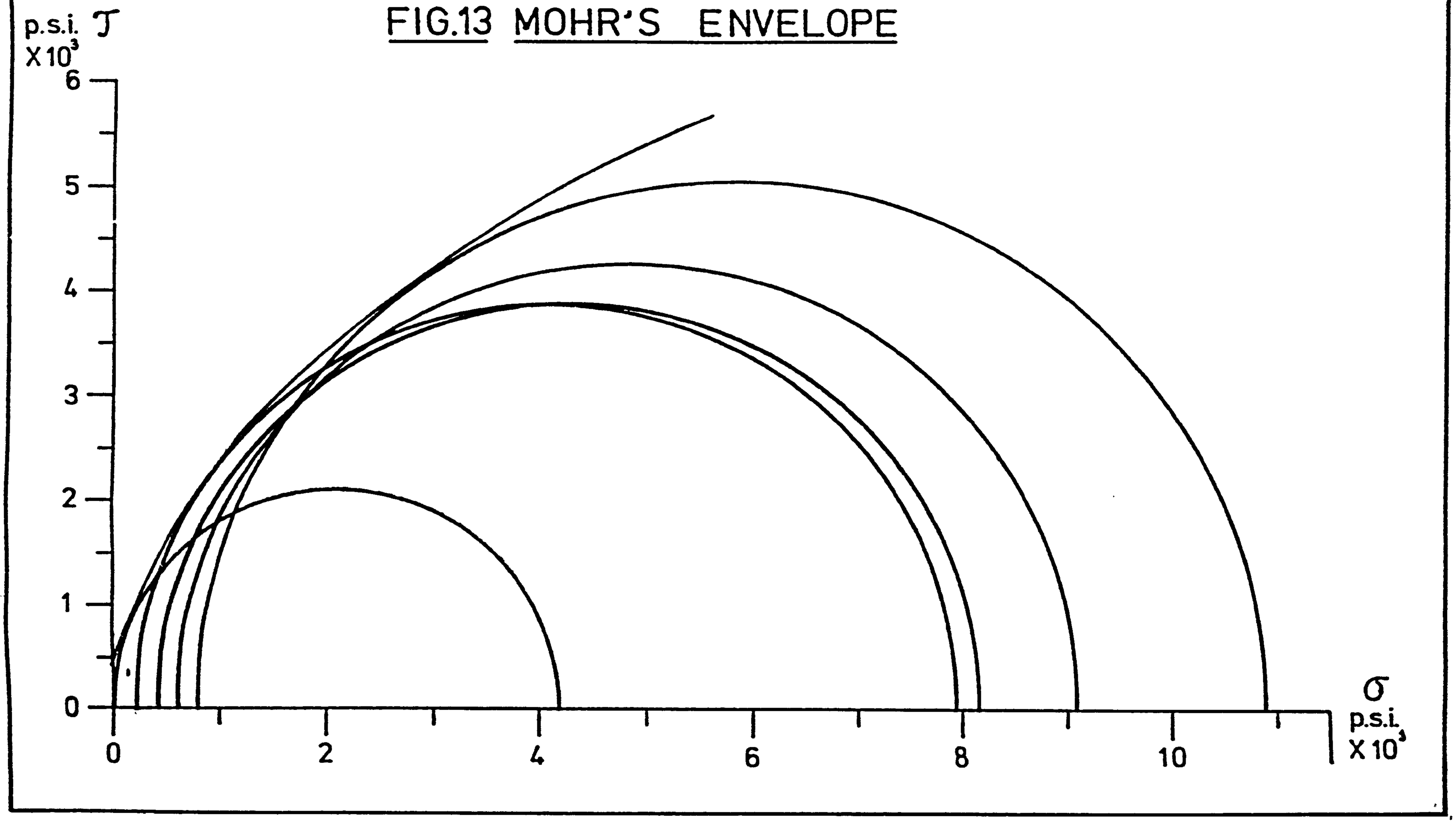

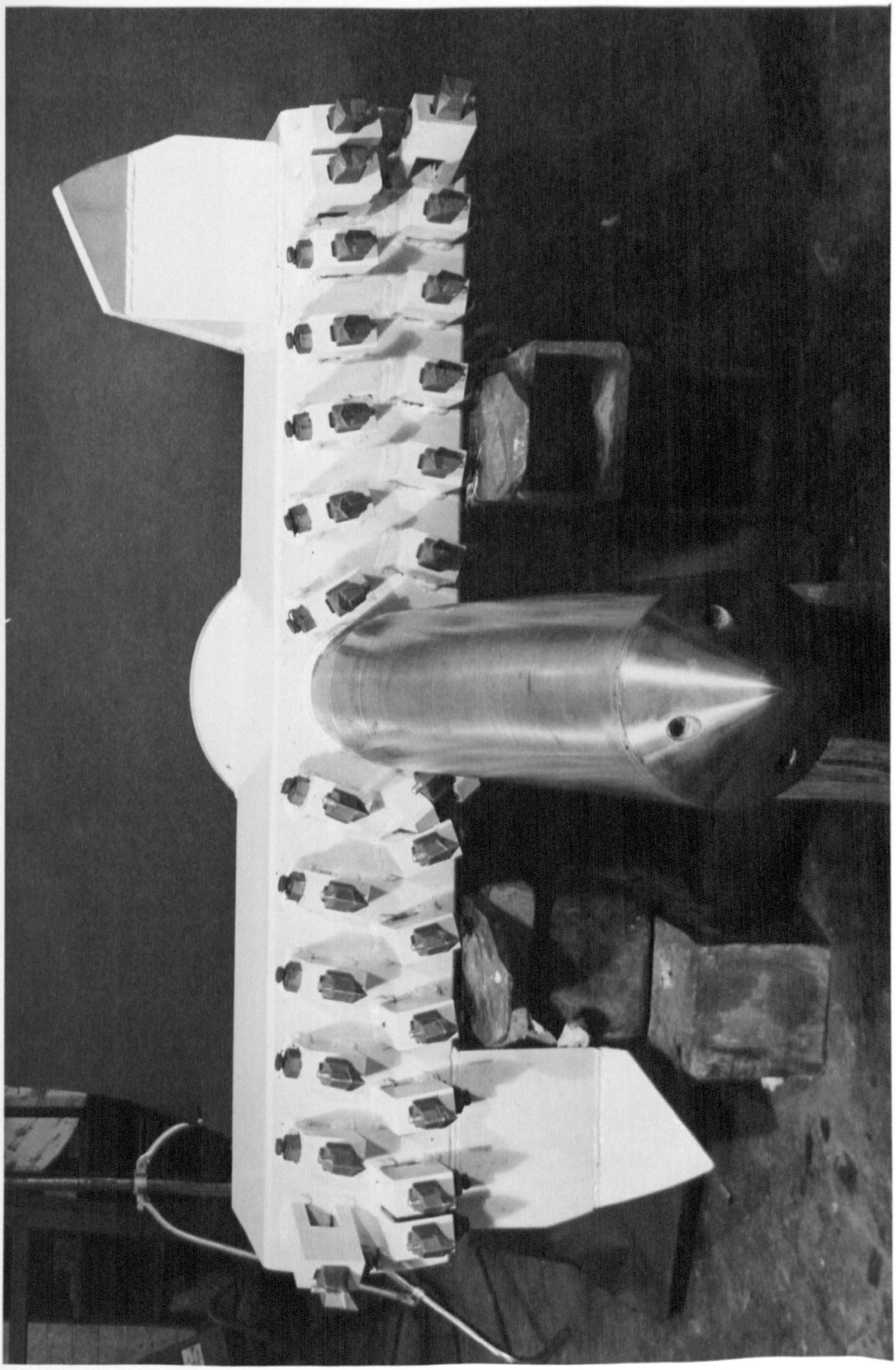

FIG. 14 THE JASON AUGER CUTTER HEAD

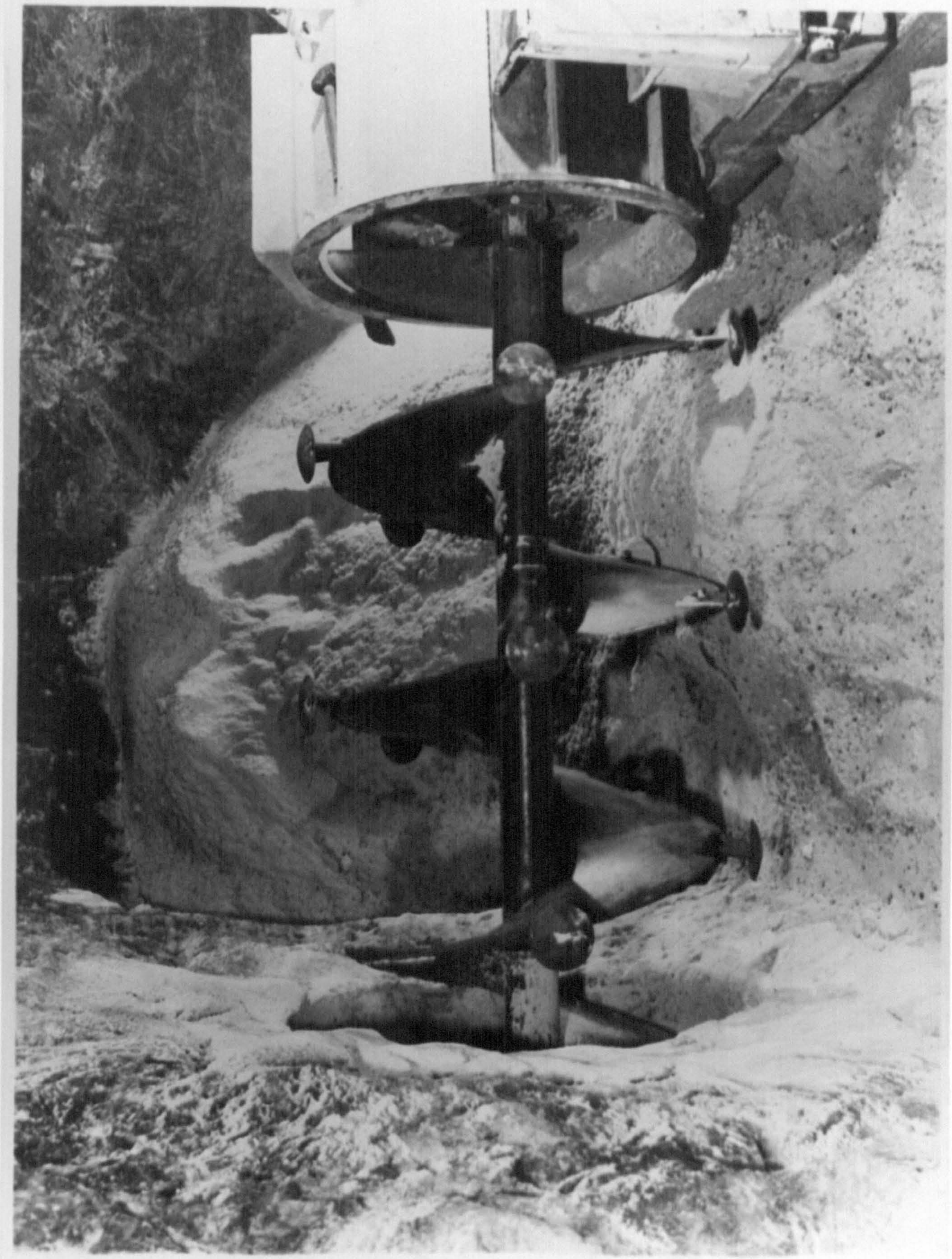

FIG. 15 THE JASON AUGER BORING CAVITY R

FIG. 16 DRILL STRING STABILISATION

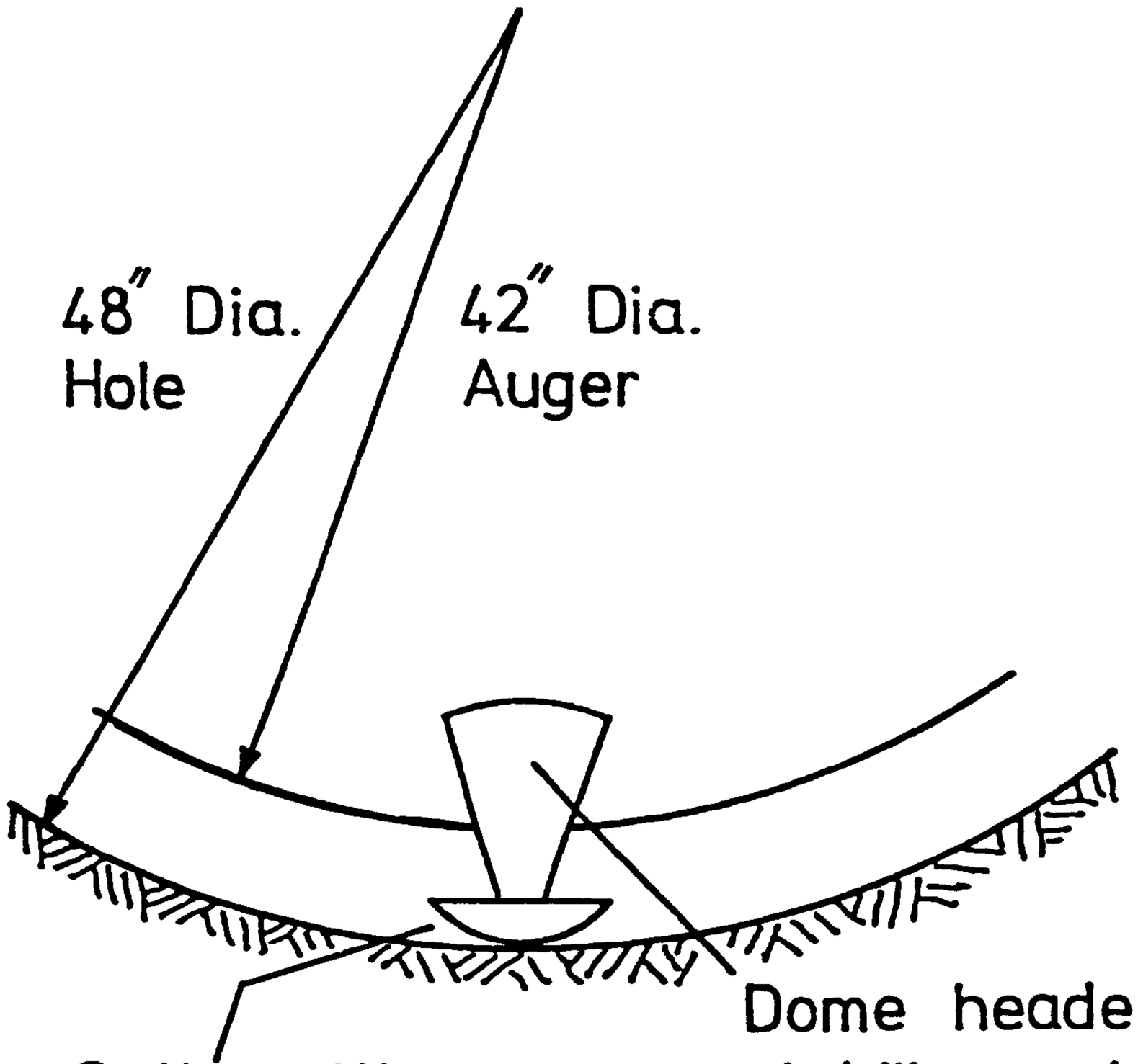

(a) Mushroom heads

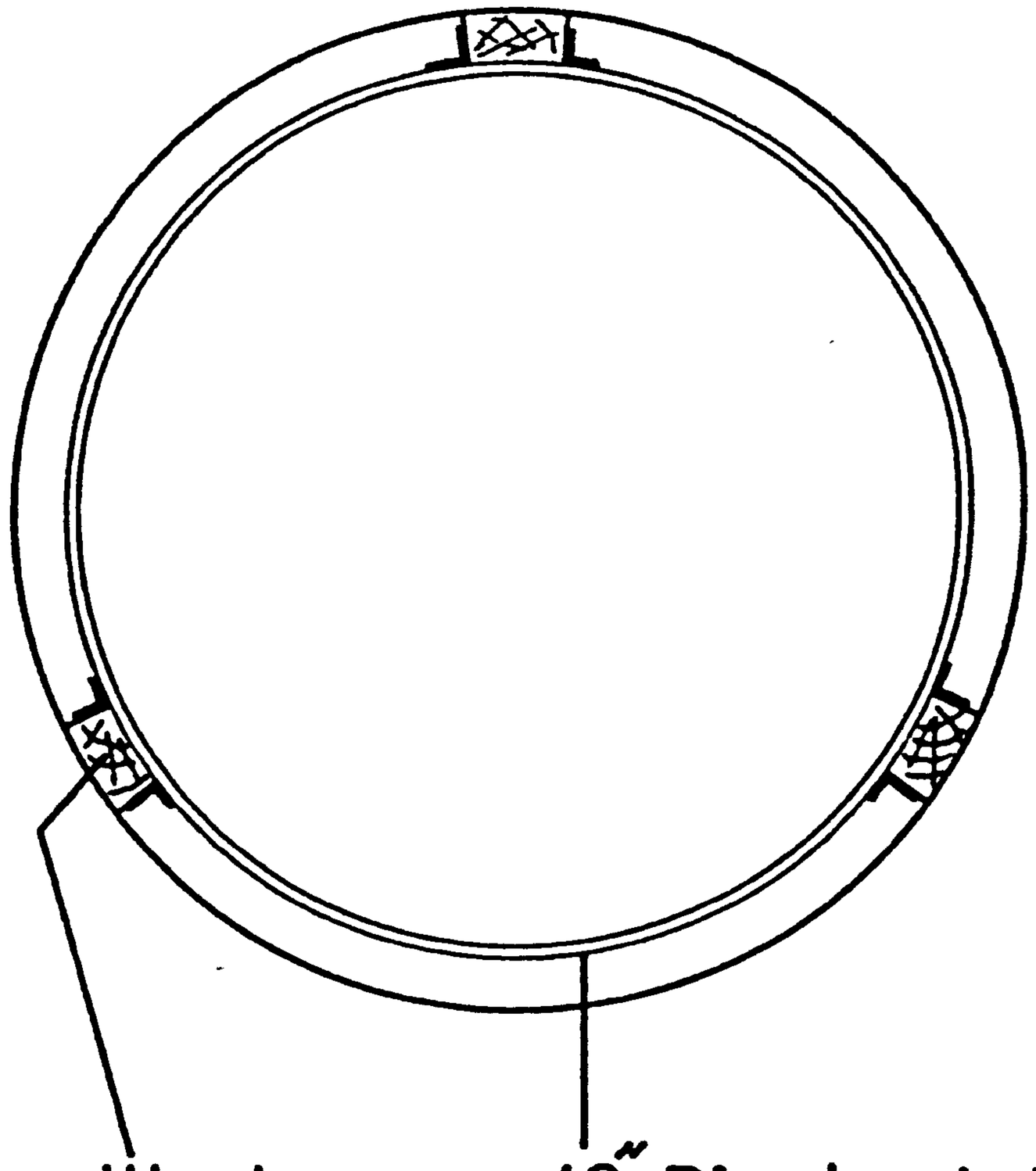

(b) Borehole liners

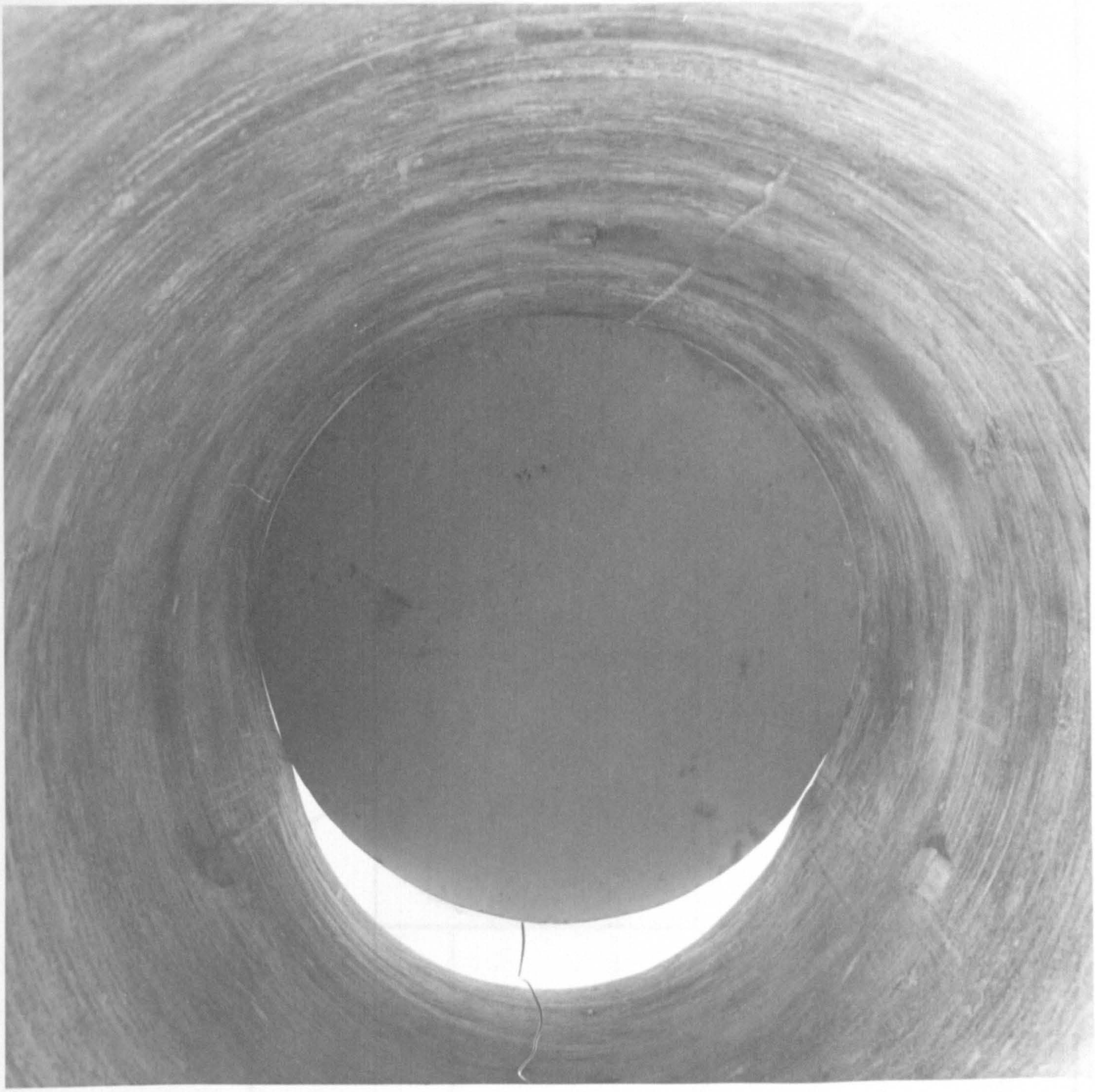

FIG. 17 INTERIOR VIEW OF CAVITY R

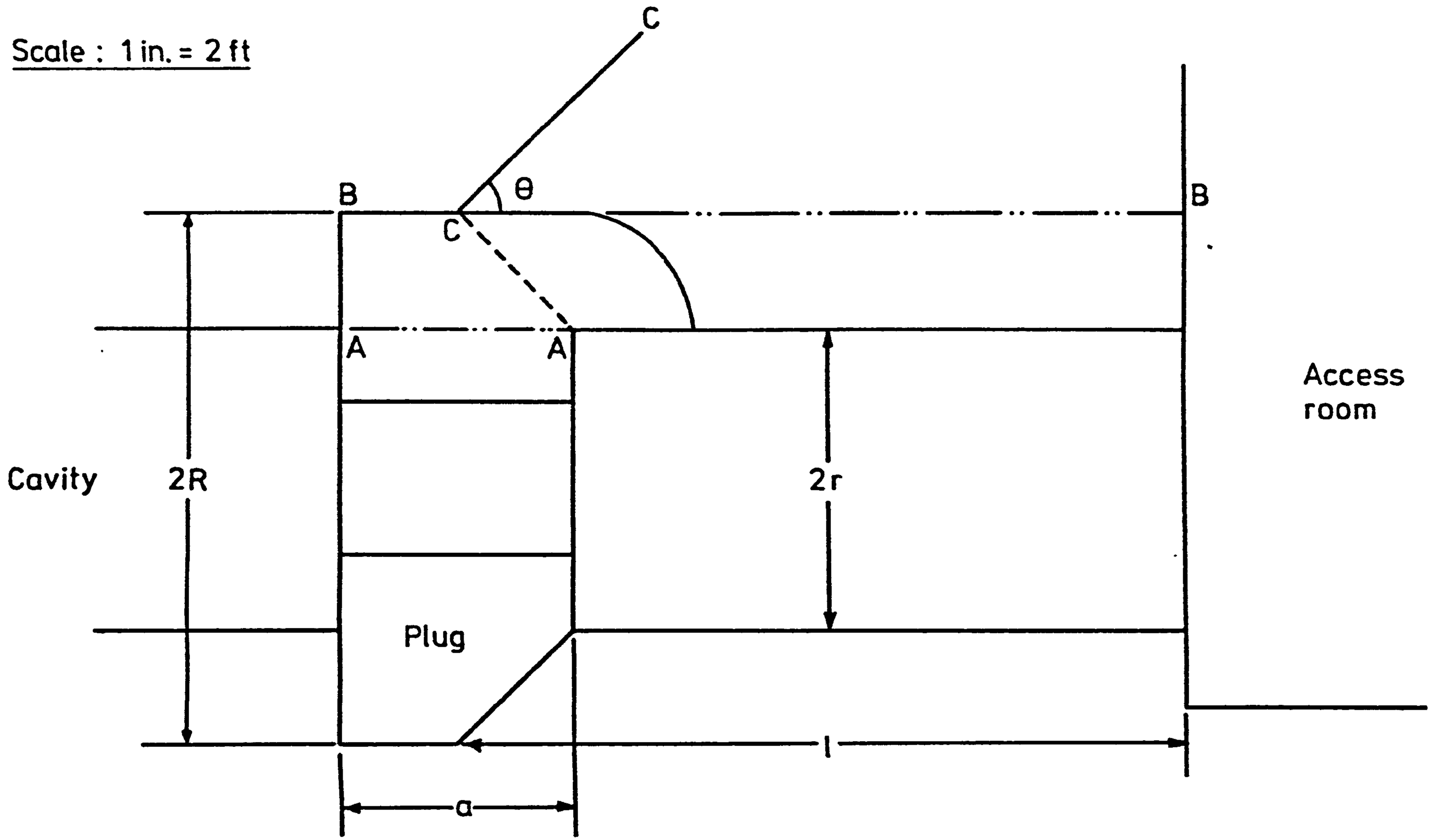

FIG. 18 LONGITUDINAL SECTION THROUGH CAVITY PLUG

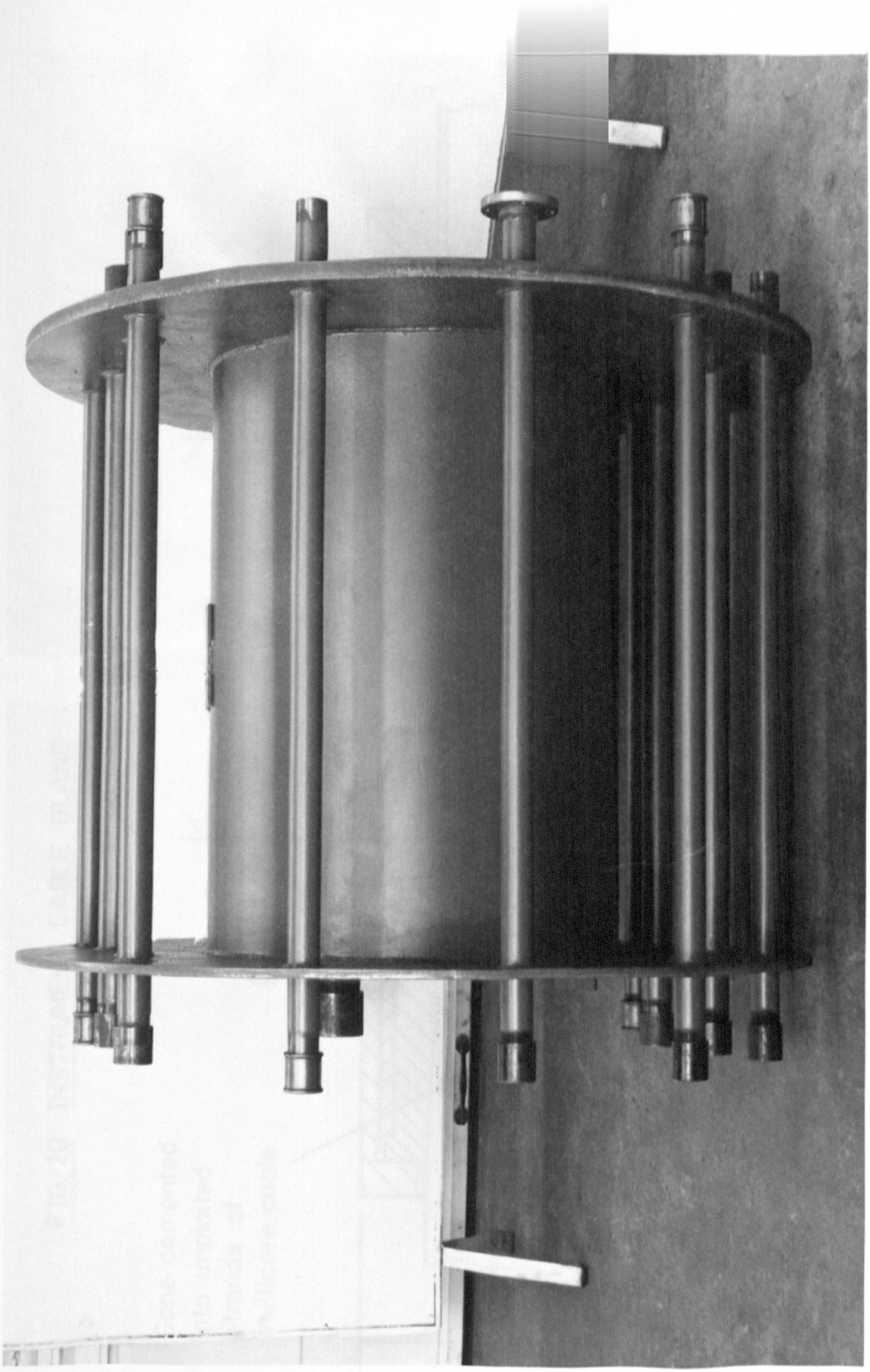

FIG. 19 PLUG REINFORCING CAGE

FIG. 20 INSTRUMENT CABLE GLAND

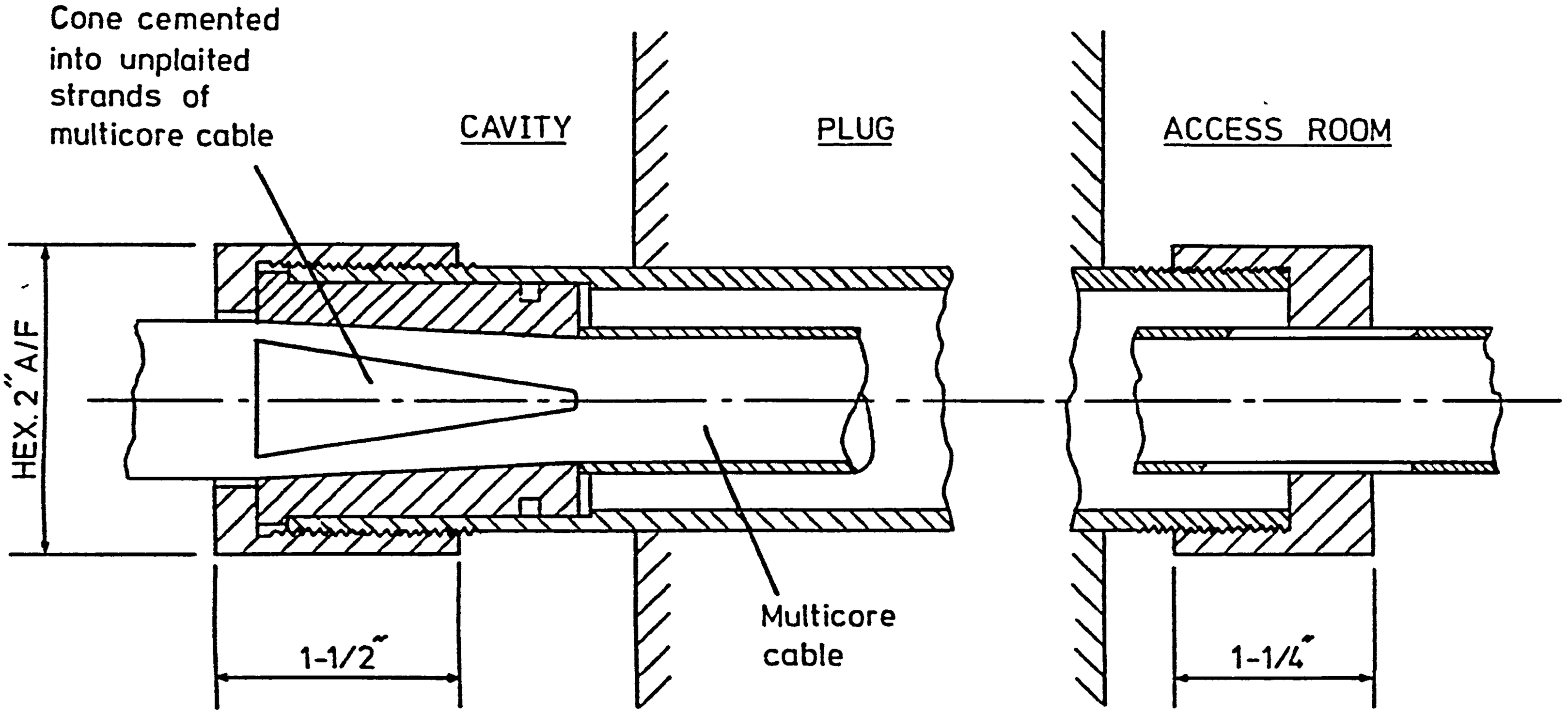

FIG. 21 GLAND ASSEMBLY PROCEDURE

FIG. 22 PLUG ANNULUS SHOWING WEDGE SHAPED EXCAVATION FOR THE INTRODUCTION OF THE CONCRETE FILL

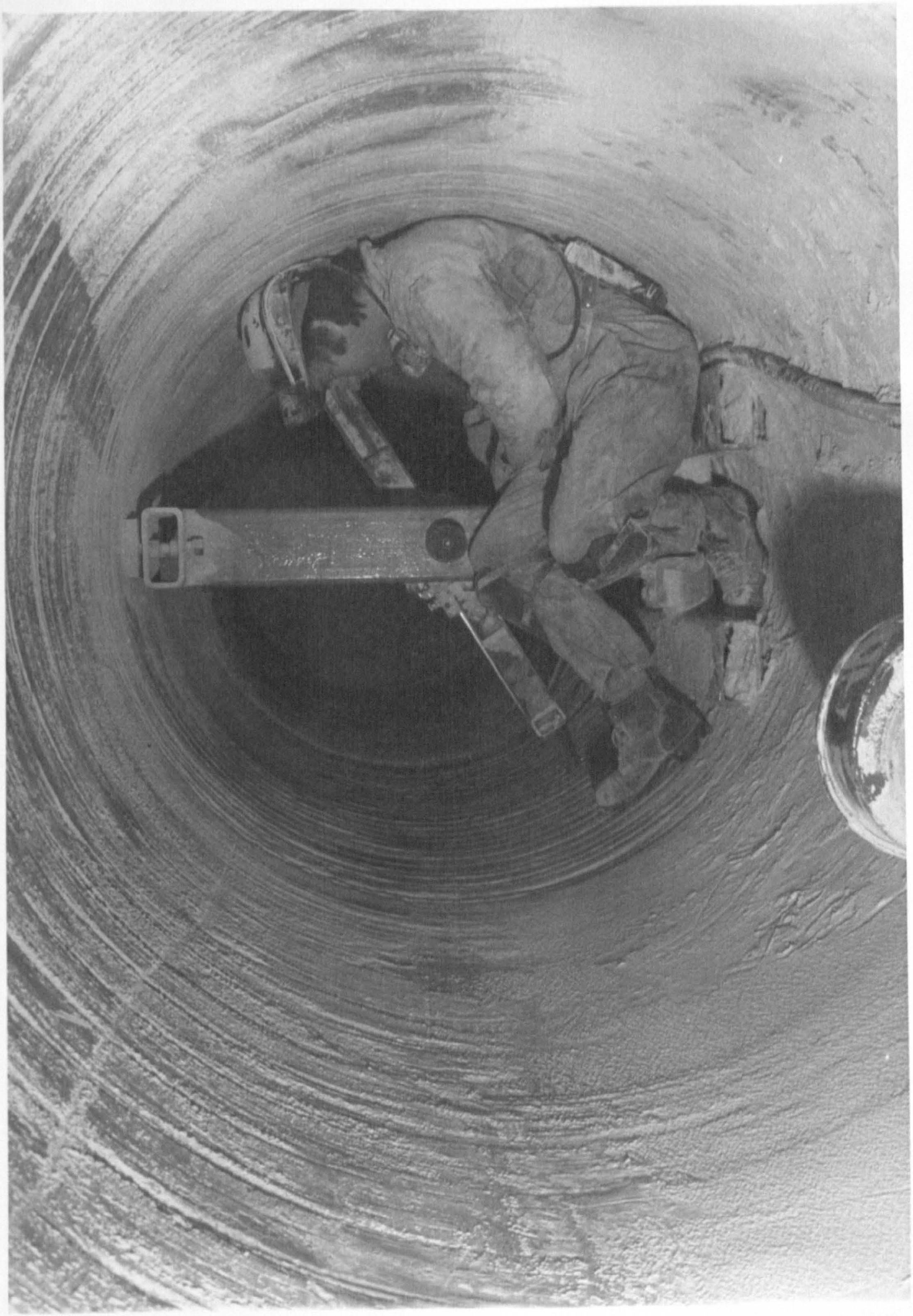

FIG. 23 DRILLING THE RADIAL BOREHOLES

CHAPTER 5

DEFORMATION MEASUREMENT

CHAPTER 5

5. DEFORMATION MEASUREMENT

5.1 Introduction

5.1.1 Requirements of the measuring system

In order to accurately determine the behaviour of rock salt under physical and thermal stress it is necessary to measure the magnitude and direction of rock movements caused by the application of pressure and temperature variations. The rock movements to be monitored may be divided into four categories:-

i) Radial deformation, measured along the nine radial boreholes. These measurements may be made with reference to either the cavity centreline or the anchors installed ten feet along the boreholes.

ii) Diametral deformation, three measurements being taken at each of the three diametral deformation stations. The positions of these stations coincide with the positions of the radial deformation stations.

iii) Longitudinal deformation measurements, to establish that the cavity deforms under plane strain conditions and no longitudinal movement takes place.

iv) Plug movement transducers, used to provide information on plug consolidation and to give prior warning od an impending plug failure.

The first three of these measurement categories require a high order of accuracy, whilst the accuracy of the plug movement measurements is not so critical.

A theoretical study of the expected behaviour of the salt mass indicated that deformations of the order of several thousands of an inch could be expected to take place in many of the tests, whilst deformations as small as 0.25×10^{-3} could be encountered in some of the less severe tests. The desired accuracy of the deformation measurements was set at 10% of lower figure, i.e. $\pm 25 \times 10^{-6}$ in. and the minimum permissable accuracy set at $\pm 10^{-4}$ in. An acceptable accuracy of $\pm 10^{-3}$ in. for plug movement measurements was arrived at after consideration of the expected plug behaviour.

5.1.2 Survey of deformation measurement techniques

The very nature of the experiment dictates that the chosen measurement system must have a remote reading facility, and this precludes any technique other than electrical. The high degree of accuracy required and the distance over which displacement was to be monitored put further constrainments on the choice of system.

Electrical transducers may work by inducing a change of resistance, inductance, capacitance or static eletric charge. They can also depend upon magnetic, piezoelectric, and many other electrical phenomena. (17). The transducer, rigidly attached to a point in the rock mass, is mechanically connected to a remote point in the rock mass, and is activated by relative movements between the two points. (18).

The survey of instruments which could be used to measure deformation in this experiment was not limited to technical considerations; the physical size of transducers and their commercial availability were closely investigated.

The study of electrical characteristics, physical size and commercial availability indicated that the linear voltage differential transformer would satisfy the basic requirements of the instrumentation scheme. An L.V.D.T. type D2/500 manufactured by R.D.P. Electronics Limited, had the physical size for a cluster of four to be assembled in the radial boreholes and provided the necessary accuracy of measurement.

5.2 Linear voltage differential transformers

5.2.1 Transducer construction and input requirements

The transducer bodies consist of thick-walled cylinders containing the transformer windings and the d.c. - a.c. - d.c. conversion components. Three windings are employed, a central primary winding with a secondary winding on each side. The two secondary windings are connected so that when the armature is in the null position, their outputs are equal and opposite in sign.

The primary winding is fed from a square wave generator powered by the 6 V d.c. supply. Any movement of the armature from the null position biases the coupling between the primary and secondary coils such that the output from one decreases whilst the output from the other secondary winding increases. This net output is demodulated into a d.c. signal which is linearally proportional to armature movement. The reverse coupling of the secondary windings generates a posative or negative output according to the direction of armature movement.

5.2.2 Variations in transducer sensitivity

Variations in the voltage supplied to the transducers gives rise to variations in transducer sensitivity. The sensitivity of a transducer may be defined as:-

$$\text{Sensitivity} = \frac{\text{Output voltage}}{\text{Deformation}}$$

Nominally the D2/500 type transducers have a sensitivity of four volts per inch of deformation when supplied with 6 V d.c., but if the supply voltage differs from 6 V, then transducer sensitivity is affected. The variation in the lengths of supply leads to transducers, and unequal numbers of transducers taking their supply from the various power lines, subjected the transducers to different levels of volt drop. This created a situation in which few transducers were being supplied with 6 V and resulted in their sensitivity being affected. For accurate deformation measurement it was necessary to measure the voltage being supplied to each transducer and then to apply a sensitivity correction factor to the transducer readings.

This correction factor was obtained by clamping the transducer in a test rig in a static temperature environment, and noting the variation in output voltage with a varying input voltage. Repetitions of this experiment, with the transducer clamped at different extensions, produced a series of straight lines when output voltage was plotted against input voltage. Such a graph is shown in Fig. 24.

The deformation of the transducer clamped in the test rig was calculated by dividing the output voltage, (when the transducer was being supplied with 6 V d.c.), by the sensitivity indicated by the maker's calibration certificate. If this deformation is known, it is possible to calculate from Fig. 24, a table of sensitivities at different supply voltages for each of the experiment repetitions. The sensitivities, (at a certain supply voltage), of each experiment repetition, were averaged, and this information used to plot a graph of sensitivity versus supply voltage. The sensitivity correction factor was calculated from the slope of this graph, shown in Fig. 25. It was found that the correction factor has the value of :-

Change in sensitivity = 0.893/volt

The correction factor may be positive or negative depending upon whether the supply variation takes the transducer input voltage above or below 6 V d.c.

5.2.3 Transducer temperature variations

Almost all the effects of temperature on the deformation measuring system may be calculated; the materials used in the construction and their temperature coefficients are known. The only exception is the effect of temperature upon the transducers. As it is proposed to vary the temperature of the experimental cavity it was necessary to investigate the effects of temperature on transducer performance.

This investigation was conducted by clamping the transducer in a test rig and allowing the transducer body and armature to expand due to temperature variations. The test rig was constructed such that the transducer body and armature expanded, in different directions, as they would under actual test conditions in the experimental cavity. The supply to the transducers was kept constant at 6V d.c.

The test rig was immersed in a parraffin bath placed in a thermostatically controlled oven and a temperature monitoring thermistor taped to the body of the transducer. The temperature of the bath was reduced to approximately -15°C by means of solid carbon dioxide and then allowed to slowly rise. The transducer output was measured every 5°C from -10°C to +35°C and a graph of temperature versus transducer output was plotted. This procedure was repeated to check the accuracy of the test rig and measuring systems.

The graph of temperature/transducer output, shown in Fig. 26, suggests that the relationship is non-linear but the degree of non-linearity, when converted to apparent deformation, is less than the accuracy of the measurement system. For the purposes of this investigation, the relationship may be regarded as linear, the slope of the straight line indicating the value of the temperature correction factor expressed in millivolts per degree centigrade. The division of this correction factor, -0.289 mV/°C, by the sensitivities of the individual transducers gives a correction factor, expressed in unit length per degree centigrade, for each transducer. Repetitions of the experiment at different armature positions indicated that the temperature correction factor was independent of armature position.

5.3 Radial deformation transducers

5.3.1 Introduction

The measurement of radial deformation was made along the eleven foot boreholes shown in Fig. 5 and Fig. 6 of Chapter 3. A theoretical consideration of the stresses imposed upon the cavity indicated that a point ten feet away from the cavity surface would remain unaffected by the imposed stresses. It was decided, from this theoretical study, to measure the deformation between the cavity surface and four points along each borehole. These points were nine inches, two feet, four feet and ten feet up the boreholes. The deformations between these points and the cavity surface were later converted to give the deformation between the stable ten foot point and the other four points, one of which being the cavity surface.

It was therefore necessary to design an instrumentation scheme whereby the transducers could be installed in a frame at the mouth of the borehole and their armatures connected, by means of extension rods, to some form of anchor gripping the rock at certain points up the radial boreholes.

5.3.2 Anchor design

The design of an anchor to rigidly connect the transducer armature extension rods to a predetermined point in the rock mass must satisfy the following requirements:-

i) It must have the capability of being accurately set at pre-determined points along the borehole

ii) The anchor must allow the extension rods and thermistor cables of anchors further along the borehole to pass through it for termination at the borehole mouth.

iii) The anchor must firmly and rigidly grip the borehole and continue to do so for several years after installation.

The design for such an anchor may be seen in Fig. 27, and is shown attached to the end of the insertion tube. The installation procedure is quite complex, but may be explained briefly as follows.

The first anchor is bolted to the end of a length of the insertion tube by means of a socket screw B (Fig. 27) with the transducer extension rod and thermistor cables passing through the centre of the tube. This assembly is pushed up the hole and further lengths of insertion tube and transducer extension rod added. The procedure is repeated until the required length of extension tubing is in place. The last length of extension tube has a flange at the bottom which, when bolted to the borehole mouthplate, accurately locates the anchor.

The anchor is set by passing a rod, terminating in a hexagonal section bar, up the middle of the insertion tubes, through the centre of socket screw B, to connect with socket screw A. When this socket screw is tightened, the cone of the anchor is drawn into the cup, thus causing the split ring to expand and tightly grip the borehole. This

tightening rod is removed and replaced with one to fit socket screw B which is unscrewed to release the anchor from the insertion tubes. The other three anchors are installed in a similar manner, with the transducer extension rods and thermistor wires of previously installed anchors passing through the anchor and insertion tubes. A general view of anchors, push rods and transducers is shown in Fig. 28, whilst Fig. 29 shows a close-up of the push rod-transducer armature connection.

This installation procedure is shown in the series of photographs, Figs. 30, 31 and 32. The insertion tubes shown together with the tightening rods in Fig. 33, are made in such lengths that they can be built up to the length required to instal an anchor in any one of the four positions.

5.3.3 Radial borehole mouth assembly

The first six inches of the 1 15/16 in. diameter boreholes were overbored to a diameter of 2 5/16 in., this enlargement being used to accommodate the cluster of four transducers. The transducers were supported and accurately located by a framework connected to the borehole mouth plate. The mouth plate, with its inner surface machined to match the cavity radius, was attached to the area surrounding the mouth of the borehole by means of a cement. A series of tests indicated that "Devcon Plastic Steel" was the most suitable adhesive for this purpose.

The presence of high pressure air in the instrument boreholes would complicate the stress fields around the cavity. Therefore it was necessary to ensure that these boreholes be maintained at atmospheric pressure. This was achieved by connecting vent pipes from the borehole cover plates to the outside face of the plug.

Compressed air was denied access to the boreholes by fitting the mouth plate with a pressure tight borehole end cover. Fig. 34 shows the borehole mouth plate with vent pipes and transducer assembly.

5.4 Diametral and longitudinal transducer design

5.4.1 Introduction

Diametral and longitudinal deformation measurements were made with basically the same instrument, shown in Fig. 35., thus allowing for simplicity in design and manufacture, and providing data logging compatibility. In addition, the same type of transducer employed in radial deformation measurements was utilised, simplifying the problem of spare parts and replacements in the event of instrument malfunction.

The instruments were constructed by mounting a transducer in a duralumin tube and connecting the transducer armature to a spring loaded extension rod. Centralisation and freedom of movement of the extension rod was assured by PTFE bushes fitted inside the duralumin tube. This extension rod was constructed from invar in order to minimise temperature effects. Provision was made for approximate mechanical nulling of the instruments by a screwed extension rod at one end of the duralumin tube. The extreme ends of the instruments were fitted with ball bearings which mated with dimples machined into the extensometer housing brackets.

5.4.2 Diametral deformation measurements

The extensometers described in the previous section were used to measure diametral deformation at the measuring stations discussed in Section 3.2.2. The measurements were made between the radial borehole end covers and a bearing plate cemented to the cavity wall. The power supply and signal leads to the extensometers were of such a length that the extensometers could be removed from their measuring position and stored in racks bolted to the heat exchanger pipework. This was arranged to allow access to further points along the cavity for removal of camera film and for instrumentation checks and repairs.

5.4.3 Longitudinal deformation measurements

For the reasons given in Section 5.4.1 the longitudinal extensometers were of the same basic design as those measuring diametral deformation. These instruments were used to measure the relative movement between two pegs set, four feet apart, into the cavity walls. The pegs, $\frac{3}{8}$ in. in diameter and 3 in. long, were set $1\frac{1}{2}$ in. into the rock and cemented in position with an adhesive. A flat face, machined into the uppermost half inch of the pegs, had a dimple which mated with the ball bearings on the ends of the extensometers.

5.5 Plug movement monitoring scheme

Although the pressure retaining plug was designed to a high factor of safety there still existed the remote possibility of a catastrophic plug failure. In view of the physical behaviour of rock salt, it was though that such a failure would not be instantaneous, and that the failure would be preceded by a slow but rapidly increasing plug movement. If this proved to be true, then it would be advantageous to have some prior warning of a plug failure. If on the other hand a plug failure proved to be an almost instantaneous event, then this would result in severe damage to most of the instrumentation scheme.

Desirable features of a plug movement monitoring scheme include both a continuous plot of plug position and an "excessive movement alarm", audible above the ambient noise level created by the experiment plant and ventilation system. The plug movement transducers were identical in all respects to the longitudinal extensometers, with one end bearing on a peg set into the rock and the other on the inner face of the plug. The output from these three instruments, arrayed in the normal pattern of one along the roof and two each displaced by 120°, was fed to both a chart recorder and an alarm system. The chart recorder, as well as indicating plug movement, also gave plots of relevant information such as cavity temperature and pressure. The alarm system included a red warning light and an audible alarm.

In the event of an alarm being sounded the chart recorder could be used to confirm an alarm condition and not alarm malfunction. The pressure in the cavity could then be rapidly dropped by means of a 6 in. diameter blowdown valve, and all the plant electrically isolated by means of two master switches. This work could be completed within a matter of seconds of the alarm sounding. The plug monitoring and alarm system was designed to minimise installation damage, not to prevent it occurring. The rapid dumping of pressure from the cavity, dropping the pressure from perhaps 200 psi to zero in a short space of time, would result in such severe temperature drops that the cavity surface would undoubtedly suffer damage.

FIG. 24 TRANSDUCER OUTPUT FOR A VARYING SUPPLY VOLTAGE

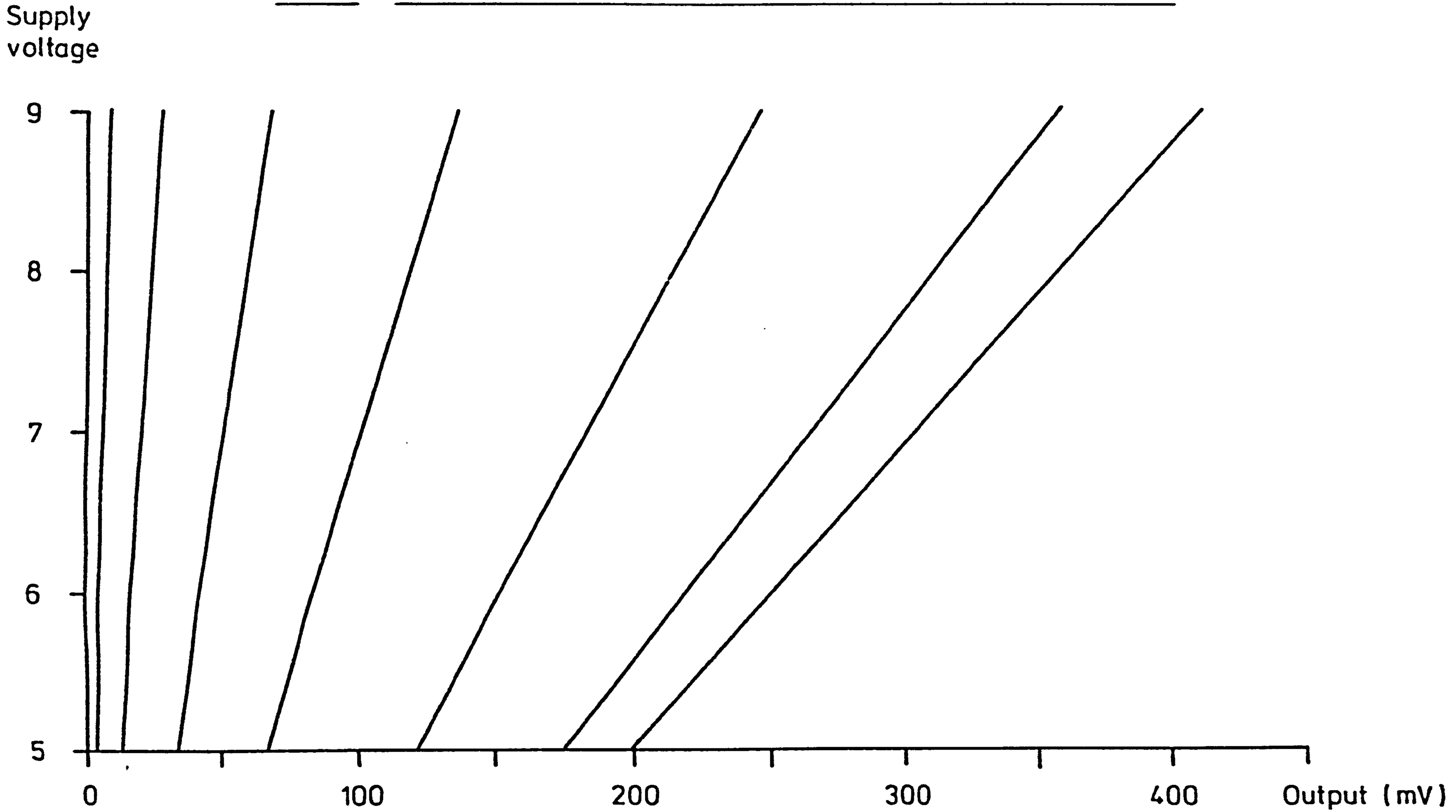

FIG. 25 TRANSDUCER SENSITIVITY VERSUS SUPPLY VOLTAGE

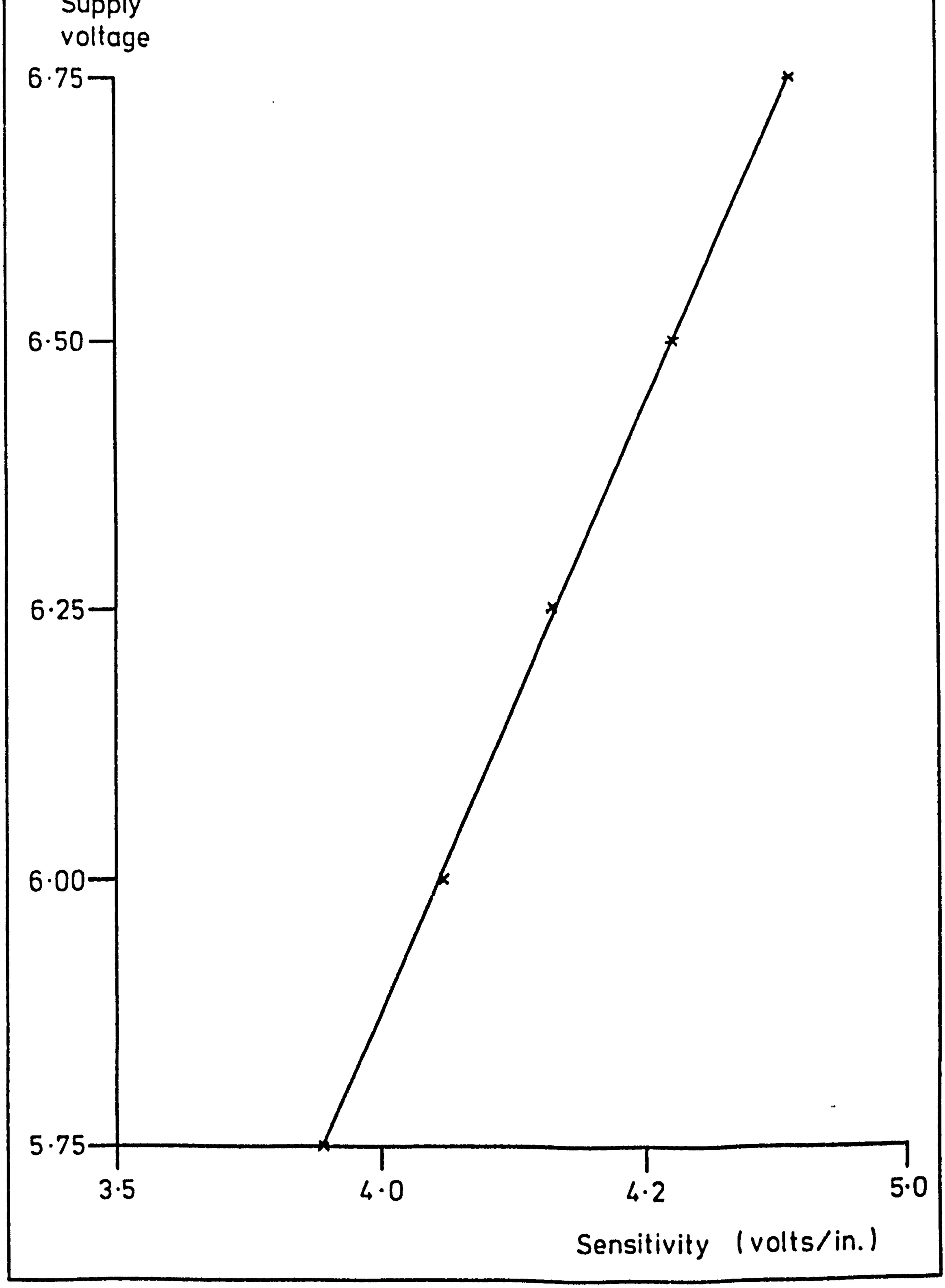

FIG. 26 TRANSDUCER TEMPERATURE / TRANSDUCER OUTPUT

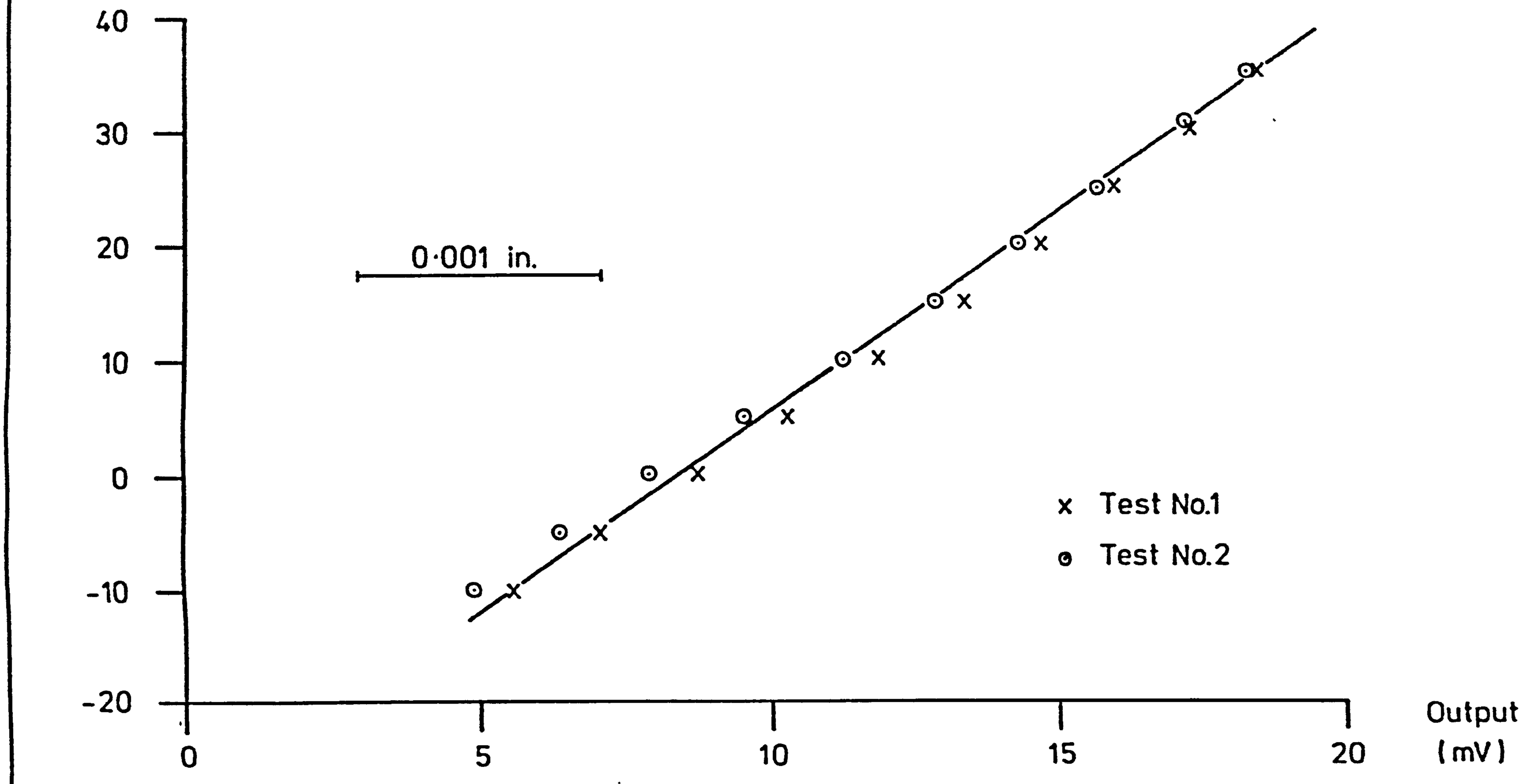

FIG. 27 ANCHOR ATTACHED TO INSERTION TUBE

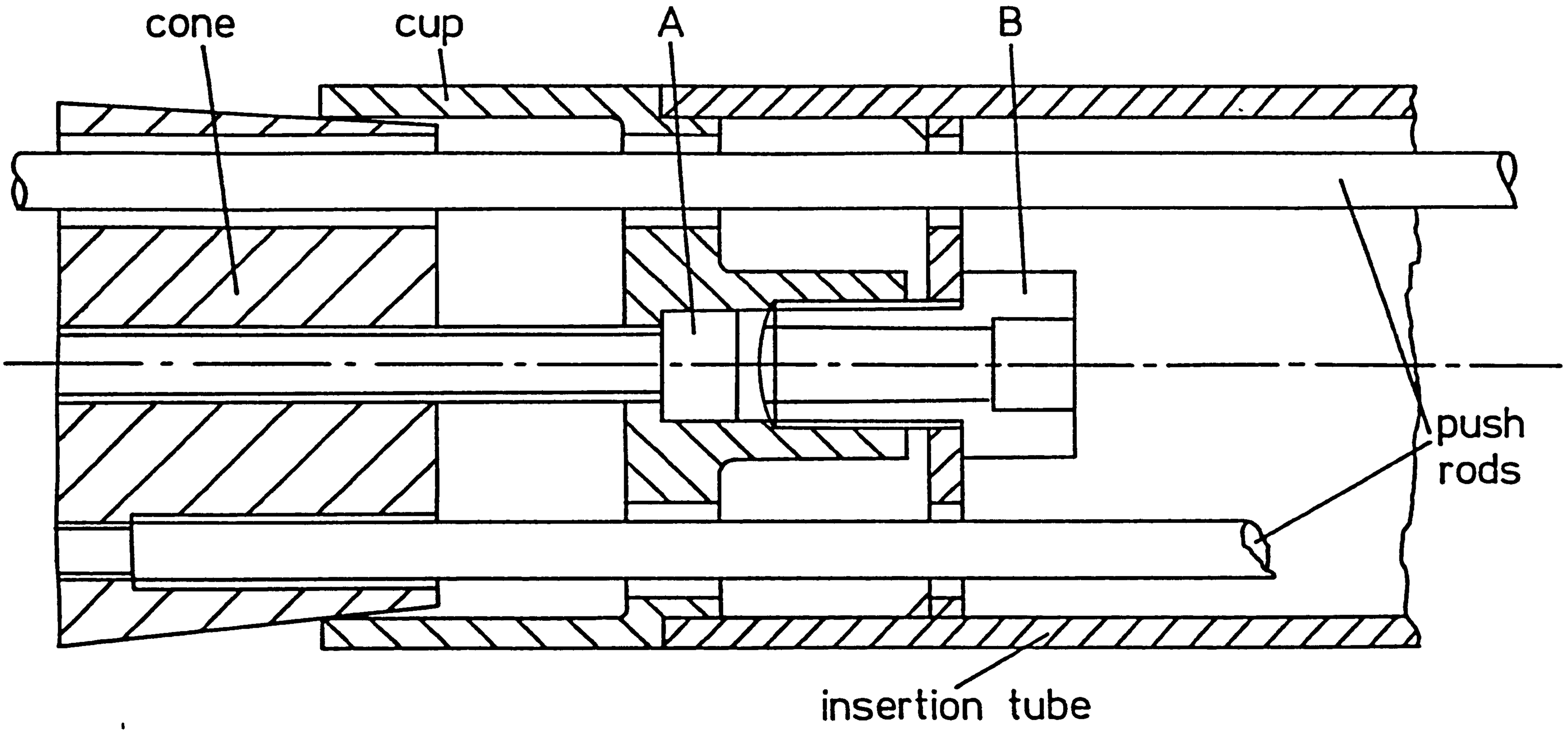

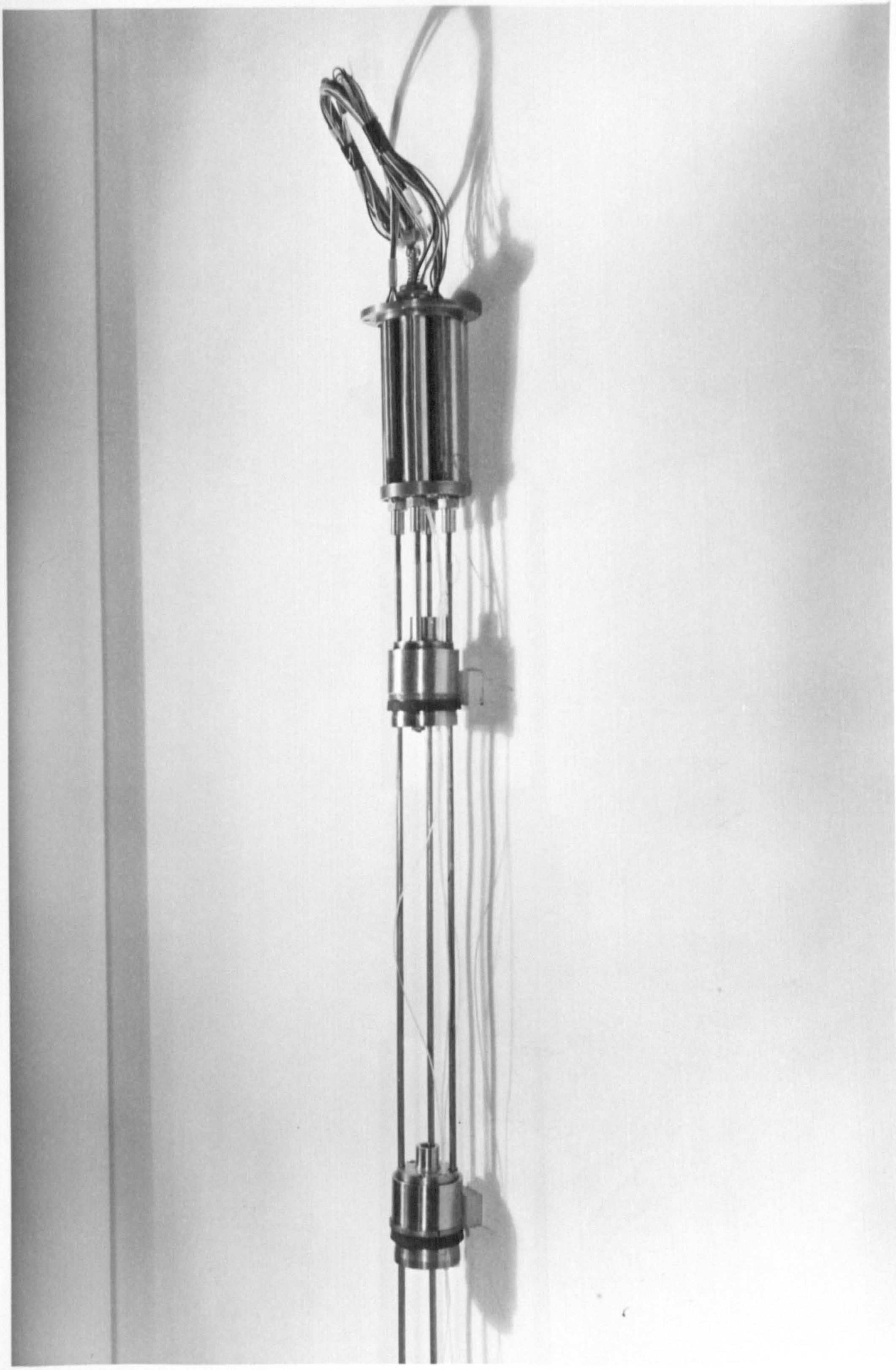

FIG. 28 ANCHOR, PUSH ROD AND TRANSDUCER ASSEMBLY

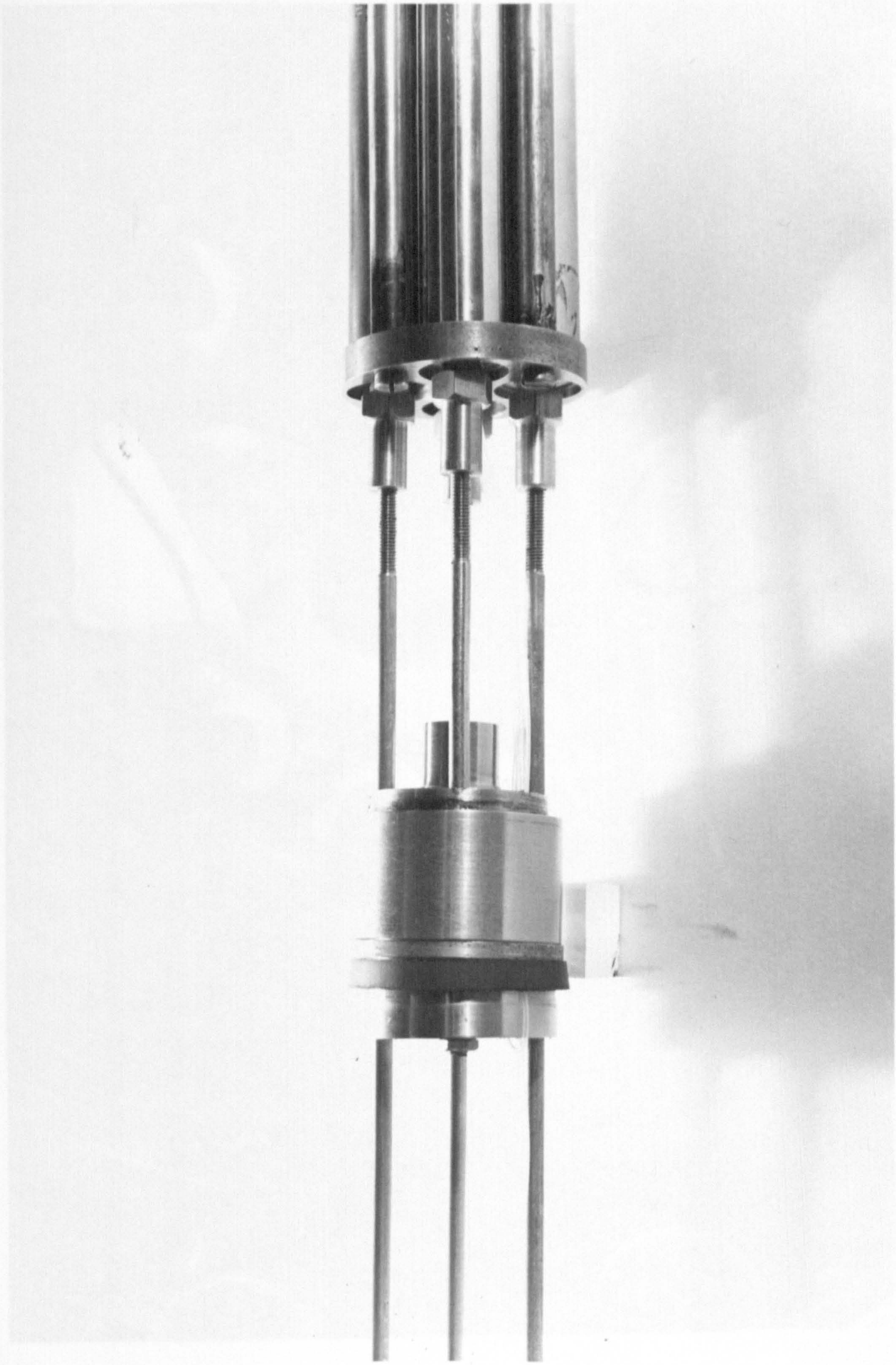

FIG. 29 CLOSE UP OF ANCHOR SHOWING PUSH ROD TO TRANSDUCER ARMATURE CONNECTION

FIG. 30 INSERTION OF ANCHOR NO. 3

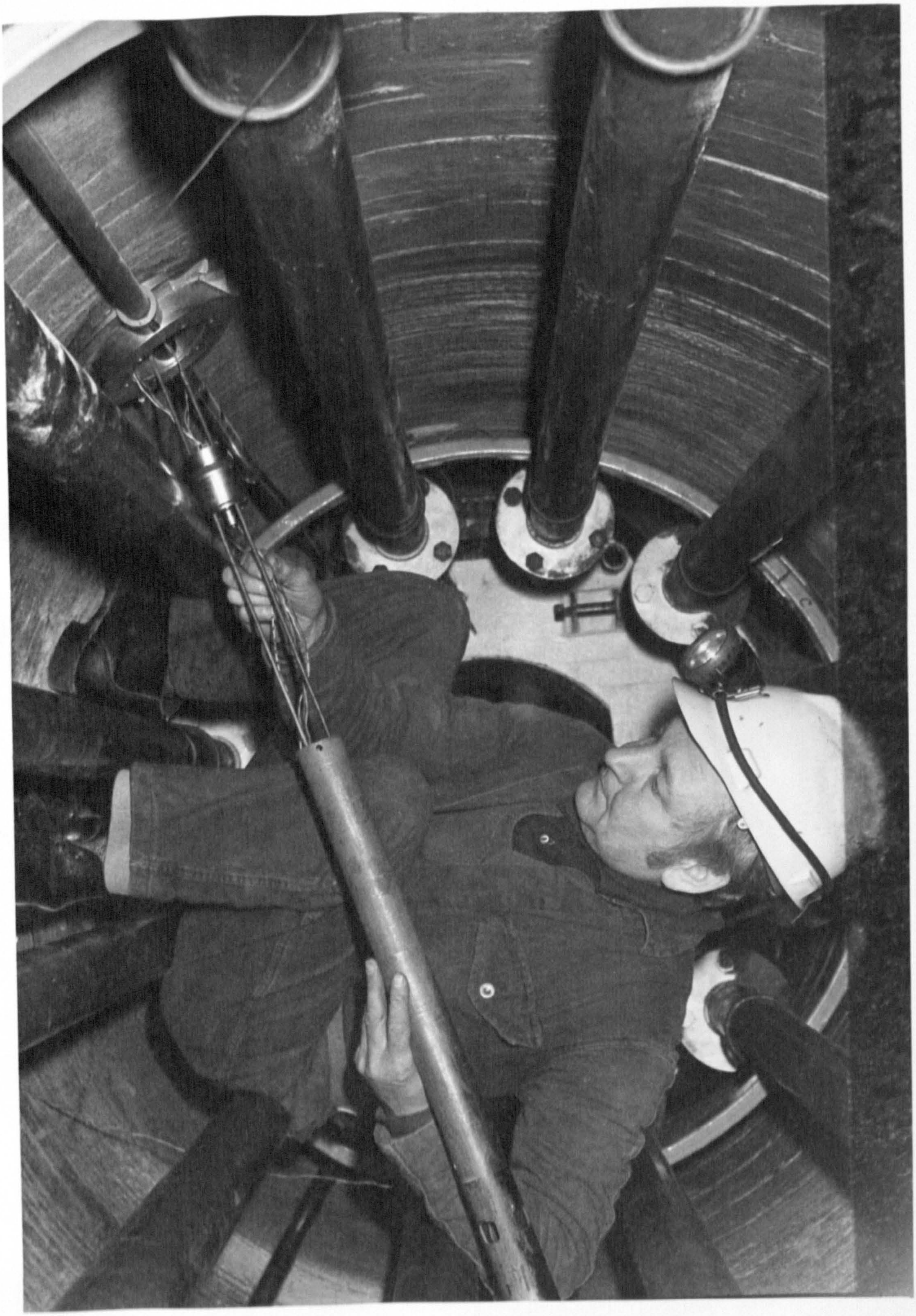

FIG. 31 INSERTION TUBE BEING PUSHED ALONG THE BOREHOLE

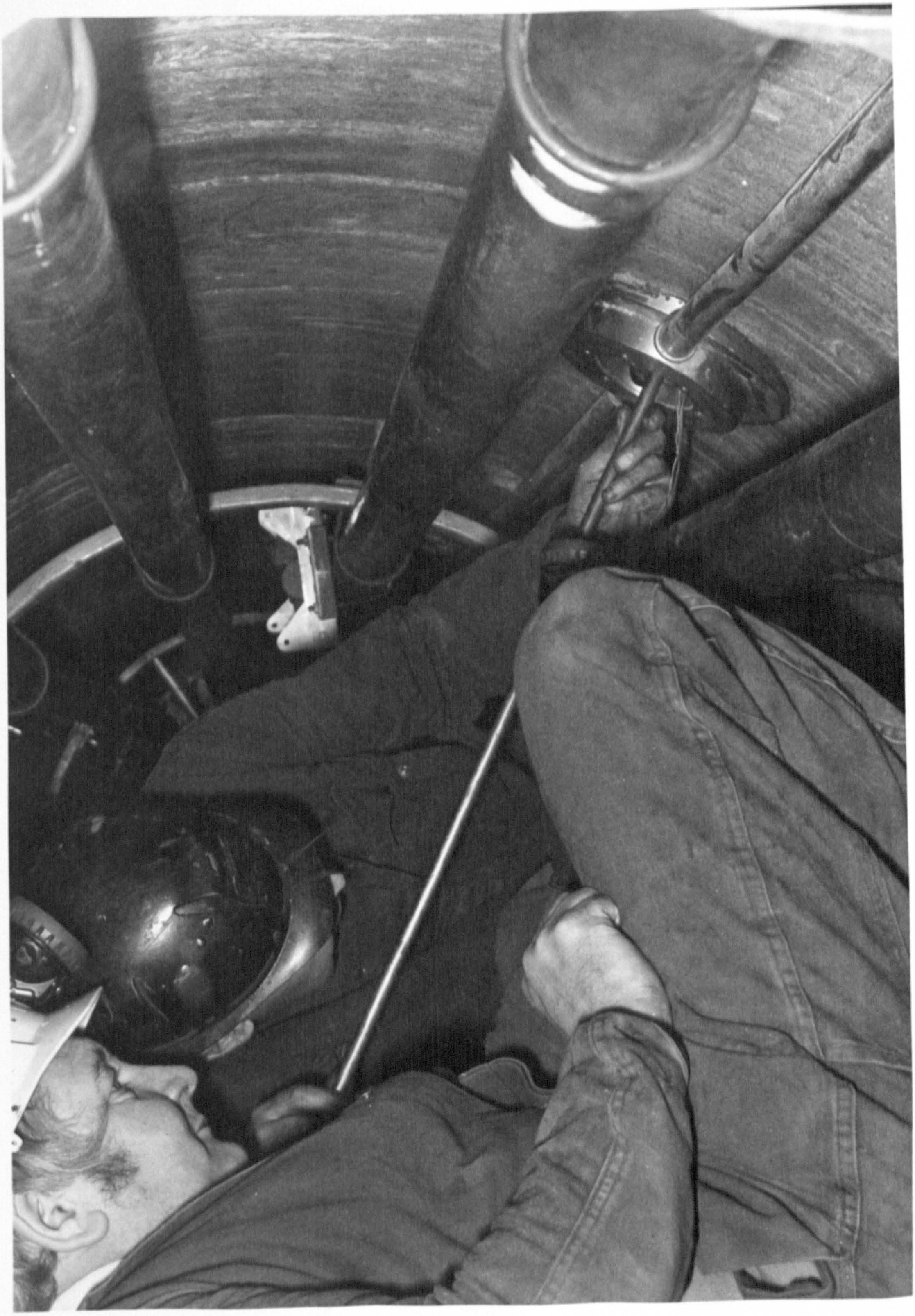

FIG 32 TIGHTENING AN ANCHOR

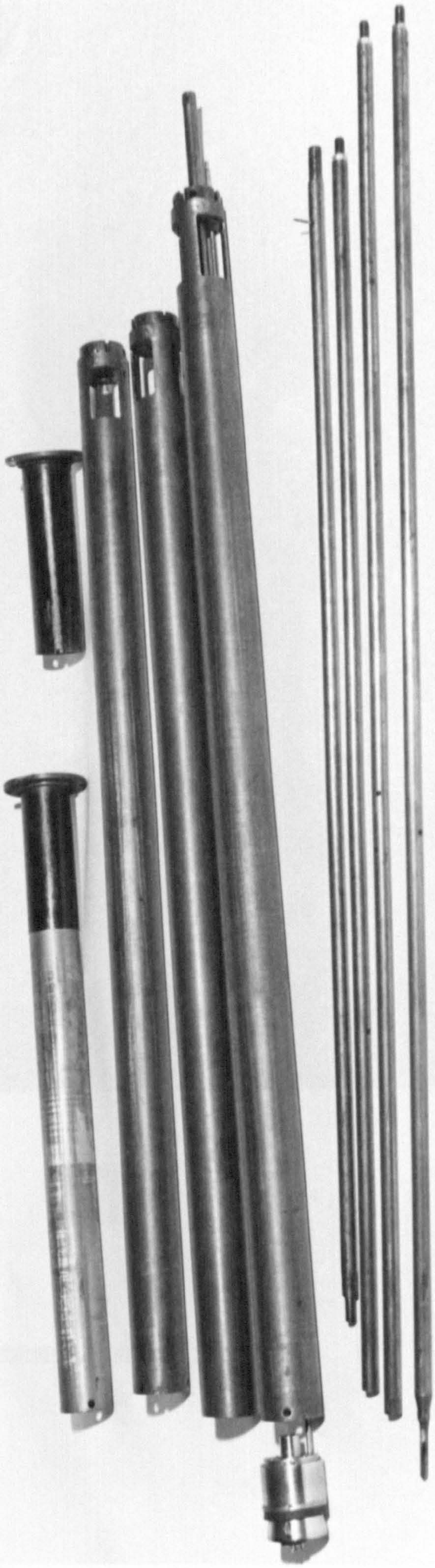

FIG. 33 ANCHOR INSERTION TOOLS

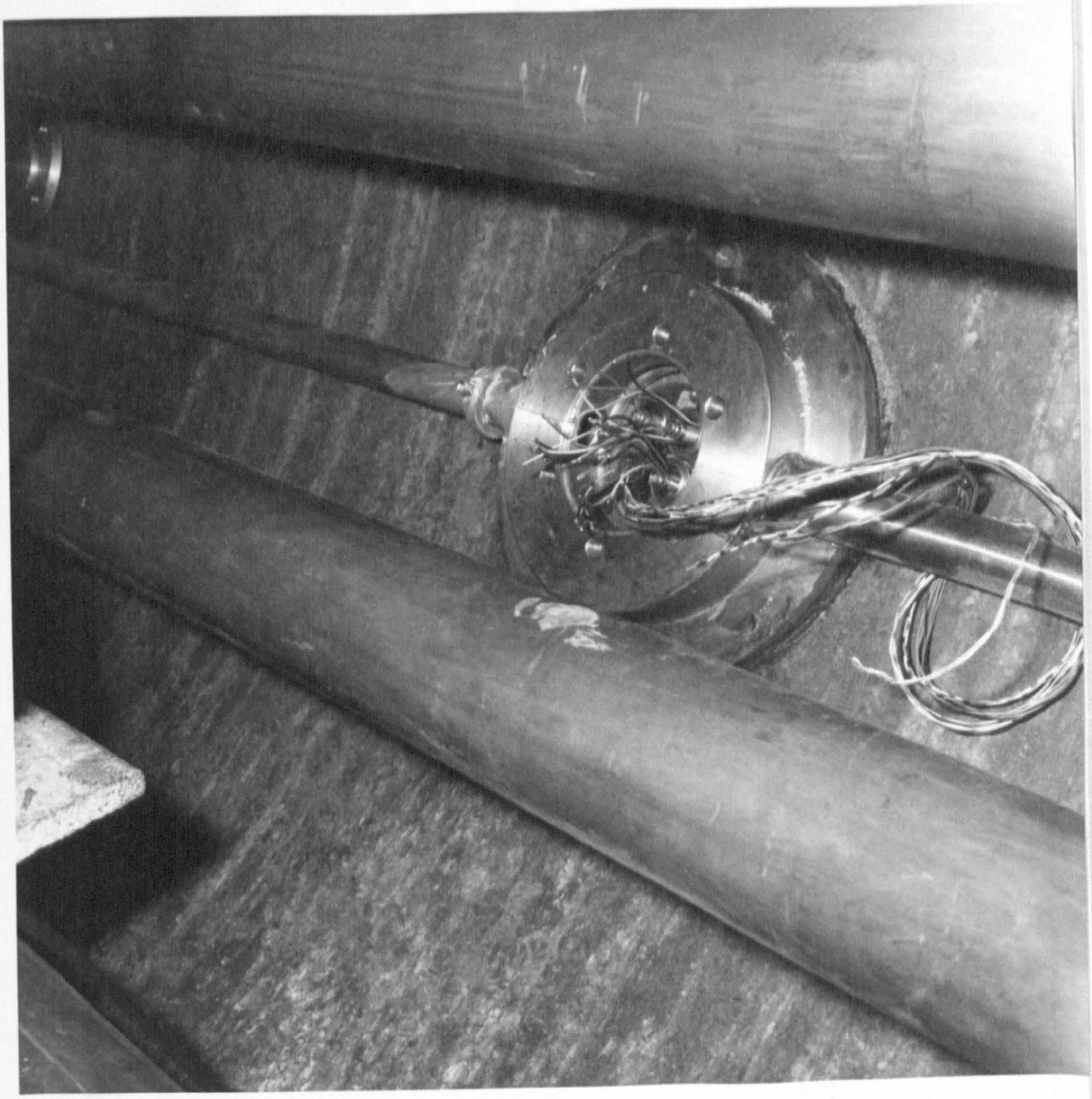

FIG. 34 RADIAL BOREHOLE MOUTH PLATE

FIG. 35 LONGITUDINAL SECTION THROUGH A DIAMETRAL EXTENSOMETER

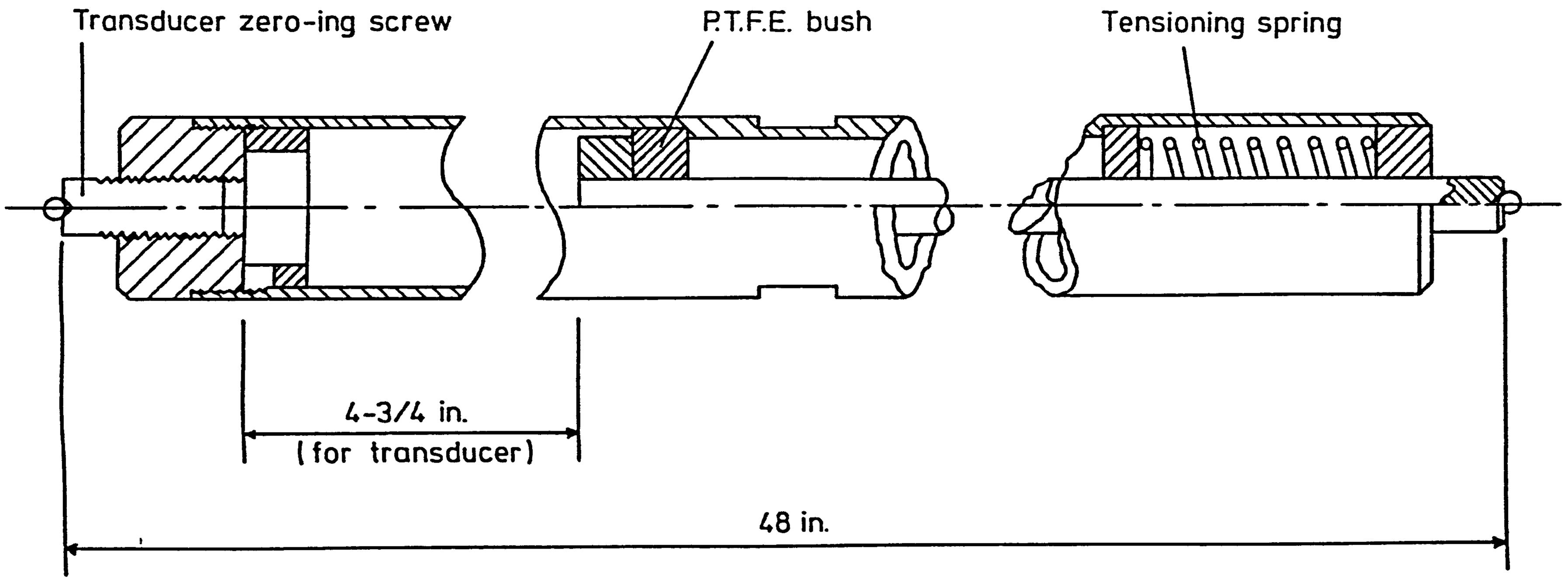

CHAPTER 6

THE TEMPERATURE MEASUREMENT SYSTEM

CHAPTER 6

6. The temperature measurement system

6.1 Introduction

The experimental programme proposed the application of pressure and temperature differences in the experimental cavity environment. The measurement of the temperature gradients in the rock mass is described in Section 2.4 and Figs. 5 and 6. This section discusses the merits of various measurement systems and covers in more detail the design, installation and calibration of the chosen system.

The ideal temperature measurement system must have several basic features. It is required to accurately measure temperature in a confined and pressurised environment and to transmit this intelligence to data recording equipment. This first requirement immediately precludes the use of any system other than an electrical technique, and this leaves only two possibilities; thermocouples or resistance thermometers. Both of these methods satisfy, in a greater or lesser degree, the remaining requirements of: accuracy, stability, sensitivity, speed of response, size and cost. Consequently both methods must be evaluated in greater detail.

6.1.1 Survey of temperature measurement techniques

The thermocouple is perhaps the simplest of all primary elements used in electrical temperature measurements. However, its advantages of simplicity, cheapness and the independence of thermoelectric effect on wire length and diameter are greatly outweighed by the disadvantages of employing such a technique in the experimental cavity. (21b). A thermoelectric sensing element could be married to the Modulog data logging system but this would involve the use of ML1033 type commutating units. These units cost appreciably more than the ML100B type, which operates on a bridge imbalance principle, that is consequently more suited to resistance themometry. An accuracy of $\pm 0.1^{\circ}C$ requires the measurement of small voltages to an accuracy of $\pm 4\mu V$ and at these low values stray thermoelectric effects would greatly influence measurement accuracy. These, and other disadvantages, indicated that thermocouples would prove to be unsuitable temperature sensors. (19b)

The resistance thermometer is replacing the thermocouple in many industrial and scientific applications (21.a) It is inherently capable of greater accuracy, often achieved using less expensive measuring equipment. Resistance thermometers generally employ platinum, copper or nickel elements; alternatively the sensing element may be a thermistor. The principle of operation depends upon an accurately known change of resistance with temperature, and a measurement of resistance permits the temperature to be computed or read off directly on a calibrated scale.

A resistance thermometer with a metallic primary element undergoes an increase in resistance with temperature; a thermistor, which has a semiconducting element, suffers a decrease in resistance with increase in temperature. For accurate measurements platinum is the primary metallic element most used in precision resistance thermometry and consequently the comparison of resistance techniques is limited to platinum thermometers and thermistors. This comparison, which for completeness also includes thermocouples, is summarised in Table 7. The advantage of both platinum resistance thermometers and thermistors greatly outweighed their disadvantages and both types were found suitable for use in this experiment. The chief disadvantage of the platinum type is the cost, whilst the disadvantage of thermistors have no great importance in the context of this experiment. Therefore it was decided to use thermistors as the sensing device of the temperature measurement system.

6.1.2 The use of thermistors in precision thermometry

The resistivity of metals is usually quite small, having values of 10^{-5} or 10^{-6} ohm. cm. at $0^{\circ}C$, which is readily explained by the high electron concentrations found in metals. Conductivity in metals is almost exclusively dependent upon electron mobility and as temperature increases reduce this mobility, due to displacement of ions undergoing thermal motion, the resistance of metallic conductors increases with temperature.

TABLE 7

COMPARISON OF THREE THERMOMETRIC TECHNIQUES

	ADVANTAGES	DISADVANTAGES
THERMOCOUPLES	Cheap Small sensing elements, i.e. hot junction Thermoelectric effect independent of length and diameter of wire	Difficult to achieve a high degree of accuracy Design problems due to relative bulkiness of thermocouple wire Involves the use of a more expensive type of commutating unit in the data logger.
PLATINUM RESISTANCE THERMOMETERS	High edgree of accuracy can be achieved Relatively small sensing element Approximately linear temperature coefficient of resistance.	Expensive Not entirely free from strain effects
THERMISTORS	High degree of accuracy can be achieved Very rapid response to temperature changes Very small sensing elements Fairly cheap for such an accurate device Its high resistance eliminates most resistance problems encountered in the extension leads.	Unstable if held at above 100°C for long periods of time Temperature coefficient follows an exponential law, making linear calibration difficult

Semiconductors have typical resistivities at $0^{\circ}C$ ranging from approximately 10^{-2} to 10^{9} ohm. cm., considerably higher than those of metals but well below the values found for insulators. It is quite common in semiconducting materials for both electrons and positive holes to contribute to the conductivity. Electron and hole concentration decreases quite rapidly with decreasing temperature producing temperature changes of resistivity often much more significant than those caused by changes in electron and hole mobility. It is this principle of large decreases in resistivity for small increases in temperature that is employed in thermistor thermometry. (19 a). The resistance temperature relationship for the thermistors used in this experiment is shown in Fig. 36.

Reproducability appears still to be the principle problem faced in thermistor thermometry. Thermistors undergo systematic resistance changes with time, generally becoming more stable after aging at elevated temperatures. For this reason most manufacturers subject their precision thermistors to some form of aging process to increase stability. In general, however, if thermistors are subjected to temperatures much greater than $100^{\circ}C$, or if they are continually cycled to temperatures above $100^{\circ}C$, their resistance tends to increase such that the maker's tolerance may be exceeded. Soldering connections to the thermistor leads must be done with care as overheating of the bead could cause these resistance changes. If thin-nosed pliers, acting as a heat sink, are used during installation, this problem can be avoided.

6.2 The design of the thermistor circuits

6.2.1 The Modulog data logging system

The Modulog data logging system includes five commutating units. The first unit, designated ML1033, logs 100 channels by direct e.m.f. measurement; the other four units, ML100B's, each log 50 channels in five blocks of ten. The ML100B commutating unit was designed primarily for strain gauge work and operates by measuring the imbalance of the strain gauge bridges. It is these units which are used to record the output of the thermistor bridges.

The commutating units house the two arms of the reference side of the bridge. Each of the arms contain a high stability precision resistor of 100 ohms. The signal lead from the measuring half of the bridge enters the logger circuit through several operational amplifiers into which is connected the digital voltmeter.

6.2.2 Design of the measuring bridge

The sensing elements used were precision thermistors type 44001 made by the Yellow Springs Instrument Co., (Ohio, U.S.A.) The experimental programme proposed an operating temperature range of 30°C and this gives a change of thermistor resistance of approximately 150 ohms. However, the imbalance caused by the changing resistance of the thermistor placed in a simple Wheatstone bridge would be so great that the data logger could not accommodate it. This necessitated slight modifications to the bridge circuits. A circuit diagram is shown in Fig. 37.

A factor of safety was applied to the design of the bridge circuits. Although it was only necessary to measure from 0°C to +30°C (approximately) the extended range of -20°C to +60°C was catered for. In order to be able to record this temperature range, the sensitivity of the bridge had to be reduced. This was done by adding 2.2 k resistors to each arm of the measuring half of the bridge, instead of using 100 ohm resistors to match the internal half bridge. (20, 22).

The high value resistors used to desensitise the bridge circuits created an almost constant current supply to the thermistors, creating favourable conditions for approximate linearisation of the bridge output. The linearisation was achieved by putting 220 ohm resistors in parallel with the thermistors.

However, resistors are normally supplied to a tolerance of 5% or 10% and unless placed in accurately matched pairs, could cause bridge imbalance of such magnitude that the data logger bridge balancing potentiometers would not be able to provide adequate compensation. Additional balancing facilities were provided by incorporating 200 ohm potentiometers into the bridge circuits.

Bridge imbalance caused by the use of electrical components specified to a tolerance of say ±5%, would create a situation whereby two thermistors at the same temperature would give different outputs via their respective bridges. There are two possible solutions to this problem:-

i) High precision resistors (±0.1%) could be used as the basic components of the bridges. The tolerance of these resistors would have to be added to the thermistor tolerance, and would result in an accuracy no better than ±0.5°C. Precision resistors would have to be specially ordered to our specifications, introducing the possibility of delivery delays, and would be relatively expensive.

ii) The second solution to this problem involves the calibration of the thermistors and associated bridge components to produce an accurate graph of temperature against data logger read-out. The facilities of the data logger are such that this calibration could be carried out with a group of up to ten thermistors at one time.

This latter recourse was considered to be more accurate, faster and cheaper than the use of precision resistors. It was decided to use standard thick film resistors (±2%) with a low temperature coefficient (100 ppm/°C.)

6.3 Thermistor calibration

6.3.1 Requirements of accuracy

The instrumentation scheme for the in situ experiment was designed to give a comprehensive picture of the behaviour of the salt mass under various imposed conditions. In order to define this behaviour with condidence precise measurement of small quantities was required, so a high degree of accuracy became necessary.

As there is a limit to meaningful measurement, a limit was set on this accuracy; very great accuracy is both difficult to achieve and expensive. The ideal degree of accuracy is that which is most compatible with precision of measurement and the technical practicality of method and interpretation.

However, the petrology of rock salt is such that the halite is intermixed with a small and varying percentage of red marl. The presence of the marl will have a small but definite effect on the temperature at a single point, and as such will have a bearing upon the determination of the level of temperature measurement accuracy.

A theoretical analysis of the imposed conditions on the salt mass indicated that it was necessary to detect temperature changes of less than $1^{\circ}C$. It was therefore proposed to set the thermometric accuracy at $\pm 0.1^{\circ}C$, although it would be possible to derive meaningful conclusions from the experiments if the accuracy was much less, say up to $\pm 0.5^{\circ}C$.

6.3.2 Thermistor calibration technique

The output of the thermistor bridges proved to be only approximately linear; although the centre portion of the output graph was linear, both ends tended to curve away. Also, the output of the bridges differed from each other when their respective thermistors were all at the same temperature. This necessitated thermistor calibration, giving a graph of temperature against data logger read-out.

The thermistor calibration required an independent temperature measuring system to record thermistor temperature. It was decided to use thermistors for this purpose and consequently two were sent to the National Physical Laboratory for accurate calibration of temperature against electrical resistance. The calibration range was $-20^{\circ}C$ to $+60^{\circ}C$ and the method used at the N.P.L. was as follows:-

The thermistors were mounted in close-fitting pyrex glass tube and completely immersed in well stirred liquid baths. The resistance of the thermistors were measured at a series of steady temperatures over the required range, the temperature being determined by a Laboratory Standard platinum resistance thermometer. From this data, the values for a resistance-temperature table were computed; the overall accuracy was estimated to be $\pm 0.05^{\circ}C$.

As the estimate for the completion of this work was six to eight weeks, it was decided that the thermistors to be installed should be calibrated in two stages, in order not to delay site installation work. This two stage calibration was undertaken in the following manner:-

The read-outs of the thermistors (at certain unknown temperatures) in one block of channels on the data logger were compared with the read-out of an arbitrarily selected thermistor (the intermediate standard), installed in the same block of channels. This procedure was repeated for the thermistors in the other blocks of channels using the same intermediate standard thermistor. This gave a data logger read-out /data logger read-out relationship between the intermediate standard thermistor and all the other thermistors. The thermistors could then be installed in the experimental cavity without causing delay to the rest of the installation work.

When the calibrated thermistors were received from the National Physical Laboratory, they were used to give a temperature/data logger read-out relationship for the intermediate standard placed in each block of channels. This allowed a temperature/data logger read-out relationship to be computed for each individual thermistor.

6.3.3 Primary calibration

The thermistor-data logger channel number allocation may be seen in Table 8 and is referred to in the following discussion on primary calibration.

The nine thermistor bridges associated with channels 100 to 108 were wired into the data logger with the intermediate standard thermistor wired into channel 109. The intermediate standard thermistor was removed from its bridge and replaced by a resistor with the same resistance as the thermistor at -20°C. By adjusting the data logger coarse and fine scaling potentiometers and the bridge balancing potentiometers, the data logger was set to read approximately -9000. This resistor was then replaced by a resistor of the same resistance as the thermistor at +60°C and the data logger adjusted to read +9000. A third resistor was substituted for the thermistor, this time representing the temperature of 20°C (laboratory temperature) and the data logger reading noted.

The intermediate standard thermistor was returned to its bridge and the group of ten thermistors immersed in a pool of light oil in a steel heat sink. The group of thermistor beads was a tight fit in the oil pool. The heat sink was placed in a thermostatically controlled oven and left there until it reached +20°C, as indicated by the intermediate standard.

The coarse and fine scaling of the channels associated with the thermistors to be calibrated were set at the same value as the standard thermistor channel, and the bridge balancing potentiometers adjusted so that all ten channels gave approximately the same reading. The heat sink was placed in a small cardboard container partly filled with finely powdered solid carbon dioxide. When the temperature of the heat sink reached approximately -30°C, the carbon dioxide was removed and sprinkled around the oven to create general cooling, enabling the temperature of the oven and heat sink to rise slowly. When the temperature of the heat sink reached approximately -20°C the data logger was allowed to scan the channels monitoring the thermistor bridges. The temperature of the heat sink was allowed to rise at the rate of approximately 1°C every two to three minutes, the oven heating element being used as and when necessary.

TABLE 8

THERMISTOR - DATA LOGGER CHANNEL ALLOCATION

Thermistor location coding refers to measuring stations A, B or C at points in the vertical, left or right directions. Reference to Figs. 5 & 6 will clarify the coding system.

Data Logger Channel No.	Thermistor Location		Type of Temperature measurement
100	A	V	Radial Borehole
101		L	
102		R	
103	B	V	Rock Temperature at Anchor No. 1.
104		L	
105		R	
106	C	V	
107		L	
108		R	
109	-	-	Calibration Channel
110	A	V	Radial Borehole
111		L	
112		R	
113	B	V	Air Temperature at Anchor No. 1.
114		L	
115		R	

Table 8 continued

Data Logger Channel No.	Temperature Location		Type of Temperature measurement
116	C	V	Radial Borehole
117		L	Air Temperature
118		R	At Anchor No. 1
119	-	-	Calibration Channel
120	A	V	Radial Borehole
121		L	
122		R	
123	B	V	Rock Temperature
124		L	
125		R	
126	C	V	At Anchor No. 2
127		L	
128		R	
129	-	-	Calibration Channel
130	A	V	Radial Borehole
131		L	
132		R	
133	B	V	Air Temperature At Anchor No. 2
134		L	
135		R	
136	C	V	
137		L	
138		R	
139	-	-	Calibration Channel

Table 8 continued

Data Logger Channel No.	Thermistor Location		Type of Temperature measurement
140	A	V	Radial Borehole
141		L	
142		R	
143	B	V	Rock Temperature
144		L	
145		R	
146	C	V	At Anchor No. 3
147		L	
148		R	
149	-	-	Calibration Channel
150	A	V	Radial Borehole
151		L	
152		R	Air Temperature
153	B	V	At Anchor No. 3
154		L	
155		R	
156	C	V	Radial Borehole
157		L	Air Temperature
158		R	At Anchor No. 3
159	-	-	Calibration Channel
160	A	V	Radial Borehole
161		L	
162		R	
163	B	V	Rock Temperature
164		L	
165		R	
166	C	V	At Anchor No. 4
167		L	

Table 8 continued

Data Logger Channel No.	Thermistor Location		Type of Temperature measurement
168		R	
169	-	-	Calibration Channel
170	A	V	Radial Borehole
171		L	
172		R	
173	B	V	Air Temperature
174		L	
175		R	
176	C	V	At Anchor No. 4
177		L	
178		R	
179	-	-	Calibration Channel
180	A	V	Temperature at Radial Borehole Cover Plate
181		L	
182		R	
183	B	V	
184		L	
185		R	
186	C	V	
187		L	
188		R	
189	-	-	Calibration Channel
190	A/B	V	Temperature 6" From Cavity Surface
191		L	
192		R	
193	B/C	V	
194		L	
195		R	
199	-	-	Calibration Channel

Table 8 continued

Data Logger Channel No.	Thermistor Location		Type of Temperature measurement
200	A/B	V	Temperature 4" From Cavity Surface
201		L	
202		R	
203	B/C	V	
204		L	
205		R	
206	-	-	Calibration Channel
210	A/B	V	Temperature 2" From Cavity Surface
211		L	
212		R	
213	B/C	V	
214		L	
215		R	
219	-	-	Calibration Channel
220	A/B	V	Temperature 1" From Cavity Surface
221		L	
222		R	
223	B/C	V	
224		L	
225		R	
229	-	-	Calibration Channel
230	A/B	V	Temperature ½" From CavitySurface
231		L	
232		R	
233	B/C	V	
234		L	
235		R	
236	-	-	Calibration Channel

Table 8 continued

Data Logger Channel No.	Thermistor Location		Type of Temperature measurement
240	A/B	V	Temperature $\frac{1}{4}$" From Cavity Surface
241		L	
242		R	
243	B/C	V	
244		L	
245		R	
246	-	-	Calibration Channel
250	A/B	V	Temperature at Cavity Surface
251		L	
252		R	
253	B/C	V	
254		L	
255		R	
256	-	-	Calibration Channel
260	A	V	Diametral Extensometers
261		L	
262		R	
263	B	V	
264		L	
265		R	
266	C	V	
267		L	
268		R	
269	-	-	Calibration Channel

Table 8 continued

Data Logger Channel No.	Thermistor Location		Type of Temperature measurement
270	A/B	V	Longitudinal Extensometers
271		L	
272		R	
273	B/C	V	
274		L	
275		R	
276	-	-	Calibration Channel

The data logger scanned the channels every minute and the information recorded on both printed paper roll, punched paper tape and eventually stored on magnetic disc mountable on the IBM 360/67 computer. Graphs of the intermediate standard thermistor read-out against the individual thermistor read-outs were plotted on the on-line graph plotter, and as expected, indicated a straight line relationship.

6.3.4 Secondary calibration

The National Physical Laboratory calibration report included a table of resistance against temperature for every C^{o} throughout the range -20 to +60°C. One of the thermistors so calibrated was used to accurately measure the temperature of the oil pool in the heat sink. This accurately calibrated thermistor was placed in one arm of a Post Office type potentiometer, the other three arms being two fixed resistors and one variable resistor. The intermediate standard thermistor was wired into the appropriate channel in the first block of channels to undergo secondary calibration. This intermediate standard and the NPL standard were placed in the heat sink and the temperature lowered to approximately -30°C. The variable resistor of the potentiometer was set to the resistance of the NPL standard at -20°C and the temperature of the oven allowed to slowly rise.

When the temperature of the heat sink reached -20°C, as indicated by the balancing of a spot galvanometer connected across the potentiometer, the "read" button of the data logger was depressed, thus recording the data logger reading of the intermediate standard at -20°C. This procedure was repeated every degree throughout the calibration range. The intermediate standard was transferred to the "calibration channel" on the next block of ten channels and the calibration continued.

The secondary calibration data was recorded on punched paper tape and stored on magnetic disc. Computer programmes were written to compute the relationship between temperature and the data logger read-out of each individual thermistor and the information presented in the form of calibration tables.

6.3.5 Bridge supply voltage

At the commencement of the calibration work, it was assumed that the stabilised voltages supplied by each ML100B commutating unit were identical. It was subsequently discovered that this was not true, the supply from each unit differing from each other by a millivolt or two. It transpired that this difference in supply voltage rendered inaccurate the results from one block of channels.

The pair of thermistors attached to each anchor are wired in such a way that they must work off the same supply. It can be seen from Table 8 that all the thermistors measuring rock temperature on the No. 3 anchors are connected to channels 140-8, and the thermistors measuring air temperature at the No. 3 anchors are connected to channels 150-8. Channels 140-8 and channels 150-8 are on different commutating units which have slightly different supply voltages. Therefore, the air and rock temperature thermistors on the No. 3 anchors, having been calibrated with the supply voltage from their own commutating units, must work from the same supply. If the supply is taken from the first commutating unit, the air temperature readings will be inaccurate, and if taken from the second unit, the rock temperature readings would be inaccurate. As the rock temperature readings are more important, the pairs of thermistors on the No. 3 anchors are supplied from the first commutating unit, and the air temperature readings rejected as inaccurate.

6.3.6 Final calibration precautions

After each block of channels had been calibrated, note was taken of the value of the energising supply and the settings of the coarse and fine scaling potenticmeters. The bridge balancing potentiometers were all sealed with sealing wax to prevent accidental disturbance of the setting.

The data logger bridge balancing potentiometers have no facilities for indicating their exact setting. If one such potentiometer malfunctioned and had to be replaced, a method was devised whereby the replacement could be set at the same value as the original. The potentiometer settings were indirectly recorded by plugging a calibration box into each channel and noting the channel reading. If a potentiometer failed, the replacement could be adjusted until the required data logger reading was achieved.

6.3.7 In situ recalibration

When the thermistors were installed, large errors in temperature readings were discovered. Although ambient rock temperature was approximately 13°C, most of the thermistors indicated temperatures between 30°C and 35°C. An investigation of this problem, discussed in Section 8.3, indicated that the only recourse was to effect an in situ recalibration of the thermistors.

6.3.7.1 Limits of accuracy

A table of resistance values for every Centigrade degree between -80°C and +120°C was supplied with every thermistor received from the manufacturers. Fig. 36 shows a graph of the accuracy of this table, indicating that within the proposed temperature range of this experiment, an accuracy of between $\pm$0.30° and $\pm$0.350° may be expected. Despite this large error inherent in the manufacturers tolerances, a consideration of the statistics of the readings suggest that better accuracies should be possible. Within the manufacturers tolerance of $\pm$1% on resistance, a normal distribution of resistance values would be expected. If this is so, it was reasonable to expect a 68% probability that the error on any thermistor would be less than $\pm$0.165°C.

An increase in accuracy of the final results was achieved by taking mean values of the temperature at a specific depth. An analysis of the variance of the temperature readings leads to an estimate in confidence of this averaging procedure. Since it is the integral of the temperature gradient that must be considered in the displacement equations, and since the variation of integrals is likely to be less than the variation in temperature readings, averaging of these integrals is likely to be justifiable even if the temperature readings show a fairly wide spread. A further analysis of the variance of these integrals will lead to a measure of confidence in the final result.

It was concluded that an acceptable degree of accuracy could be achieved by using the table of temperature - resistance values supplied by the manufacturer in the recalibration procedure.

6.3.7.2 Thermistor recalibration

Thermistor recalibration involved the removal of the thermistors from their circuits at a point inside the cavity and the substitution of a resistance box. The resistance box was connected to the thermistor terminals using wire of a similar type and length to that used to connect the thermistors. Any temperature may be simulated by adjusting the resistance box to the resistance of the thermistor at that temperature.

Using this technique, the data logger scaling and balance was adjusted to give a reading of -0500 at -5°C and approximately +3000 at +30°C. Data logger readings were then recorded for every C° between -20°C and +60°C. A set of readings for each thermistor channel was recorded on punched paper tape for subsequent analysis on the IBM 360/67 computer.

An investigation of the temperature readings after recalibration indicated that this calibration was successful; the variations in temperature at a specific depth was never greater than $0.3C^{o}$. Both the resistance box and a calibration box was plugged into the data logger immediately after recalibration to provide information to enable any future shift in balance or scaling to be quickly and easily detected. This information allows simple adjustments to be made to the data logger in the event of any unexpected shifts.

6.4 Measurement of the radial temperature distribution

The radial temperature measurements were taken by equipping each of the anchors used in the radial deformation instrumentation with a pair of thermistors. One of these thermistors was embedded in a rubber ring fitted around the anchor cone just above the expanding anchoring ring. Setting the anchor in the borehole expanded the rubber ring until its outer face, containing the thermistor, was pressed tightly against the borehole wall. This may be more clearly understood by referring to Fig. 27. The other thermistor fitted to the anchors was used to monitor borehole air temperature, and is discussed in Section 6.6.

The borehole mouth plates and borehole end covers were both made from stainless steel. Any temperature change in the cavity would be conducted through this metal and cause convection currents in the borehole air-space. The convection currents could quite easily change the temperature of the borehole instrumentation and rock surface, and would invalidate the measurement of the rock temperature gradient. To minimise these effects, the boreholes were stuffed with glass wool during anchor installation.

6.5 Near surface thermometry

The temperature gradient near to the cavity surface was predicted to be quite steep, especially during the early stages of a temperature test. The steepness of the temperature gradient demands that measurements must be taken at a number of points within a short radial distance of each other if a high degree of accuracy is required. A study of the predicted temperature gradients advised measurements at the rock surface and at $\frac{1}{4}$", $\frac{1}{2}$", 1", 2", 4" and 6" deep into the rock mass. The radial borehole temperature measurements would complete the survey of radial temperature distribution.

6.5.1 Host material tests

A short discussion of the siting of the near surface thermometry stations and the problems involved in obtaining accurate temperature measurements is given in Section 3.3. It was suggested in Section 3.3 that a temperature probe could seriously affect, by its presence, the temperature gradient in area of rock under investigation. Consequently a series of tests were conducted to ascertain the most suitable material for the temperature probe.

Three methods of measurement were considered, using three different types of temperature probes:-

i) An araldite rod, thermistors cast in place
ii) A salt/araldite rod with thermistors set in longitudinal grooves.
iii) A salt cylindor with thermistors housed in radial holes.

The thermistors were set ¼", ½", 1", 2", 4" and 6" from one end of the host material. In methods i) and ii) the heat path crosses a salt or salt/araldite film which separates the thermistor bead from the salt. Although the film was quite thin, less than ⅛", a time lag was predicted before the thermistor bead came up to the temperature of the surrounding salt. The thermistors could not register a higher temperature than the surrounding salt as the thermal conductivity of araldite or an araldite/salt mix is less than that of rock salt. The purpose of this test therefore, was to evaluate the time lag in methods i) and ii); if this was not significantly large, the technically difficult salt cylinder method could be dispensed with. The three temperature probes were constructed as follows:-

i) Six thermistors were cast into an araldite rod 6¼" long by ¼"diameter with the leads brought straight to the front face of the rod. The thermistor beads were less than 1/32" from the rod surface.

ii) A rod was cast, 6½" long by ½" diameter, from a material consisting of 50% araldite and 50% - 120 mesh rock salt. Grooves ⅛" deep by 3/16" wide were milled longitudinally to house the thermistors. The 6" and 4" thermistor leads came straight to the front; the other four thermistor leads were taken to the back and then brought out. The thermistors were cemented in position using the same araldite/salt mix as the host material.

iii) The principle involved in using a rock salt probe supposes that an element of salt has been removed from the cavity, fitted with thermistors, and then replaced. The cylinder was made as long as possible to minimise the effects of temperature gradient disturbance on the temperature gradient within the first six inches of the probe. Radial holes, 3/32" in diameter were drilled into a cylinder of salt 1 31/32" diameter by 12" long, to house thermistors. The depth and circumferential position of the four front holes was varied to preserve the strength of the cylinder. Longitudinal grooves, ⅛" deep by 3/16" wide, were milled into the salt such that the leads from thermistors ¼" to 2" were taken to the back of the cylinder before being brought to the front; thermistors 4" and 6" had their leads brought straight to the front.

The three probes were cemented into tight fitting holes in the upper surface of a block of salt 3' by 2' 3" by 2' 6" deep. Surface temperature of the block was monitored at several points by cementing in thermistors. The surface was covered with a steel hood, cemented in place, and steam used to raise the surface temperature. The thermistors were connected, via suitable bridges, to the data logger to give continuous monitoring of surface and sub-surface temperatures. The conclusions of this test are as follows:-

a) The steam generator was not efficient enought to produce a uniform temperature distribution along the top surface of the salt, i.e. there was a temperature gradient from inlet to outlet.

b) The steam near the inlet removed the coatings of aluminium paint protecting the salt surface and created a vent to the bottom of the salt block. The vent did not invalidate certain comparisons between the two araldite probes as they were equidistant from the vent. The previously drawn conclusions made the interpretation of the data more difficult, but the following points may be accepted as a generalisation of the situation.

c) The time lag between salt temperature, measured by the salt probe, and the araldite probe was greater than that of the araldite/salt probe. This time lag appeared to increase with time, rate of temperature rise and the depth of temperature measurement.

d) There was no indication that the temperature readings were influenced by heat conduction along the thermistor leads.

In view of the uncertainty of the results of this experiment and the implied time lag of araldite probes, it was decided to construct the near surface temperature probes from rock salt. After many attempts, six cylinders 12" long by 1 15/16" in diameter were machined from rock salt. This test indicated that there was no noticable heat conduction along the leads and consequently design of the rock salt probe was simplified by bringing the thermistor leads straight out to the front of the probe. A front view of the probe is shown in Fig. 38.

6.5.2 Temperature probe installation

Six holes 12" long by 2" in diameter were drilled into the cavity surface at the locations described in Section 3.3. The backs of the holes were ground flat for a good thermal contact with the end of the probes. The probes, fitted with thermistors in the pattern described, had an additional thermistor cemented to the front end to monitor surface temperature. Installation of the probes into their respective holes proved to be quite difficult due to the tight fit (1/16" on diameter). The araldite used to cement the probes in position acted as a seal making the probe behave like a piston in a cylinder, but time and patience solved this problem.

6.6 Instrument thermometry

The experimental programme proposed changes in the cavity air temperature of $\pm 15c^{o}$ from ambient. In view of the high degree of accuracy required from the deformation transducers, a temperature variation of $30C^{o}$ would have a noticeable effect on the results of these measurements, even though most of the active components of the instrumentation were constructed from invar. Section 5.2.3 describes the precautions taken to compensate for electrical and mechanical transducer output variations due to temperature changes, but does not indicate the correction factors to be applied for temperature variations in the instrumentation connected to the transducers.

The radial deformation transducers were sited in a cluster near the borehole mouth and mechanically connected to the points under investigation by anchors, and push rods made from invar. These rods would tend to take on the temperature of the surrounding rock, and due to the precautions taken to eliminate convection currents, a temperature gradient would exist along the rods. Although constructed from invar, the temperature variations would cause small changes in the lengths of the push rods which would be especially noticable in the longer lengths.

Ideally the temperature of the rods should be measured at various points and a correction factor derived from some integral of the temperature gradient. However, technical difficulties prohibited measurements of this type and the air temperature at each anchor was measured instead. From these readings a subroutine in the data handling program calculated the appropriate correction factor.

The variations in the temperature of the diametral and longitudinal extensometers were monitored by means of thermistors tightly taped to the duralumin transducer housings. Although ideally the actual invar push rod temperature should be measured it was felt that the rate of change of temperature was low enough to permit this simplification. Once again, a subroutine in the main handling program calculated the temperature correction factor and automatically compensated for changes in temperature.

6.7 Temperature monitoring and alarm system

The experimental procedure involved several hours of intense activity in bringing the cavity to the required state of temperature and /or pressure followed by several days of routine instrument monitoring. It was felt that some system giving a quick visual appreciation of cavity condition would be useful during the early stages of a test. An alarm system, to be switched on during the routine phase of the tests, would protect the experiment operatives from overlooking any malfunction of the temperature and pressure control systems.

Several thermistors were cemented to the cavity wall and connected by suitable bridges to a chart recorder. The recorder could be set to give a semi-continuous plot of approximate rock surface temperature, thus leaving the data logger completely free for instrument monitoring. Two more thermistors were wired into a temperature drift alarm system. The alarm could be set to operate a warning light and audible signal should cavity temperature drift above or below predetermined limits.

FIG. 36 THERMISTOR RESISTANCE–TEMPERATURE CURVE

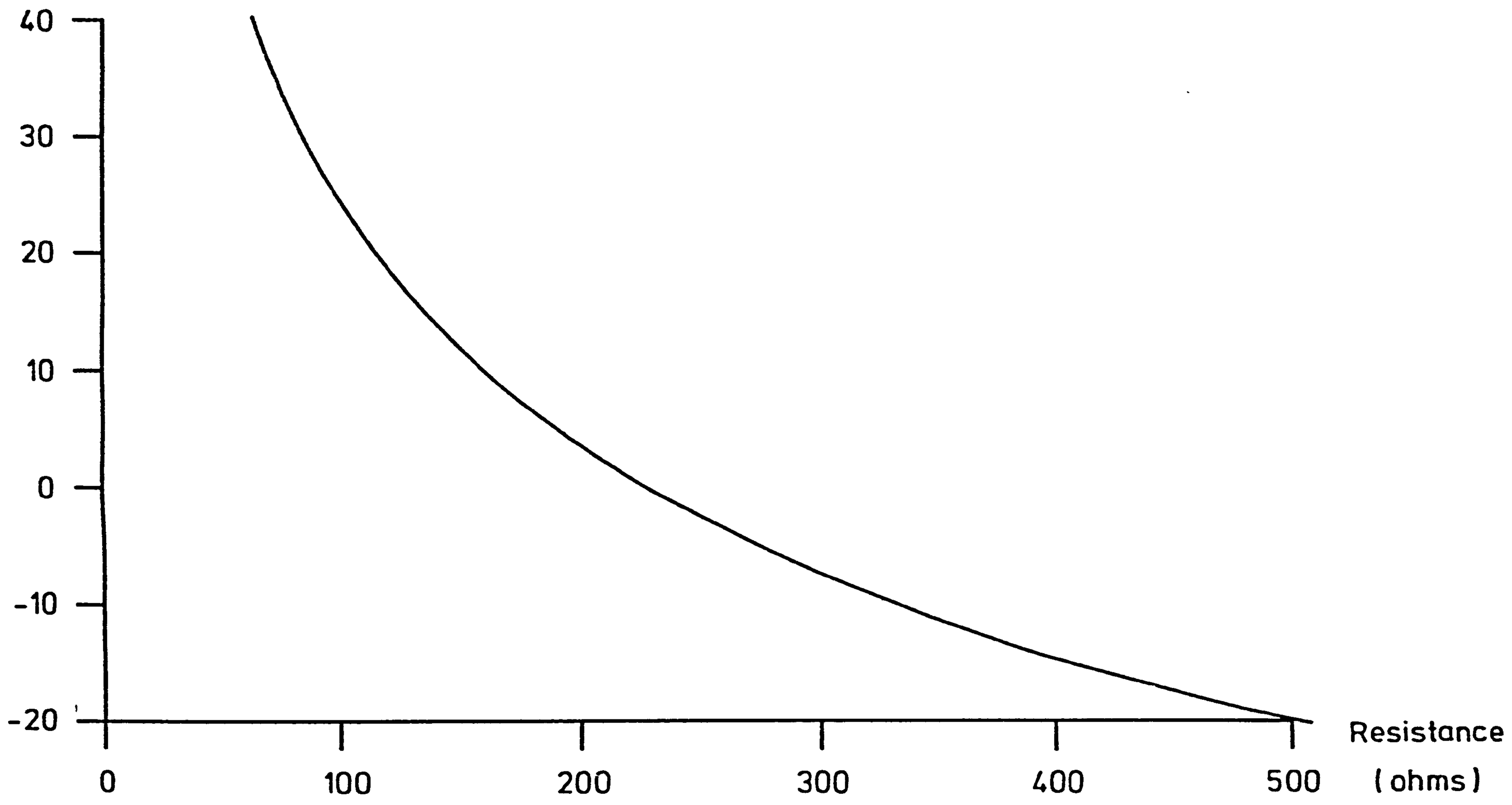

FIG.37 THERMISTOR BRIDGE CIRCUIT

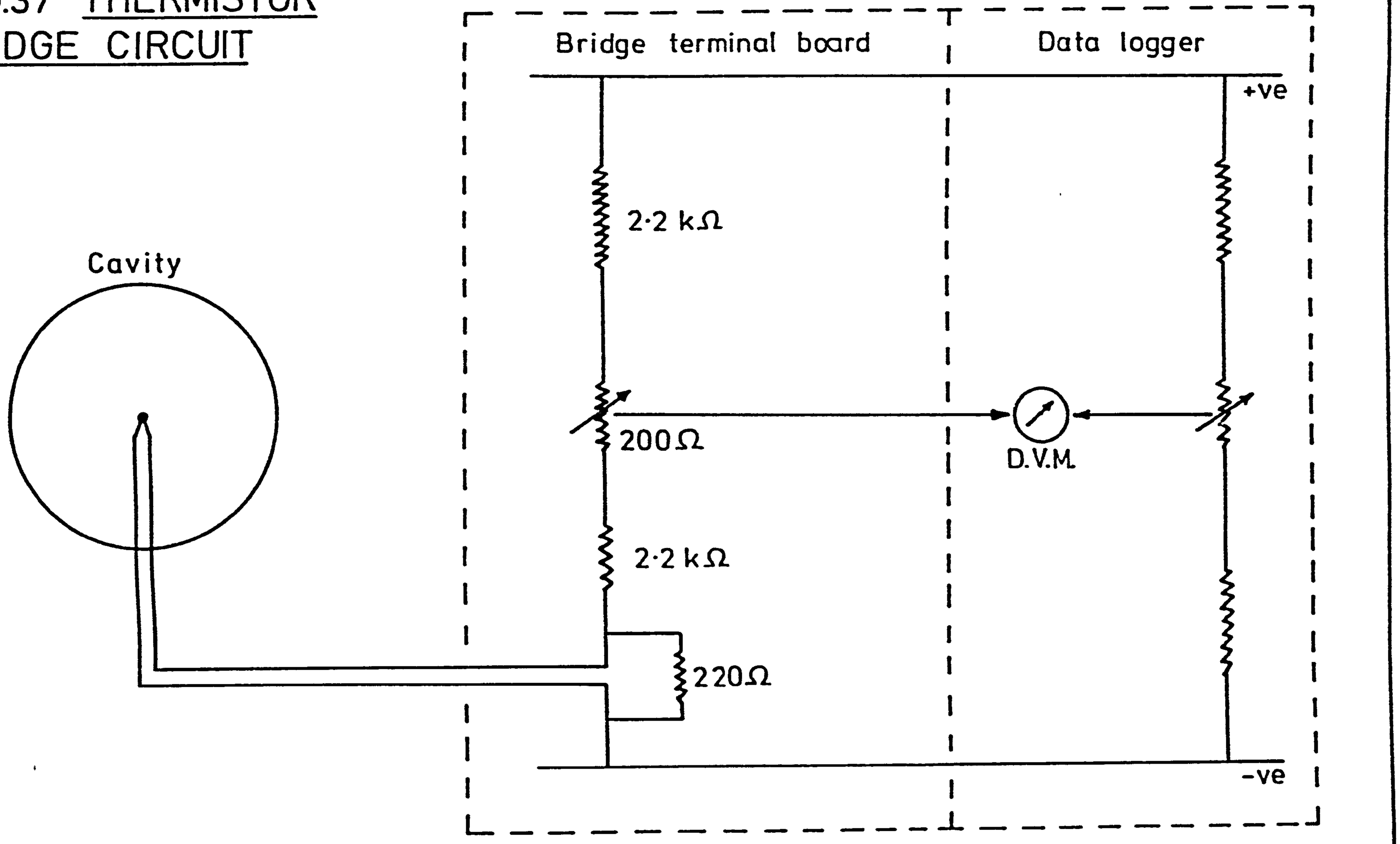

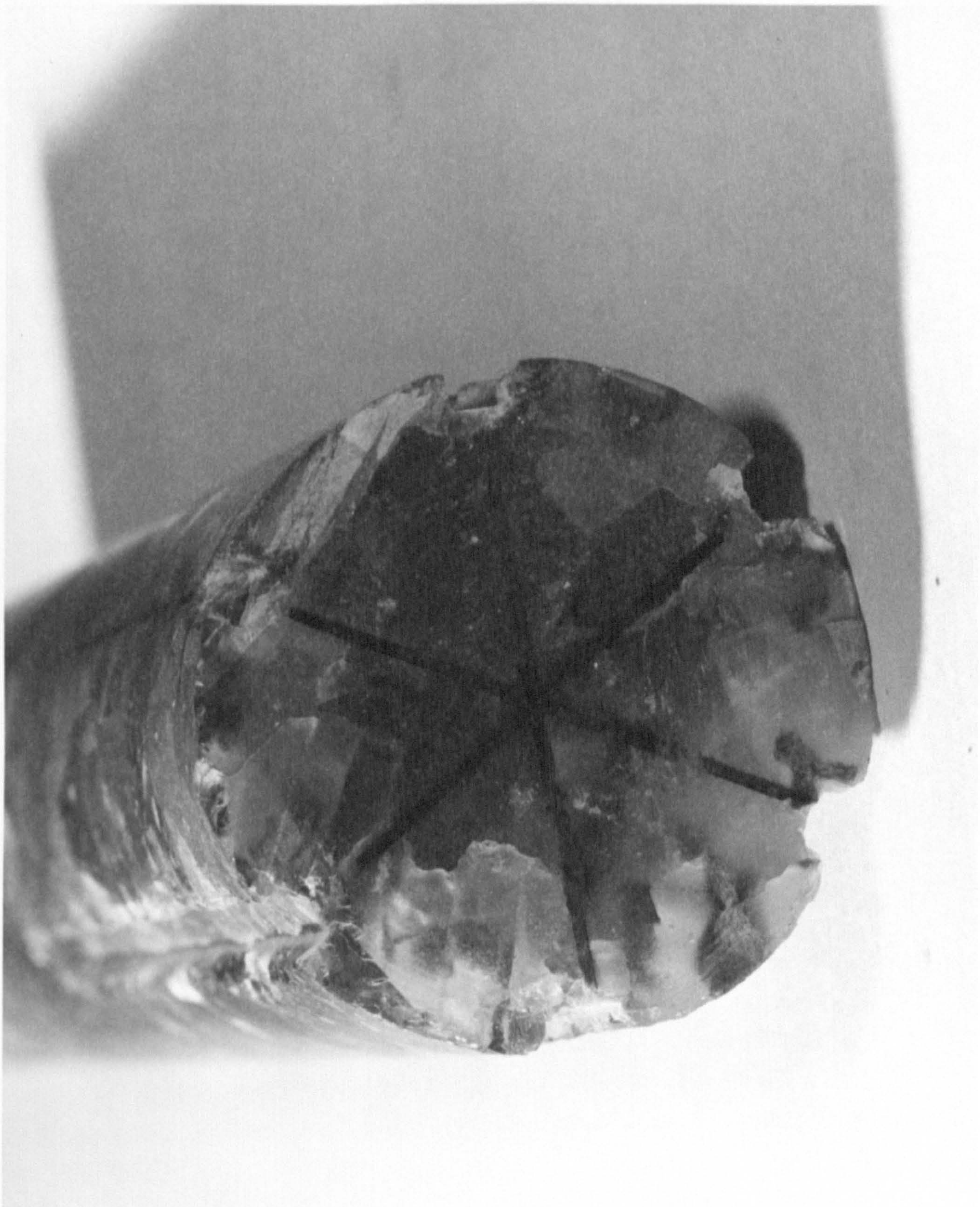

FIG. 38 FRONT VIEW OF ROCK SALT TEMPERATURE PROBE

CHAPTER 7

EXPERIMENTAL PLANT AND ANCILLARY EQUIPMENT

7. EXPERIMENTAL PLANT AND ANCILLARY EQUIPMENT

7.1. Introduction

The account of the in situ experiment so far has been limited to theoretical considerations and to the detection of physical changes in the rock mass due to imposed loading conditions. It is now proposed to discuss the means of achieving the desired loading conditions. This discussion also includes some aspects of the engineering problems encountered and briefly describes ancillary instrumentation and equipment.

7.2. Electrical power supplies

The power supply to the site is taken from the Moulton No. 2 Panel feeder rated at 3.3 KV, 200 KVA, and is transmitted to the electrical plant by means of several transformers and two distribution boards. The incoming power is collected by the main transformer, stepped down to 415V 3 PH 50 Hz and is fed to the main distribution board. This distribution board supplies the compressor, heater/chiller and a transformer feeding the instrument hut distribution board with single phase 240V. The hut distribution board supplies the data logger, chart recorder, hut lighting and heating systems and a water boiler; two transformers in the hut step this power down to supply 110V and 50V a.c. sockets.

The compressor control panel is tapped to provide one phase for transformation down to 240V which is used to feed a distribution board in the access room. This board is used to power the cavity fans, access room lights, and two transformers. One transformer supplies the photographic equipment with 24V d.c. whilst the other feeds sockets with 50V and 25V a.c. The electrical distribution scheme is shown schematically in Fig. 39.

7.3. Instrument wiring and data logging system

The instrumentation and alarm systems involve the use of 54 displacement transducers and 144 thermistors, and obviously requires some form of data logging equipment if readings are to be taken at frequent intervals. A survey of the market indicated that the Modulog data logging system, manufactured by Intercole Systems Ltd., best suited the needs of this experiment.

The equipment is shown in Fig. 40. On the left is the main control cabinet showing, from top to bottom, the digital clock displaying the time 16.09 on the 13th day, the digital voltmeter displaying the reading -0388, the commutator drive unit and the printer/punch drive unit. On the right are the commutating units, from top to bottom, type ML1033 capable of monitoring up to 100 channels and used to log transducer readings below which are four ML10013 units, each capable of monitoring 50 channels and used to log thermistor readings. On top of the cabinets, from left to right, are the punch, printer and remote digital voltmeter. Fig. 41 shows the data logger installed in the instrument hut.

It is beyond the scope of this thesis to describe in detail the circuitry connecting the instruments to the data logger, although an indication of the complexity may be gained from Fig. 42 and Fig. 43. A schematic circuit diagram is shown in Fig. 42 whilst Fig. 43 shows the access room junction boxes.

7.4. Cavity pressurisation equipment

For reasons of safety, convenience and economy it was decided to pressurise the experimental cavity with compressed air. This gives a fair approximation to operational gas storage conditions as air is in many respects thermodynamically similar to natural gas. The elastic model predicted that rock movements large enough to be conveniently analysed could be induced by an internal pressure of 200 psi. The free air delivery rate was not thought to be critical as once the cavity was at the required pressure the compressor would only have to power ancillary equipment and compensate for leaks.

7.4.1. The air compressor

The cavity was pressurised by an Atlas Copco BT414D air compressor delivering 126 c.f.m. of free air at a maximum pressure of 200 psi. The compressor, fitted with an intercooler and discharge pulsation damper, fed compressed air to an aftercooler. Leaving the after cooler, the air was lead through a dryer, a filter to take out any oil mist, and finally to an air receiver. Pressure was controlled by a control valve, which could be set anywhere between atmosphere and 200 psi, and was installed just after the air receiver. The equipment may be seen on the right of Fig. 44.

7.4.2. Compressed air pipework

Compressed air was supplied to Cavity L by means of 3" N.B. pipework, installed at gradients suitable for the extraction of condensates by strategically placed drain valves. The pipework shown in Fig. 45 is extended so that Cavity R may be pressurised if so desired. The pipework, including interconnections between the compressing plant, is fitted with several pressure gauges for visual checks and monitoring, with two pressure transducers installed in the pipework near the cavities. One of these transducers transmits information to the data logger whilst the other is connected to the chart recorder for semi-continuous monitoring.

The compressed air pipework was extended to allow for rapid cavity depressurisation in the event of an emergency. A 6" N.B. main, installed just after the air control valve, could discharge compressed air at a point remote from the working areas. The large diameter valve which controlled this operation was fitted near the pressure control equipment at the ramp top.

7.5. The heater/chiller system

The heater/chiller system was designed to perform two functions:-

(i) To raise or lower cavity temperature, maintain cavity temperature at this level, and then to bring cavity temperature back to ambient rock temperature.

(ii) To maintain cavity temperature at ambient rock temperature, counteracting heat changes induced by adiabatic compression or expansion of air during compression tests.

The experimental programme proposed raising and lowering the temperature of the cavity surface a maximum of 15C° from the ambient rock temperature. This temperature differential was imposed by using a heat exchanging system to adjust the temperature of the cavity air space. Control equipment, monitoring cavity surface temperature, could raise, lower or maintain any temperature between -15°C and 50°C. This was done by mixing refrigerant coming from two tanks, one held at -15°C, the other at 50°C, and passing it through a heat exchanger installed in the experimental cavity.

7.5.1. The chiller

The chiller has a capacity for removing 115,000 BTU/hr and can induce a cavity surface temperature as low as -15°C. The chilling system consists of an electrically driven compressor and air cooled condenser which supplies chilled refrigerant to a cold storage tank. This equipment is fitted in a closed loop, with the chilled refrigerant (ethylene glycol) drawn from the cold storage tank as and when required.

7.5.2. The heater.

The heating system consists of a 36 KW thermostatically controlled immersion heater pumping ethylene glycol to a hot storage tank. The refrigerant in the hot tank is maintained at approximately 50°C. Once again, this equipment is installed as a closed loop with hot refrigerant being drawn from the hot storage tank as required.

7.5.3. The heat exchanger

The heater and chiller provides hot and cold reservoirs of ethylene glycol, both activities being operated from a control panel. The control panel may be adjusted to supply the cavity heat exchanger with refrigerant at a required temperature. Six platinum resistance thermometers, monitoring cavity surface temperature, provide a reference for automatic cavity surface temperature adjustment and control.

The control circuits incorporating the resistance thermometers activate a motorised mixing valve which can vary the demand from the hot and cold reservoirs. The control panel gives a visual indication of the proportion of the liquid being drawn from each tank and continuously plots cavity surface temperature on a built in chart recorder.

The cavity heat exchanger, consisting of upper and lower loops, may be seen in Fig. 46, and was constructed from 6" N.B. copper pipes. The flow through each loop can be adjusted to counteract the tendency for the upper half of the cavity to be warmer than the lower half. The inlet pipe divides outside the cavity to provide an inlet for each of the loops and a similar arrangement exists for the refrigerant outlet. The valve assemblies controlling this operation may be seen in Fig. 45. Other valves were fitted so that the refrigerant supply to Cavity L could be cut off and Cavity R supplied instead.

The refrigerant was pumped to the cavity heat exchanger through 1½" N.B. pipework covered with 1½" thick polystyrene insulation. Fig. 45 shows the five purge valves used for releasing trapped air from the system. A header tank, installed near the roof of the ramp top area, was connected to both the heating and chilling systems and catered for volumetric changes in the refrigerant due to temperature variations.

7.6. Air circulation fans

Although the cavity heat exchanger was designed to minimise the effects of convection currents, it was thought some stratification of air temperatures would take place. To counteract this, a form of ventilation system was required to thoroughly mix the air in the cavity, attempting to achieve a uniform cavity air temperature. Rather than specially design fans for this purpose, it was thought more advisable to modify commercially available fans. Consequently orders were placed for two PVD90 ceiling fans, manufactured by Electric Fans & Controls Ltd.

The swept diameter of these fans was 3'0" and the bearings were of such a type that the fan could be operated in the horizontal position. The modifications were limited to reducing the fan blade length, so that the fan could be operated within the confines of the heat exchanger, and to the design of suitable supporting brackets. The fans were installed at opposite ends of the cavity and run in contrary directions. The fan support brackets were designed to allow the fans to be swung to one side, allowing easier access to the cavity. This was done by unscrewing two clamping bolts and removing two of the three fan blades. The fans, cut down to 2' 4¾" swept diameter and running at 280 r.p.m., were operated by a low voltage relay energised from the instrument hut. The fan motor starting capacitors, being unable to withstand high pressures, were resited outside the cavity and connected to the motors via the cable gland through the plug.

7.7. The photographic equipment

Whichever mathematical model was found to be most suitable for predicting long term cavity stability, some criteria of failure would have to be defined. In view of the weakness of rock salt in tension it was decided that the primary criterion of failure should be a zero stress condition. However, crack initiation and propagation in the cavity walls would provide invaluable data on the behaviour of rock salt, and so crack initiation was adopted as a secondary criterion of failure.

Information on crack initiation and propagation was to be recorded by means of remote controlled photography. It was decided to photograph the rock at two points along the cavity, with the cameras rotating about the cavity axis such that a series of photographs of the circumference of the cavity could be taken. The two cameras were sited between the diametral measurement stations.

7.7.1. The cameras

The photographic equipment was built around Agfa R.C.B. cameras fitted with 60 mm f4.5 Solagon lenses. The lenses, were vented to enable them to withstand the 200 psi pressure. The camera magazines accepted 51 ft (17 metres) of 35 mm film which was wound onto the take-up cassettes by a 12V motor. Variable power ring flash units, coupled to the camera trigger mechanism, provided the necessary illumination.

7.7.2. Camera rotation mechanism

The camera rotation mechanism was designed to direct the cameras at twelve points on the cavity circumference. The cameras, rotating about the cavity axis, would move the first position, stop, expose the film and wind on to the next frame, and continue to the next position until all twelve exposures had been completed. The camera would then be rotated back along its original path to the start position to await the time signal to begin the next scan.

The camera rotation mechanism shown in Fig. 47, consists of a framework with a power unit at one end and a shaft at the other. This shaft is fitted with a large sprocket which is chain driven by the power unit. The camera and flash are fitted to an arm located radially at the opposite end of the shaft to the sprocket. Twelve cams and two pegs are attached to a large disc bolted to the sprocket. The two pegs each operate a microswitch mounted on the frame, one starting and the other stopping and reversing the rotation mechanism. The cams operate a microswitch which activates the camera and flash mechanisms. The camera rotation mechanism is designed to contra-rotate after a complete scan in order to eliminate sliprings from the mechanism design. It was felt that slipring contacts would not withstand the corrosive atmosphere of the salt cavities.

7.7.3. Camera control equipment

The camera control equipment was designed to allow the camera to take a photograph every 30° in such a manner that the same twelve positions were photographed during each rotation. When the rotation mechanism is in the "start" position a peg, mounted on the sprocket disc, rests on a microswitch which maintains the control circuits in a de-energised state. The circuits can be energised manually from a push button or by a signal from the control clock; either of these devices overrides the open microswitch and allows the motor to turn the camera. When the camera driving sprocket turns, the peg on the sprocket disc allows the microswitch to close, providing continuous energisation of the control circuits.

The camera driving sprocket continues to turn until a cam mounted on the sprocket disc strikes a microswitch. This microswitch disconnects the motor from the supply, and signals the power unit to disengage the clutch and apply the brake, causing the camera to come to an abrupt halt. The control cams are sharp edged, thus ensuring that the camera halts at the same position in each complete rotation.

The control circuits allow the cameras to pause, enabling vibrations caused by the abrupt halt to subside. A few seconds later the camera shutter and flash circuits are activated and a photograph taken. After this exposure the camera automatically winds the film on to the next frame. A relay then short circuits the cam-operated micro-switch for a short time, re-energises the drive motor, and allows the camera to rotate to the next area to be photographed.

When all twelve photographs in the scan have been taken, the cameras continue to rotate for a short distance until the second peg on the sprocket disc hits a microswitch. This switch reverses the direction of camera rotation, simultaneously de-energising circuitry not directly involved with simple camera rotation. The camera continues to turn in the reverse direction until the "start" peg engages the microswitch which de-energises the whole circuit. Another complete sc be ordered by the manual push button or an automatic signal from the control clock.

The control clock can be set to activate the circuits from every five minutes to every six hours. The fifty-one feet of 35 m film in the magazine allows up to 450 exposures of 24 x 36 mm frames. This permits up to 37 complete scans without reloading the camera magazines. The aperture, shutter speed and flash power were determined experimentally and designed to allow sufficient depth of field to cater for minor surface irregularities. Fig. 48 shows a photograph taken by this recording system.

7.8. Site ventilation

The experiment site, located in a dead end off the north west corner of Moulton No. 2 Panel, required ventilation to satisfy statutory regulations and to cool experimental plant. Suitable ventilation was achieved by an auxiliary forcing fan taking air from the main return airway. The airstream was directed through ducting to the ramp top area to assist in cooling the compressor and heater/chiller.

FIG. 39 POWER DISTRIBUTION SYSTEM

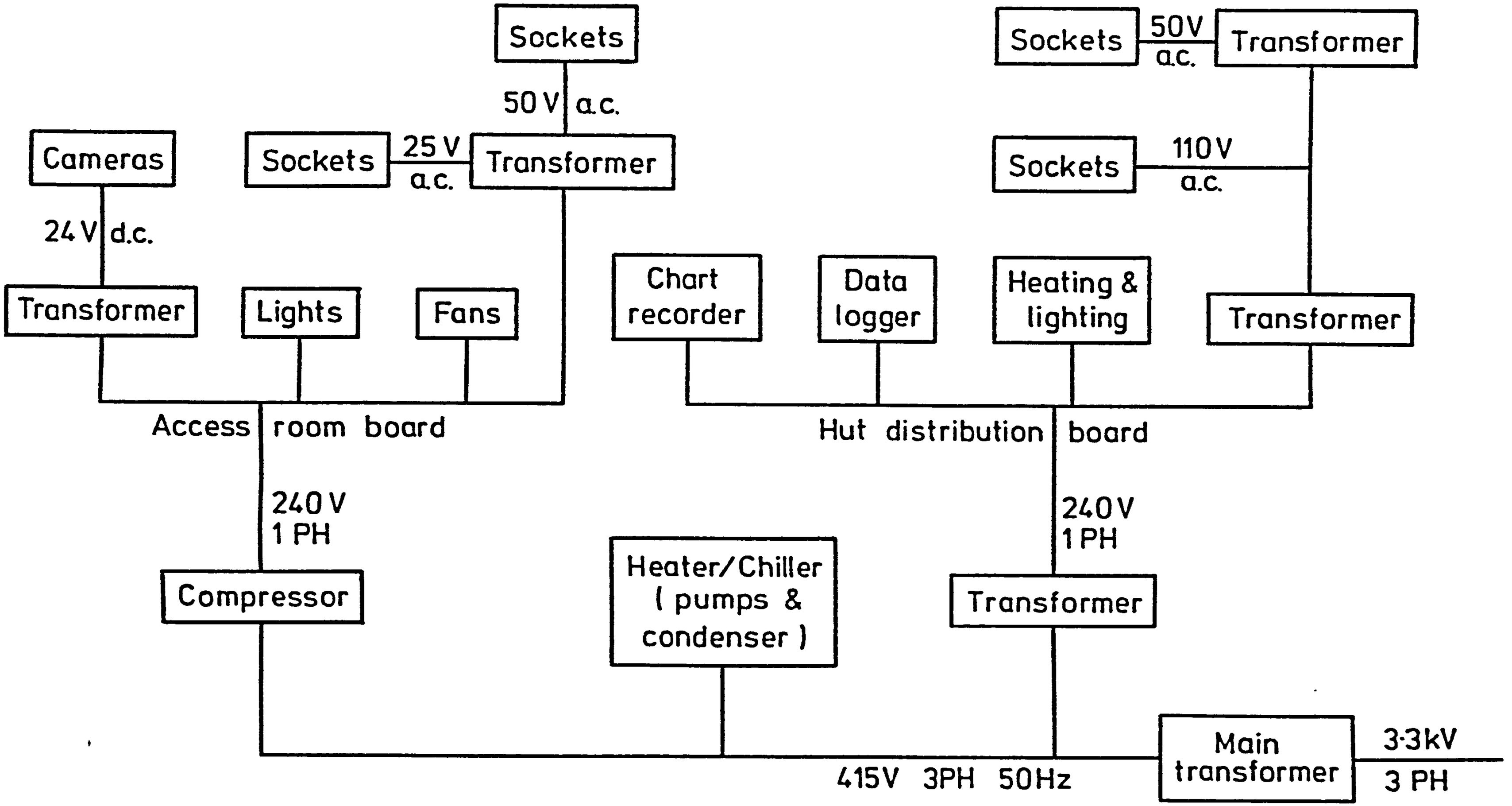

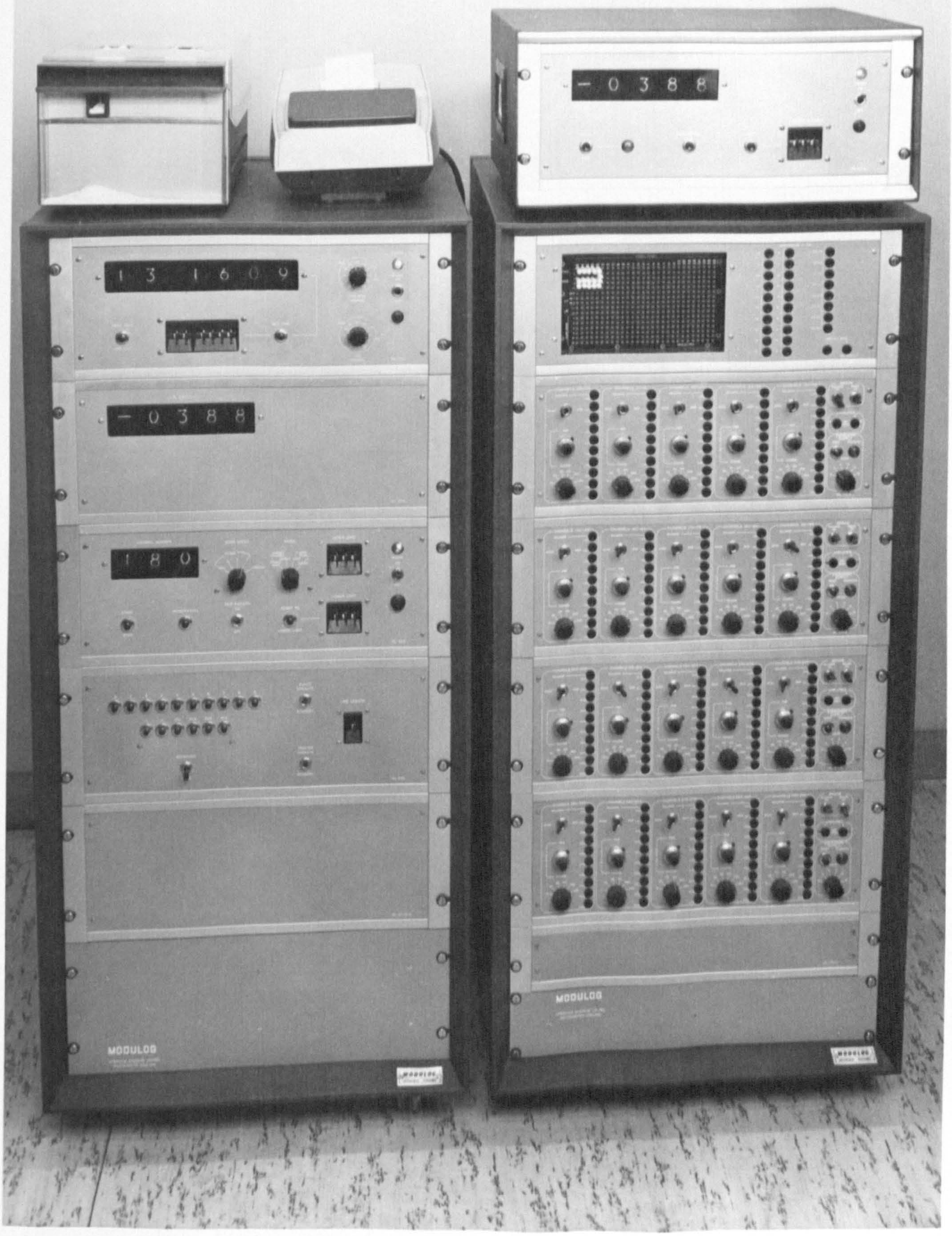

FIG. 40 MODULOG DATA LOGGING SYSTEM

FIG. 41 INTERIOR OF THE INSTRUMENT HUT SHOWING THE CHART RECORDER AND DATA LOGGER

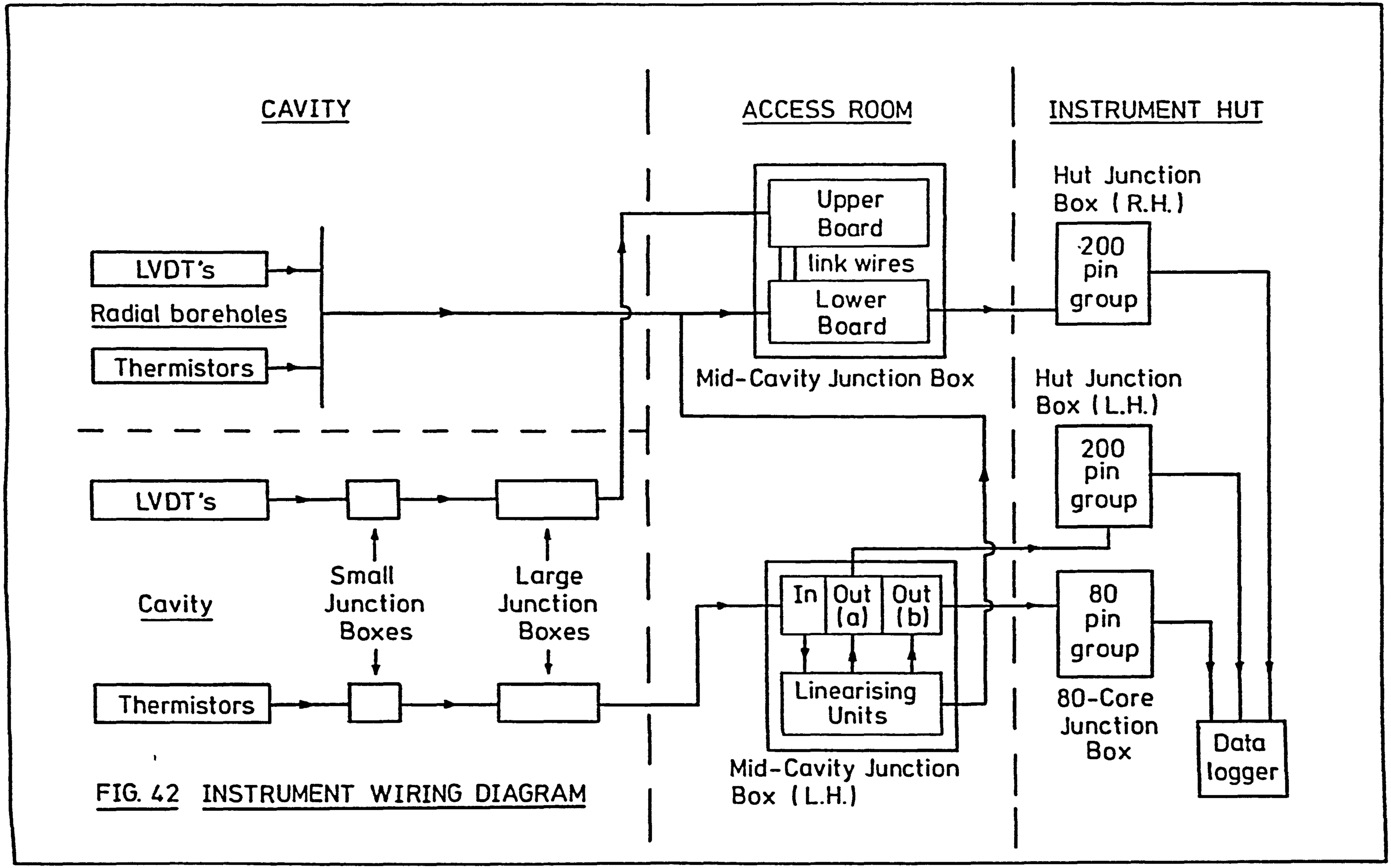

FIG. 42 INSTRUMENT WIRING DIAGRAM

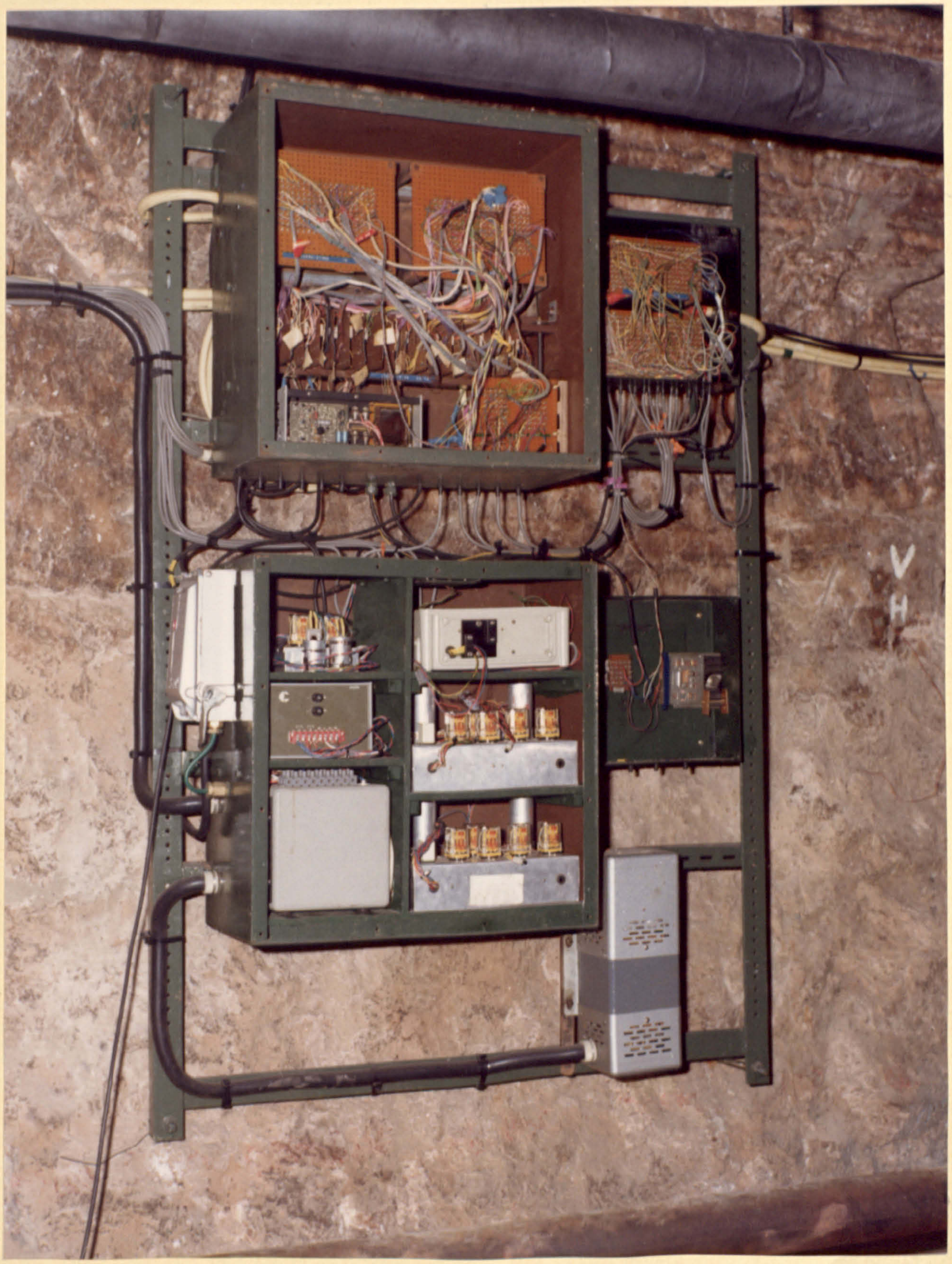

FIG. 43 INSTRUMENT WIRING JUNCTION BOXES

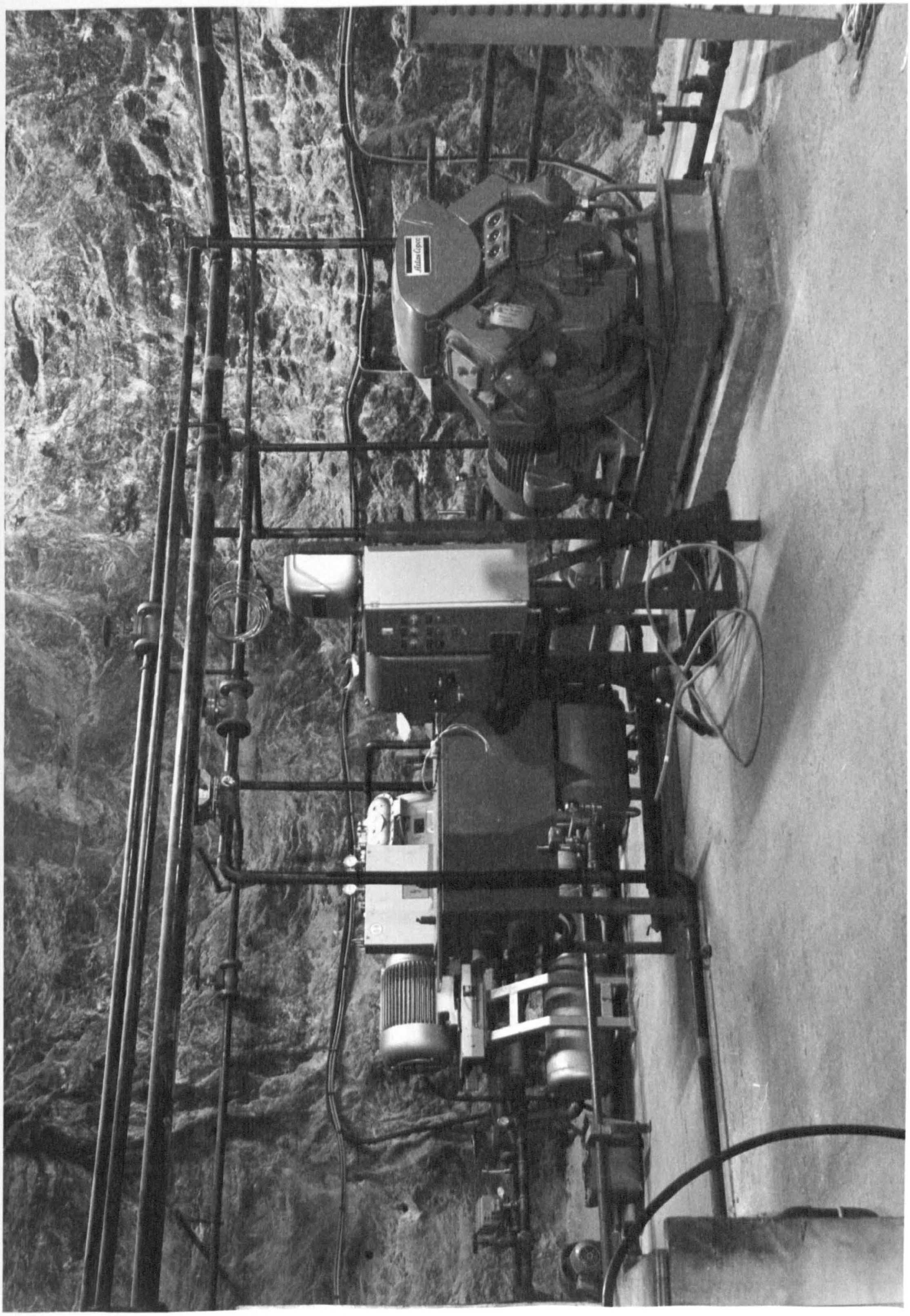

FIG. 44 VIEW OF THE RAMP TOP, WITH THE HEATER/CHILLER ON THE LEFT AND COMPRESSOR ON THE RIGHT.

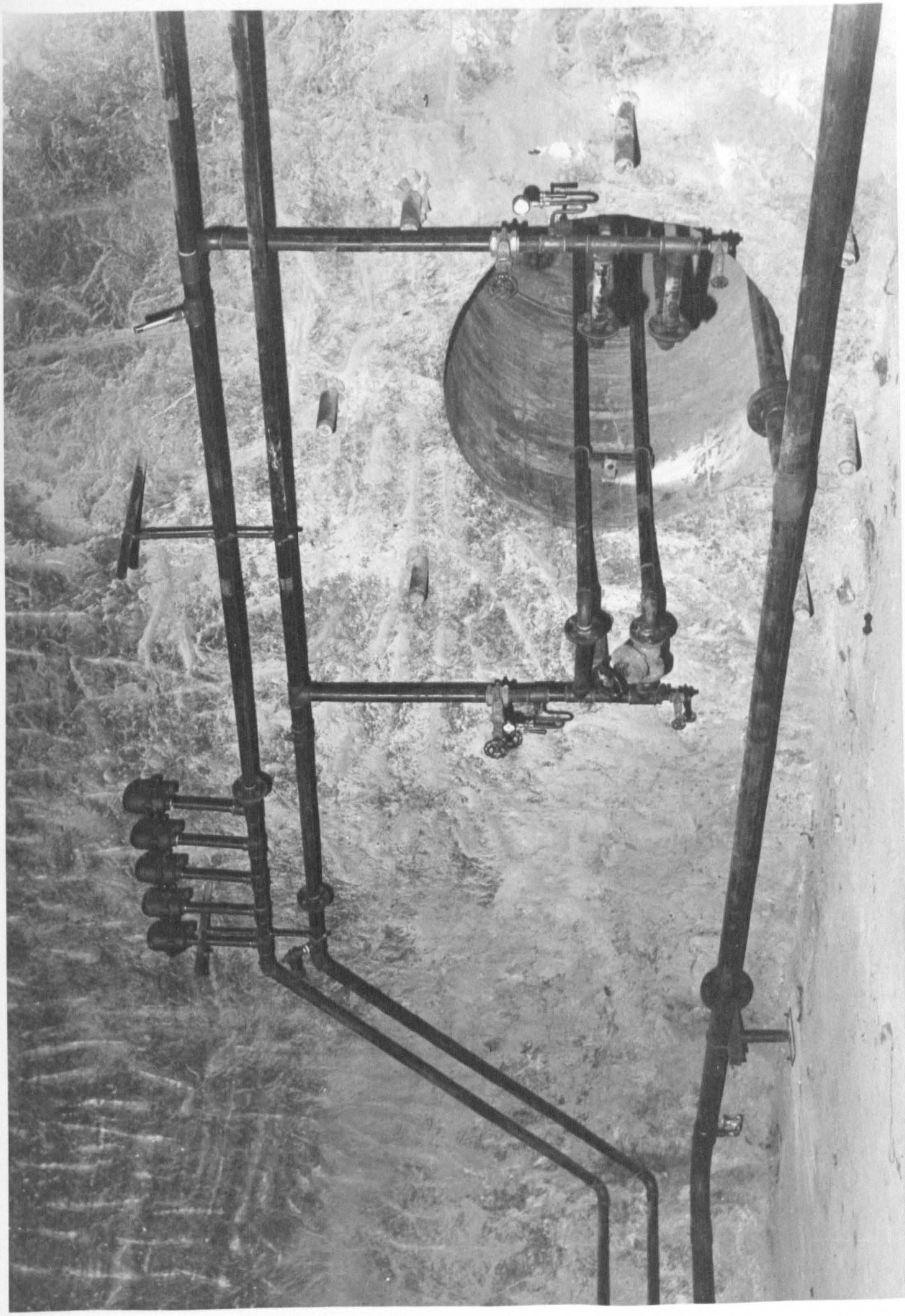

FIG. 45 GENERAL VIEW OF THE ACCESS ROOM SHOWING HEATER/CHILLER AND COMPRESSED AIR PIPEWORK

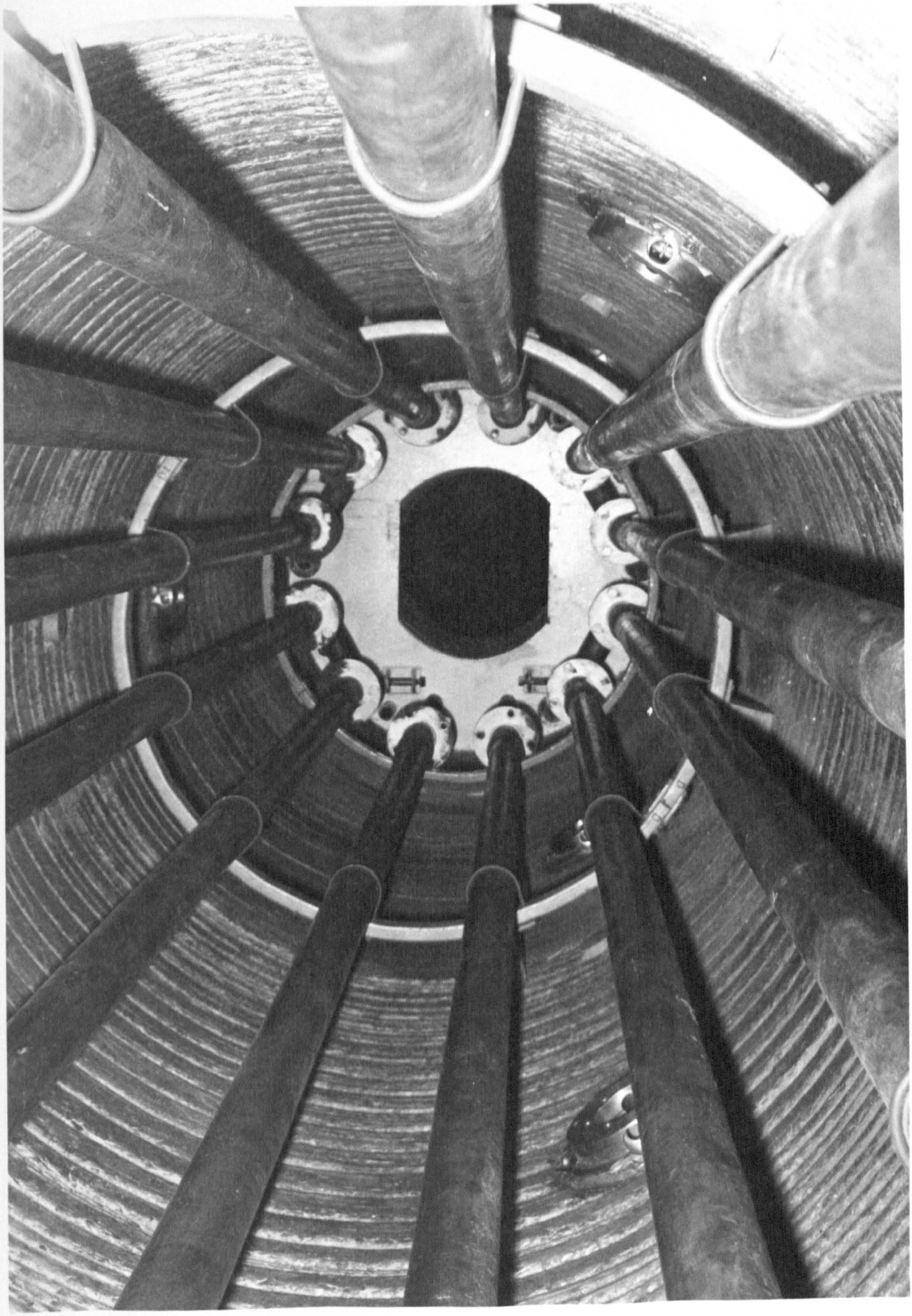

Fig. 46 CAVITY HEAT EXCHANGER

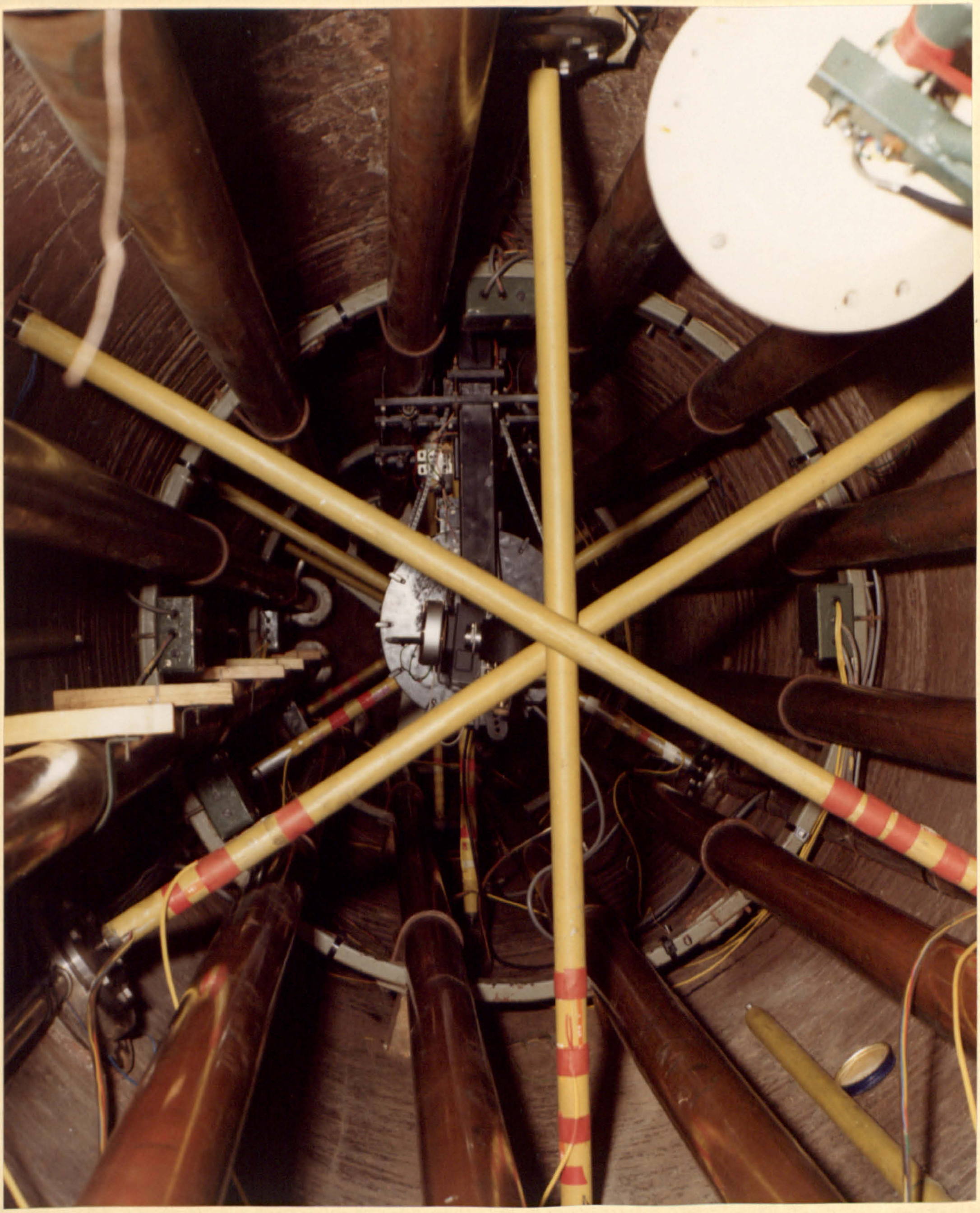

FIG.47 THE INTERIOR OF THE INSTRUMENTED CAVITY

Fig. 48

A PHOTOGRAPH OF THE CAVITY SURFACE TAKEN BY ONE OF THE RECORDING CAMERAS

CHAPTER 8

PROBLEMS ENCOUNTERED DURING THE COMMISSIONING OF THE IN SITU EXPERIMENT

8. PROBLEMS ENCOUNTERED DURING THE COMMISSIONING OF THE IN SITU EXPERIMENT

8.1. Introduction

An in situ experiment of the size and scope described in the previous chapters includes both complex instrumentation problems and engineering difficulties which must be solved before any experimental work can begin. Some of these problems were encountered before the commissioning tests took place whilst others were only discovered during the preliminary runs preceding the actual experiments.

The instrumentation scheme, because of the difficult installation conditions, had many minor faults such as dry soldered joints, short circuits and broken wires but these minor difficulties will not be discussed in any detail. However, both the temperature and deformation measurement systems developed major faults which took many weeks to trace and rectify.

The heater/chiller system posed several problems both during the installation phase and under operational conditions. The compressed air system, apart from cavity sealing problems which were quickly rectified, functioned satisfactorily.

8.2. Deformation transducer problems

A survey of the transducer readings soon after they were installed revealed large fluctuations in their outputs. These fluctuations were of the order of several thousands of an inch. Several explanations could account for the random variations in transducer output:-

(i) Variations in the transducer supply from the 6V d.c. power pack

(ii) Variations in the mine supply to the transducer power pack

(iii) Shunting conductance across transducer terminals due to the hygroscopic salt dust

(iv) Mechanical vibration caused by dump trucks running along a main roadway 150 yards from the cavity.

8.2.1. Investigation of possible causes of transducer failure

(i) The 6V d.c. supply from the transducer power pack was monitored over a period of several hours. This supply was found to be stable to within $\pm$0.17% (the limit of the measuring equipment available at that time) and consequently the transducer power pack was eliminated as a cause of transducer malfunction.

(ii) The stability of mine electrical supplies is notoriously poor due to voltage fluctuations caused by switching of high powered equipment such as winders, crushers and production machines. Electrical power at the Meadowbank Mine can be taken from three sources; the C.E.G.B. grid, the I.C.I. local grid and an emergency generator. Various switching arrangements assured a minimum of 230V from the feeder transformer supplying the transducer power pack.

The supply to the transducer power pack was monitored by a slow-response clockwork recording voltmeter for two days and was at all times between 240V and 250V. The supply was closely monitored over a two hour period and was seen to vary between 246V and 248V.

An ultra violet recorder with a response of 2kHz was connected across the mains supply. This showed a voltage dip of 12V when the cavity compressor was switched on and the winder at No. 3 shaft produced a change of 6V every 25 seconds. The ultra violet recorder was used principally for the detection of transients and none were found. The same trace, shown on a cathode ray oscilloscope, indicated a minor signal of approximately 2 kHz imposed on the mains supply.

These minor variations in the voltage and frequency applied to the transducer power pack could not induce the large fluctuations in transducer output. Although an investigation of the power supply eliminated this as a possible cause of transducer failure it was still felt that the problem was an electrical one. Consequently it was decided to install a transducer power supply system that was completely independent of mains supply.

The alternative power supply was provided by two 12V lead-acid batteries connected in series. These batteries were continuously trickle charged and the 24V output fed to a pair of cascading stabilising transformers. The first transformer took the relatively stable 24V from the batteries and converted it to a stable 12V. The second transformer converted the 12V to 6V and increased the degree of stabilization to 640,000:1. In other words, a fluctuation of one volt from the batteries would be passed on as 1.5uV to the transducer input. The transducer output variation was directly proportional to the input variation, i.e. the percentage output variation would be the same percentage of input variation. The use of this alternative supply ensured that transducer malfunction could not be attributed to random supply variation. The improvement effected by the alternative supply was minimal, and this turn of events directed the investigation towards the transducers themselves.

(iii) Shunting conductance across the transducer terminals was eleminated early in the investigation by drying the cavity with dry air from the cavity air compressor. The transducer terminals were smeared with a desiccative gel with no effect.

(iv) Previous investigations eliminated vibration as a cause of transducer failure. Geophones were cemented to the access room walls and ground vibrations monitored by an oscilloscope. This vibration was negligible and could not cause the transducer malfunction.

8.2.2. Variations in transducer demand

The failure of the alternative supply to rectify the transducer output variations indicated that the problem lay in the wiring or the transducers themselves. Consultations with the transducer manufacturers revealed that the transducers took their supply in pulses to feed the square wave oscillators, and not as a steady d.c. drain. Once this became clear the reason for transducer malfunction was at once apparent. The radial deformation transducers were supplied in groups of four and the diametral deformation transducers in groups of three, i.e., due to space restrictions the groups had common supplies.

The use of a common supply resulted in very fast voltage fluctuations due to the transducer supply pulses occasionally being superimposed on each other. This meant that a transducer supply voltage was often decreased due to the drain imposed by the previous pulse from another transducer. This problem could be eliminated by two methods.

Rewiring the transducer supply so that each had a separate supply would rectify the situation, but this solution was impractical due to lack of space in the cavity. The alternative solution was to connect capacitors across the transducer terminals. Tests in the laboratory indicated that 1000 uF capacitors would effectively decouple the transducers and that the capacitors could withstand at least 3000 psi without damage. When all the transducers were fitted with capacitors, transducer output variations were brought within design limits.

8.3. Investigation into the failure of the temperature measurement system

8.3.1. Discussion of the problems encountered

After the temperature measurement system was installed, it was discovered that the thermistors indicated a temperature much higher than anticipated. Ambient rock temperature was approximately 13°C near the surface, but the thermistors on the first three commutating units indicated between 30°C and 35°C whilst the fourth commutating unit indicated between 8°C and 12°C. These large errors could not be accounted for by a design fault and accordingly the following possible faults were investigated:-

(i) Errors in the wiring system
(ii) Fluctuating power supply
(iii) Short circuits due to condensation
(iv) Thermistor malfunction
(v) Excessive imbalance due to the effect of long extension leads
(vi) Data logger malfunction
(vii) Calibration errors

8.3.2. Errors in the wiring system

The instrumentation circuits were thoroughly checked, and apart from a few minor faults on individual channels, the circuits were found to be in a satisfactory condition and constructed exactly to the design specifications.

8.3.3. Power supply fluctuations

The data logger is powered by 240V a.c. current taken from the mine supply and in turn provides the thermistor bridges with a stabilised 4V d.c. supply. The data logger can tolerate a 10% fluctuation in power supply before its efficient operation is affected. An investigation into the 4V supply indicated a variation of approximately 0.075% which cannot account for the erroneous thermistor readings.

8.3.4. Short circuits due to condensation

Fluctuations in the temperature of the mine air and the exhalation of water vapour by personnel working in the cavity produced a certain amount of condensation. This condensate tended to collect in small pools along the cavity floor and had to be periodically dried out. It was possible that condensation precipitated at certain critical points in the instrumentation circuits could produce short circuits which could in some way affect the thermistor readings. The cavities were dried out using dry air from the cavity compressor and the circuit junction boxes treated with a water dispersent. This treatment did not affect the thermistor readings in any way.

8.3.5. Thermistor malfunction

It was remotely possible that the thermistors could have been damaged by over-heating in the process of soldering on the extension leads. If this had occurred, the resistance of the thermistor would have been increased, causing a low temperature to be indicated on the data logger. However, the thermistors appeared to be reading too high, so apparently they were undamaged. To confirm this nine of the more accessible thermistors were removed from the circuit and brought to Newcastle for testing. All of these thermistors were found to be well within the makers tolerance.

8.3.6. Excessive imbalance due to the effects of long extension leads

The Modulog data logger instruction manual stated that the data logger remote sensing facility eliminates voltage drop effects produced by long transmission cables between the instruments and the data logger. This was extremely misleading as it would only apply to an in situ calibration; the internal arrangements of the data logger are such that only one of the pairs of long leads is taken into account. This resulted in an unwanted imbalance in the bridge circuits.

A further investigation of this problem revealed that the imbalance could not be wholly responsible for the erroneous thermistor readings. Several of the half bridges were reconnected to the data logger on short leads with resistors in place of thermistors to simulate various temperatures. The results of these tests indicated a contraction of scaling from that set in the calibration at Newcastle, although the scaling potentiometers had not been disturbed from their original setting. The scaling contraction was constant within each commutating unit but varied between a factor 3.4 and 4.1 for different commutating units. This gave a definite indication that there was a factor other than the imbalance due to long leads to be considered.

8.3.7. Data logger malfunction

A service engineer from Intercole Systems Ltd., the makers of the data logger, subjected the data logger to a thorough examination and, apart from a faulty fine scaling potentiometer on the block of channels 100-109, found the data logger to be in good working order. The engineer also studied the instrumentation scheme and found no fault with the application of the data logging system.

8.3.8. Calibration errors

The possibility of some error in the calibration procedure causing erroneous thermistor readings was investigated. Any error in the procedure or wiring of the circuits would either cause a massive imbalance of the bridges, or prevent the logging system from working at all. No possible calibration error could account for the apparent contraction in the scaling of the thermistor readings.

8.3.9. Conclusions

It was concluded that the temperature measurement system failed because of two unforseen factors. Firstly, ambiguities in the Modulog data logger manual misled the designer of the calibration system. The manual stated that long transmission lines would not produce any voltage drop effects; internal circuits in the data logger would supply automatic compensation. In actual fact, only one arm of the transmission lines is compensated for, thus producing severe bridge imbalance. It was this factor that was responsible for the zero shift which produced erroneous temperature readings.

However, a second factor in the problem existed, that which produced a scaling contraction. Although a thorough investigation was conducted, both by Modulog and University engineers, this factor was never identified. It was therefore concluded that the only possible recourse was to repeat the thermistor calibration 'in situ'.

8.4. The pressure retaining plug

The first experiment commissioning test involved raising the cavity to 25 psi internal pressure and maintaining this pressure for several hours. The compressor was then shut down and the cavity allowed to unload through natural leakage. The ratio of compressor working time to compressor idling time and the rate of natural leakage indicated a serious leak around the pressure retaining plug.

When the pressure had dropped to 15 psi the area around the plug was treated with soapy water. The resulting bubbles indicated a leak all the way around the plug periphery, with the greatest leakage at the top near to the wedge-shaped excavation used to place the cement. The cable glands and cavity door did not leak at all, but the left hand vent pipe leaked slightly indicating a poor seal on one of the borehole and covers.

The resealing of the plug was undertaken by an I.C.I. engineer conversant with adhesive and sealing technology. Although the University recommended a plastic rather than a brittle sealant, a brittle sealant was used to construct a fillet on the inside interface of cavity and plug. The cavity was pressurised to assist in placing the sealant where it would do the most good. A second 25 psi test suggested that the cavity had been made almost completely airtight.

However, during an experiment conducted in later months, it was discovered that this sealant had broken down and that it was impossible to raise cavity pressure above 160 psi. Consequently, the sealant was removed and replaced by one with some yielding properties. Again the sealant was forced into place using internal cavity pressure. Subsequent tests indicated that the cavity could withstand an internal pressure of 200 psi without excessive leakage overloading the compressor.

8.5. The heater/chiller system

The heater/chiller system, designed to adjust and maintain cavity temperatuee, was subjected to two commissioning tests. The first test involved raising the cavity temperature by $5C^{o}$ and maintaining this temperature, within close limits, for a period of several hours. The second test, following the same procedure, lowered the cavity temperature by $2C^{o}$.

These commissioning tests revealed that the manufacturers had not completed the installation; the automatic control equipment had not been connected to the heater/chiller. Once this work had been completed a further commissioning test indicated wild temperature oscillations of approximately $\pm 2C^{o}$ during heating or cooling. A representative of the control equipment manufacturer, present on site during this test, sdved this problem by replacing a faulty unit in the control cabinet.

A further series of commissioning tests were undertaken to assess whether the heater/chiller could operate to the design specifications. These tests indicated that the response of the heater/chiller was much too slow. The counteracting of temperature changes produced by adiabatic expansion or compression of air stored in the cavity was much too slow, but once the heater/chiller did respond, overshoot occurred. In other words, the heater/chiller allowed the temperature to drift and then over compensated, bringing the temperature too far the other way.

It gradually became apparent that the heater/chiller could not adequately compensate for temperature changes during pressure tests. Adjustments to the control unit and valves in the pipework effected a compromise between sensitivity, overshoot and temperature oscillations. This produced a situation whereby, although the heater/chiller could not control temperature changes due to pressure variations, it could slowly, over a period of several hours, adjust the cavity temperature to a predetermined level, and maintain it to within $\pm 0.2C^{\circ}$.

During the commissioning tests the rock surface temperature was not allowed out of range +5 to $-2C^{\circ}$ of ambient rock temperature. The imposed temperatures were not maintained for long periods, so that the resulting thermal stresses were not high enough to affect the future behaviour of the salt mass surrounding the cavity.

8.6. Compressed air system

The air compressor functioned perfectly apart from one minor fault. The fault was not accurately identified but it exhibited itself in the form of a "high temperatuee warning" alarm. At this time site ventilation involved forcing air through ducting into the access room with a small proportion of the returning air passing over the compressor. It was thought that the compressor overheating was due to an insufficient stream of cooling air passing over the intercooler and aftercooler. Consequently the air duct was broken near the compressor and all the ventilation stream passed over or near the major plant at the ramp top. This action prevented the re-occurrence of overheating and generally improved ventilation in that area.

8.7. The photographic equipment

The photographic equipment was subjected to prolonged tests in the laboratory before installation in the experimental cavity. The initial difficulties encountered with this equipment were associated with minor wiring faults and expsure trials. The only major source of difficulty involved the balance of the camera rotation mechanism.

With the photographic equipment in the dormant position, a peg on the rotation mechanism rested on a microswitch which de-energised the control circuits. However, this microswitch also de-energised the clutch and brake (see Section 7.7.2) and the weight of the large recording camera tended to swing the rotation mechanism out of the dormant position. This allowed the microswitch to close, energise the control circuits and start a new scan. This meant that the cameras would not stop working without opening the isolator controlling the power pack supplying the rotation mechanism.

A mechanical solution to this problem was thought to be more convenient than modifying the control circuits. Consequently a friction brake was fitted to the rotation mechanism. The force exerted by the friction brake was such that the imbalance of the rotation mechanism was counteracted without overloading the camera rotation motor.

8.8. Conclusions

Once the instrumentation scheme and experimental plant had been installed, many months were spent in making the installation perform to design specifications. A great number of minor difficulties were encountered, mostly connected with faults in the complex wiring system.

Rectification of these faults was extremely time consuming due to the intricacy of the system and the cramped working conditions of the cavity.

In addition to the wiring faults, many other minor difficulties were encountered. The printer and punch, which recorded data assembled by the data logger, proved to be rather troublesome. The punch broke down twice within two years and the printer four times. Although the punch eventually gave good service, the printer was abandoned as unreliable. Fortunately the printer was not regarded as equipment essential to the running of the experimental programme. Other minor problems involved equipment connected to both the chart recorder and the data logger. The faults took the form of electrical interaction between the two sets of recording equipment and were solved by duplication of the instruments (e.g. cavity pressure transducer) involved.

The experimental plant, with the exception of the heater/chiller, operated to design specifications. The heater/chiller problem was overcome by only using it for simple temperature tests; temperature variations during pressure tests were avoided by using a very low rate of pressure change. The cavity was made relatively airtight at pressures up to 200 psi without undue difficulty.

CHAPTER 9

RESULTS OF THE INITIAL TESTS

CHAPTER 9

9. THE RESULTS OF THE FIRST SCHEDULE OF TESTS IN THE EXPERIMENTAL PROGRAMME

9.1 The Experimental Programme

The in situ experiment was designed to construct and develop a suitable mathematical model for the evaluation of long term cavity stability. It was hoped that the initial tests would provide the in situ values of the elastic and creep constants. Later tests, operated under different conditions, would indicate the degree of validity of the mathematical model employing these parameters. Finally, a series of cyclical experiments, representing the storage-discharge cycle of an operational gas storage cavity, would investigate the work hardening aspects of rock salt.

Thus the experimental programme could be divided into three phases each being distinguished by the nature of the tests included in that phase:-

(i) Pressure and temperature tests only
(ii) Pressure and temperature combined
(iii) Cyclical tests involving pressure and temperature

The experimental programme consisted of a series of provisional tests. It was intended that subsequent tests, or a whole series of tests, would be modified or even omitted in the light of the information gained from previous tests. Consequently, although a detailed test schedule had been drawn up it was in no way regarded as a rigid plan of action. The major theme of the test programme was one of flexibility, with constant revision of the programme eliminating or introducing new tests according to the results of previous experiments.

9.1.1 Phase I of the experimental programme

The first phase of the tests, immediately following the 25 p.s.i., +50° and -20° commissioning tests, was designed to determine the in situ values of the creep and elastic constants. The provisional test schedule for Phase I of the experimental programme is shown in Table 9.

TABLE 9

Phase I test schedule

Test No	Pressure Limit (psi)	Temperature Limit (°C from ambient)	Maximum surface σ_θ		Maximum surface σ_z	
			Top	Side	Top	Side
1	0 - 100 - 0	0	-350	-950	-480	-720
2	0	0 -(+10) - 0	-940	-1540	-970	-1210
3	0 - 150 - 0	0	-300	-900	-480	-720
4	0 - 200 - 0	0	-250	-850	-480	-720
5	0	0 -(-5) - 0	-205	-805	-235	-475
6	0	0 -(-10) - 0	+40	-560	+10	-230

These tests were designed to provide information without inducing failure of the cavity surface. No limits were imposed on any compressive increase in the stress components since these are never greater than 1800 p.s.i. (an increase of 750 p.s.i. from the ambient stress level) and rarely greater than 1500 p.s.i. However, to preserve the integrity of the cavity, induced tensile stress levels were restricted to an approximate zero stress condition. Thus the maximum tensile stress imposed by any Phase I test was a

tangential stress of +40 p.s.i. in the surface of the cavity roof and floor, induced by a cavity surface temperature decrease of 100°.

As far as possible, the test schedule was arranged on a principle of increasing severity of test conditions. However, test severity was estimated theoretically, using assumed values for the material parameters. Experimental results, indicating a need for significant modification of the assumed values of the material parameters, could drastically alter the test schedule.

9.1.2 Later phases of the experimental programme

Phases II and III of the experimental programme were not planned ahead in any great detail. It was felt that planning this work without any information from Phase I would be a pointless exercise. Consequently, detailed schedules of experiments involving both temperature and pressure, and cyclical experiments, were postponed until such a time when more information was available.

9.2 Experimental Procedure

An experiment in Phase I of the test schedule could take one of three forms:-

A: Pressure test at ambient temperature
B: Temperature increase at atmospheric pressure
C: Temperature decrease at atmospheric pressure

All of these tests involve a complex instrumentation scheme and the efficient operation of the experimental plant, and such was the

complexity of running an experiment that some form of check list was thought necessary. The purpose of the check list was to avoid errors in procedure and to detect equipment malfunction. The check list was divided into thirteen sections, with the code letters following each section description indicating the nature of the tests, as given by the above table.

Section		Test Application
1	Initial action	A B C
2	Instrumentation check list	A B C
3	Heater/Chiller start-up	A B C
4	Cavity check list	A B C
5	Compressor check list	A
6	Heater/chiller run-above ambient	B
7	Heater/chiller run-below ambient	C
8	Heater/chiller run-at ambient	A
9	Cavity pressurisation	A
10	Cavity de-pressurisation	A
11	Returning temperature to ambient	B C
12	Emergency shut down	A B C
13	Normal shut down	A B C

The test procedure check list deals with the minutia of running an experiment, so it is not proposed to describe it in any great detail. Very briefly, Sections 1 to 5 verifies that both the instrumentation and experimental plant are functioning correctly; these checks take approximately three hours to complete. Sections 6 to 9 describe the procedure for imposing upon the cavity the desired test conditions, whilst Sections 10, 11 and 13 deal with returning the cavity to its original state.

The time taken in altering the state of the cavity may be estimated from the loading rates employed in these experiments. Pressure was increased or decreased at the rate of 0.5 p.s.i./min; any increase of this rate tended to change cavity temperature. The rate of temperature change, limited by the capacity of the heater/chiller, was approximately 1 C°/hour.

Section 12 of the test procedure deals with an emergency condition indicated by warning lights and an audible alarm. As such an emergency could result in serious damage to the cavity and associated equipment, this Section will be described in more detail.

The alarm system could be triggered off by either the cavity temperature drifting from its set point or by plug movement. Reference to the chart recorder would indicate whether this was in fact an alarm condition and not alarm malfunction. If the alarm was due to alarm malfunction the experiment would be continued with temperature and plug movement being closely monitored on the chart recorder. A high/low temperature alarm would be answered by shutting down the heater/chiller and allowing the cavity to reach ambient temperature by natural heat dissipation. This type of alarm would not be regarded as an emergency and normal shut-down procedures would be followed.

If excessive plug movement activated the alarm system, the leader of the two man team operating the experiment would hit the compressor emergency stop button mounted on the outside wall of the instrument hut and run to the top of the ramp. At the ramp top he would open the blowdown valve, isolate the compressor air receiver from the cavity, and finally take shelter in a place of safety until the cavity was fully depressurised.

The second team member would monitor plug movement on the chart recorder, and if the plug appeared to be definitely failing despite the reduction in cavity pressure, he would push the heater/chiller emergency stop button to prevent refrigerant being pumped through ruptured heat exchanger pipes.

9.2.1 Data aquisition

The cavity loading procedure involved a great number of instrument and equipment checks. Once these checks had been completed cavity loading could begin.

The data logger was adjusted to record at a rate of ten channels per second and initially was set to take one complete scan of readings every ten minutes. When the cavity was at the required state of loading the scan cycle was changed to one scan per hour for several hours, and if the test required long term loading, the scans were reduced to one every eight hours. Similarly, one scan/hour was the scan rate employed during the few hours before and after unloading and a scan rate of one scan/10 minutes used during the actual unloading cycle of the experiment. This ensured that data aquisition was biased towards the most critical phases of the experiment.

An investigation of the punched paper tape system and data storage facilities on the IBM 360/67 computer indicates why this biassing was necessary. One complete scan of channels uses approximately twenty feet of paper tape and occupies 2,400 bytes of computer core space. The available core space limits the total number of scans to approximately 100 with a resulting tape length of 2000 feet or 3/8 mile. The core space limit is not absolute; various computing techniques can circumvent this problem but requires a great deal of computing time. It is therefore much more convenient to limit the number of recorded scans and bias these towards the loading/unloading sections of the

experiment and to record static or slow moving conditions less frequently.

9.2.2 Cavity pressurisation

Cavity pressurisation could begin after the necessary instrument and equipment checks had been completed. The drain valves in the plant and air lines were opened to release any condensate and the main blow-down valve opened. The cavity air pressure control valve was set to zero pressure and the compressor started. The drain valves were closed and cavity pressure increased by the combined operation of slowly closing the blowdown valve and adjusting the pressure control valve. The cavity pressure was increased at the low rate of 0.5 psi/min, to eliminate increases in cavity temperature, and was automatically stabilised at the required pressure by the pressure control valve. The heater/chiller, although not used in pressure tests, was kept at standbye in readiness to counteract any unexpected temperature changes.

When the cavity was at high pressures (near to 200 psi), depressurisation was initiated by lowering the set point of the pressure control valve to give an unloading rate of 0.5 psi/min. Once the pressure was down to approximately 150 psi, the compressor could be shut down and the air receiver isolated from the cavity. At these pressures the cavity could unload by natural leakage without the air discharge rate affecting cavity temperature. When the cavity was below 100 psi natural leakage did not produce a high enough air discharge rate and unloading was assisted by cracking a small diameter air cock. This air cock was used to lower the cavity to atmospheric pressure.

9.2.3 Cavity temperature control

The adjustment of cavity temperature could commence after the heater/chiller hot and cold storage tanks had reached their operating temperatures (-15°C and +50°C respectively). The pointer on

the temperature control panel was set to the desired temperature and the control panel was switched to "automatic control". Opening a valve allowed the motorised control valve to pass the refrigerant, drawn from the storage tanks, to the heat exchanger. To prevent overshoot, the control equipment was set to raise the temperature slowly and this resulted in a change of cavity temperature rate of approximately $1C^{o}$/hour.

The control equipment would maintain the cavity surface temperature at the desired level to an accuracy of $\pm 0.2C^{o}$. The cavity surface temperature was returned to ambient rock temperature by setting the control pointer to the desired temperature and allowing the heater/chiller to automatically adjust the flow of heat through the heat exchanger.

9.2.4 Combined pressure and temperature experiments

A cavity loading condition involving both the application of pressure and temperature differences is achieved by first imposing the desired pressure, as described in Section 9.2.2. and then applying the temperature difference, as described in Section 9.2.3.

9.3. The 100 p.s.i. Test

The first experiment involved raising the cavity to 100 psi and maintaining this pressure for a period of three days. This test was designed to give some indication of the in situ value of Young's Modulus and, should the pressure prove to be high enough, would provide data for creep analysis.

The cavity was raised to 98.0 psi over a period of 2½ hours without undue temperature fluctuations. Initially the temperature of the cavity was inadvertently raised (by too great a rate of pressure increase) by 1C°, but the temperature was quickly and finally stabilised at between 0.1 and 0.2C° below ambient.

The cavity was slowly returned to atmospheric pressure over a period of six hours, during which time the temperature decreased to 0.3C° below ambient. The instrumentation scheme was allowed to record for five days after the return to atmospheric pressure in order to detect any relaxation phenomena.

9.3.1 Longitudinal deformation

The accuracy of the mean of the reading from the deformation transducers, according to a statistical analysis of long term steady-state readings, was of the order of $\pm 0.075 \times 10^{-3}$ inches. The magnitude of longitudinal deformation was so small that it did not fall within the accuracy of the measuring system, and for the purposes of this test was regarded as being zero. Therefore the cavity could be considered to have been in a condition of plane strain.

9.3.2 Diametral deformation

The diametral deformation was recorded by the extensometers located at Stations A and C; the diametral extensometers at Station B, although appearing to be operational prior to the experiment, failed to record any deformation. This fault was later traced to a dry soldered joint in the instrument supply lines. The diametral deformation resulting from this test is shown graphically in Figs. 49 and 50.

Referring to Figs. 49 and 50, it can be seen that the diametral deformation increased uniformly with the uniform increase in cavity pressure. At the peak pressure of 98.0 psi a diametral deformation of 1.1 x 10^{-3} inches was recorded. The graph of deformation against time, shown in Fig. 49 indicates that either creep is absent or is too small at this pressure to be detected by the measuring system. Therfore only elastic parameters could be derived from the results of this experiment as the cavity loading was not great enough to cause time-dependent deformation.

The elastic behaviour of the rock salt mass during the loading cycle was repeated during the unloading cycle. Unfortunately, the measurement of relaxation behaviour or permanent set was prevented by a breakdown in the deformation measurement system. This may best be seen in Fig. 49. Cavity depressurisation (taking place on Day 4 of the experiment) allowed the diameter of the cavity to return to within 0.1 x 10^{-3} of its original dimension. However, immediately after depressurisation, all the transducer readings showed a steady but sudden increase. Thus the unloading cycle showed a return from the 1.1 x 10^{-3} in. deformation at 98 psi to 0.1 x 10^{-3} in. at atmospheric pressure, quickly followed by a sudden increase to approximately 0.3 x 10^{-3} in. After 3 days the transducer readings dropped to approximately 0.1 x 10^{-3} in. This erratic behaviour was traced to a fault in the transducer decoupling circuits involving the capacitors used to stabilise transducer output.

9.3.3 Radial deformation

The data obtained from the radial deformation transducers in this test was not at all conclusive. The lack of reliable information was due to two factors:-

(i) The optimum value of the decoupling capacitors in the modified transducer supply circuits had not been firmly established at this time. Consequently only 19 of the 36 radial deformation transducers performed to design specifications. Increasing the value of the decoupling capacitors to 1000uF avoided this problem in future tests.

(ii) The most important reason for the lack of conclusive data was the magnitude of the recorded radial deformation. The transducers connected to the No. 1 anchors (the anchors ten feet along the radial boreholes) registered a maximum deformation of approximately 0.3×10^{-3} inches. This deformation was thought not to be of a sufficient magnitude for meaningful analysis. A graph of deformation against time for No. 1 anchor in the vertical borehole of Station C is shown in Fig. 51 and is typical of the radial deformation recorded in this test.

It can be seen from Fig. 51 that the radial deformation transducers suffered from the same "bounce" in instrument readings as the diametral deformation transducers.

9.3.4 Conclusions

The 100 psi test was the first experiment in Phase I of the experimental programme. Although some of the results were not conclusive, and instrumentation problems were encountered, the overall pattern of results suggested that the experiment was successful and that the installation was performing to design specifications.

A cavity pressure of 100 psi was not high enough to induce either severe elastic deformation or any observable time-dependent deformation. This resulted in cancelling the planned 150 psi test and replacing it with a test involving a cavity pressure of 200 psi. It

was felt that a 150 psi test would not provide information any more conclusive than the 100 psi test and that a 200 psi test, according to data derived from the 100 psi test, would not induce cavity failure.

A comparison of the results from instruments which should indicate the same readings under test conditions showed that cavity deformation, as expected, was symetrical about the cavity axis.

The results of the 100 psi test were used to calculate the in situ value of the Young's Modulus of rock salt. The radial displacement of the cavity surface may be expressed by:-

$$U_r = \mu P a \qquad (50)$$

where $$\mu = (1+\upsilon)\frac{}{E}$$

Substituting the values of

$$Ur = 0.55 \times 10^{-3} \text{ in.}$$
$$P = 98 \text{ psi}$$
$$a = 24 \text{ in.}$$

the value of μ may be calculated. Using assumed values of Poisson's ratio the Young's Modulus can be calculated. The resulting values of Young's Modulus, and those values derived from the later 200 psi tests, are given in Table 10. The value of μ was calculated to be 0.233×10^{-6}

TABLE 10

The in situ value of the Young's Modulus of rock salt

Assumed value of Poisson's ratio	E x 10^6 p.s.i.		
	100 p.s.i.	3 - day 200 p.s.i.	10 - day 200 p.s.i.
.25	5.36	5.58	5.74
.30	5.58	5.79	5.97
.35	5.79	6.02	6.20
.40	6.01	6.25	6.42
.45	6.22	6.46	6.65
.50	6.44	6.69	6.88

Previous workers in this field (13,14) have, by laboratory tests obtained values of the Young's Modulus of Winsford rock salt ranging from 0.5 to approximately 3 x 10^6 psi, with 1 x 10^6 psi being accepted as a representative value for theoretical and design work. This may be compared with the values of 3.4 to 3.7 x 10^6 psi obtained by laboratory tests on the cavity pilot hole cores, given in Table 4 of Section 4.3.3 (iv). The in situ value of Young's Modulus, given in Table 10, clearly illustrates the problems facing the rock mechanics engineer, that of relating the values of material parameters obtained by laboratory work to the in situ condition. Thus, estimates made in the past of the in situ stress of rock salt, based upon strain measurements, should be revised.

9.4 The +10C° Test

The second experiment in Phase I of the test programme involved raising the temperature of the cavity surface by 10C°. Ambient rock surface temperature in the vicinity of the experimental cavity averaged 13.5°C and the cavity surface temperature was accordingly raised to approximately 23.5°C in just over six hours. The cavity door was bolted in the closed position and the compressed air inlet vented to atmosphere.

The cavity surface temperature was maintained between 23°C and 24°C for a period of three days, during which time the effect of the surface temperature increase upon radial temperature gradient development and rock deformation was observed. The cavity surface temperature was then returned to ambient rock surface temperature by a combination of natural heat sissipation and the heater/chiller. The return to ambient temperature took approximately 10 days, the low rate of temperature decrease being partly due to the capacity of the heater/chiller and partly due to the necessity of avoiding an accidental imposition of a large temperature decrease on the cavity surface.

This experiment had two objectives; firstly to determine the value of Poisson's ratio, ν, and also to determine the value of the coefficient of thermal expansion of rock salt, α. Although both the linear elastic model and the linear visco-elastic model predicted no movement of the cavity surface, the movement of a point in the rock mass at a distance r from the cavity centreline would assist in the determination of ν. (16, 23).

The slope of the graph of Ur against θ/r will determine the paramrter m, where :-

Ur = displacement of a point at relative to the cavity centreline

$a < r < R$ where a = cavity radius R = distance at which the rock mass behaviour is uninfluenced by the cavity

$\theta = \frac{1}{a}\int_R^a rT\,dr$ were T = temperature

$$m = \alpha\frac{(1+\nu)}{(1-\nu)}$$

The results of this experiment indicated that the transducer temperature correction system was ineffective. Section 6.6 discusses

the installation of thermistors monitoring instrument temperature used in the calculation of the temperature correction factors. Taping thermistors to the transducer housings proved inadequate as they registered much higher temperatures than the transducers themselves. Consequently, no great reliance was placed on the longitudinal and diametral extensometer readings of this test. The instrument temperature monitoring thermistors were subsequently relocated inside the housings, close to the transducers.

9.4.1 Longitudinal deformation

The longitudinal extensometers indicated an average deformation of approximately 3×10^{-3} ins. when the cavity had reached the desired temperature. This deformation could be seen to follow instrument temperature rather than cavity surface temperature and it was concluded from this that over-compensation for instrument temperature variations was taking place. Relocating instrument temperature monitoring thermistors solved this problem in future tests. Bearing in mind the apparent lack of longitudinal movement in the 100 psi test, it was tentively concluded that the 3×10^{-3} ins. movement recorded in the $+100^{\circ}$ test was due to instrument temperature effects.

9.4.2 Diametral deformation

The diametral deformation recorded in this test suffers from the same inaccuracy as the longitudinal deformation readings. However, if 3×10^{-3} ins. is subtracted from the readings at peak temperature, a very approximate quantitative result will be achieved. Although the results of this test give an approximate quantitative description of the deformation, no great reliance will be placed upon this, and the results only discussed in a qualitative manner.

A graph of cavity surface temperature against average diametral deformation, shown in Fig. 52, indicated that almost no movement of the cavity surface took place until its temperature had increased by approximately 50°. Then the cavity slowly began to deform and when the cavity surface temperature had reached approximately 100° above ambient the cavity exhibited time-dependent deformation behaviour and continued to rapidly deform despite no increase in cavity surface temperature. The cavity continued to show this time-dependent deformation at the end of the test when the cavity surface was being restored to its original temperature. The restoration of the cavity surface to its original temperature left the cavity with a permanent set of approximately -16 x 10^{-3} ins, thus reducing its diameter.

Although no great reliance is placed quantita tively on the results, a qualitative explanation of the cavity behaviour may be given. The linear elastic and linear visco-elastic models predict no movement of the cavity surface; all rock movement takes place between the cavity surface and a point remote from the cavity. However, this prediction only holds up to the elastic limit of the material, and once this has been passed, time-dependent deformation takes place. It can be shown that an imposition of a 50° temperature difference on the cavity surface, when considered in the light of the unexpectedly high in situ value of Young's Modulus, generates a tangential stress in the cavity surface of approximately -2000 psi. Investigators (13, 14) of the creep properties of rock salt have suggested, that time-dependent behaviour generally becomes most marked at stresses at and above this value.

Fig. 53 shows a graph of mean diametral deformation and cavity surface temperature against time. It can be seen from this graph that once the cavity surface was at the required temperature, the cavity diameter was progressively reduced by approximately 14.5 x 10^{-3} ins. during the three days this temperature difference was maintained. The cause of the irregular pattern of results towards the end of this

test was eventually traced to interaction between the transducer signal leads and electro-magnetic fields generated by the camera rotation mechanism. This problem was avoided in future tests by ensuring that data logger instrument scans did not take place at the same time as camera scans.

9.4.3 Radial deformation

The pattern of radial rock deformation predicted by the linear elastic and linear visco elastic models is rather complex. Although no movement of the cavity surface should take place at low stress levels, the rock surrounding the cavity should move, i.e. a density modification of certain sectors of the rock will take place.

A graph of radial deformation and cavity surface temperature against time is shown in Fig. 54. The deformation plotted is that of the rock surrounding the vertical borehole at Station B, which, being in the centre of the cavity is more likely to be in a state of plane strain than the other two stations.

The deformation plotted in Fig. 54 is the relative movement between the four anchors and the cavity surface. This graph should be referred to in conjunction with Fig. 55, which converts the deformation to strain between each of the five points in the measurement system. It can be seen from Fig. 55 that the high deformation indicated by Anchors 1 and 2 in Fig. 54 is almost entirely due to rock movement near the cavity surface. Fig. 55 suggests that the rock near to the cavity surface expands, part of this expansion causing a reduction in cavity diameter and part contributing towards the compression of the rock between Anchors 1 and 3.

The complexity of the patterns of rock deformation in this test is due to two factors; firstly, at high stresses (c. -2000 psi), time-dependent deformation is induced and the magnitude and direction of this deformation is governed by the radial temperature distribution,

which in the context of this experiment, is time dependent. At the time of writing, the radial deformations had not been subjected to a quantitative analysis, but qualitatively the results fit the linear visco-elastic model.

9.4.4 Conclusions

The inadequacies of the temperature compensating system of the longitudinal and diametral extensometers rendered inaccurate the results from those instruments. Although no great reliance is placed on these results, it appears that the zero surface movement prediction of the linear visco-elastic model is confirmed. A qualitative analysis of the recorded radial deformations suggests that the rock mass surrounding the cavity does not seriously differ from that predicted by the linear visco-elastic model, although a qualitative analysis of these results would prove more profitable.

9.5 The 200 psi Test

The cavity was raised from atmosphere to 196 psi in four hours and twenty minutes with a cavity surface temperature increase of a few tenths of a centigrade degree. This pressure was maintained for just under three days in order to observe any time-dependent deformation.

The cavity was restored to atmospheric pressure over a period of seven hours during which time the cavity surface temperature decreased by a maximum of 0.26 C^{o}. The instruments were monitored for a further four days to detect any relaxation phenomena.

9.5.1 Longitudinal deformation

Once again the magnitude of the mean longitudinal deformation was so small that it did not fall within the accuracy indicated by the

statistical analysis of long term steady-state readings. The deformation was of the order of 0.05×10^{-3} ins.

9.5.2 Diametral deformation

All the diametral extensometers were operational during this test and indicated a mean deformation 2.11×10^{-3} ins. at 196 psi. Fig. 56 shows a uniform increase in cavity diameter with increasing pressure whilst Fig. 57 shows changes in cavity diameter during the three day period of constant load.

With the cavity under the constant load of 196 psi internal pressure the mean diameter increased at a rate of 8.1×10^{-8} in/min. Although this increase in cavity diameter was indicative of time-dependent deformation the results were by no means conclusive. Further investigation of this phenomenon was undertaken by introducing two new tests:-

(i) Test 4 in the series would monitor transducer output over a period of nine days, whilst the cavity was not under any artificial load. This would give an indication as to whether the apparent creep detected in Test 3 was due to transducer drift.

(ii) Test 5 was planned to be a repeat of Test 3 with the cavity held at full pressure for ten days. It was hoped that the longer period of cavity loading would produce more conclusive data on time-dependent cavity deformation.

The elastic behaviour of the rock during the loading cycle was repeated during the unloading cycle, at the end of which a deformation of 0.34×10^{-3} in. was recorded. During the following four days with the cavity at no load, the instruments were scanned

every eight hours to detect any cavity relaxation. The mean cavity diameter was observed to decrease from the 0.34×10^{-3} above the original diameter, to 0.26×10^{-3} in.

9.5.3 Radial deformation

The results of this and previous experiments had indicated that although a high degree of accuracy could be achieved by the transducers, there was a suggestion of instrument scatter and a possibility of drift. Thus the first reading from an instrument in a test may not be truly representative, the actual reading falling somewhere within the instrument scatter range.

This situation was to some extent anticipated, although the range of scatter was higher than expected. This problem was countered in two ways. Firstly a test was planned to investigate instrument scatter and drift, and also, the zero point for each instrument in a test was obtained by averaging readings from several preliminary zero scans. Unfortunately, the procedure for obtaining realistic zero points for the instruments in this test was omitted, and although the results from the longitudinal and diametral extensometers did not appear to be seriously affected, the lower values of readings from the radial extensometers were partially obscured.

For this reason a graph of the results from the radial extensometers will not be presented here although an approximate degree of radial deformation at 200 psi may be obtained from the following table.

	Anchor No.			
	4	3	2	1
Distance from cavity surface (ft.)	10	4	2	0.75
Deformation (1×10^{-3} ins)	0.45	0.30	0.35	0.07

Detailed and more accurate results of radial deformation at 200 psi cavity pressure will be given for the extended 200 psi test following the instrument scatter test, as discussed in Section 9.5.2.

9.5.4 Conclusions

The results of the 200 psi were not conclusive. The test was designed to subject the cavity to time-dependent deformation, but the short period of cavity loading (3 days) made it difficult to distinguish between creep and a possible instrument drift. The results from the 200 psi initiated two further tests, designed to clarify this situation.

The proposed tests were:-

(i) Instrument Scatter and drift test

(ii) Long term 200 psi test with the cavity under load for 10 days.

9.6 The Transducer Drift Test

The cavity was left for a few days to stabilise at atmospheric pressure and ambient rock temperature, and then over a period of nine days, the instruments were scanned once every eight hours. The results from the diametral extensometers were selected for detailed analysis and the following conclusions drawn.

The readings from each of the nine transducers considered fluctuated about their zero point, i.e. their initial reading, and this fluctuation had a range of 0.68×10^{-3} ins. However, this high value

was largely due to two readings, erratic maximum and minimum readings recorded by extensometers BV and BR respectively. If these two readings are excluded, the range of all the transducer readings reduces to 0.41×10^{-3} ins, with a standard deviation of 0.074×10^{-3} ins.

If the average transducer readings at one scan is plotted against time there appears to be a suggestion of a slight upward drift. A linear regression of this graph, shown in Fig. 58, indicates an upward trend of 0.4×10^{-8} in./min with a standard deviation of the slope of 0.25×10^{-8} in./min. As there is no apparent instrumentational explanation for the drift, and it cannot be attributed to creep due to overburden pressure, this phenomena must be investigated in more detail. It is quite possible that further analysis could show that this drift is not statistically significant.

The importance of instrument drift in relatively short term creep measurement requires that this problem must be resolved. A statistical technique must be used first of all to establish the existence of the drift, and if the drift is proved to be statistically significant, a technical investigation in conjunction with the transducer manufacturers may provide the answer to this problem.

The range of the mean transducer readings plotted in Fig. 58 was 0.14×10^{-3} in. with a mean of 0.042×10^{-3} in.

9.7 The extended 200 psi test

The cavity was pressurised to 200 psi in just under six and half hours with a minor temperature increase of $0.2^{\circ}C$. This pressure was maintained for approximately ten days. However, on the third day of cavity pressurisation, a mine power failure cut off all electrical power to the experimental site. The enforced shut down of the

compressor allowed the cavity to depressurise to 156 psi in a period of just over one hour. The cavity was immediately repressurised once power was restored.

In previous tests the air pressure transducer was connected to both the data logger and chart recorder. Electrical interaction between the two recording instruments required a second pressure transducer to be added to the instrumentation scheme so that each recording instrument was fed by a separate pressure transducer. The new transducer, coupled to the data logger proved to be slightly unstable when compared with the original on the chart recorder, pressure gauges and experience of the pressure control equipment. This was later traced to a minor electrical fault, but resulted in the poor accuracy of $\pm$ 5 psi on data logger pressure readings. These readings were corrected by referring to chart recorder readings.

At the end of ten days at 200 psi, the cavity was returned to atmospheric pressure in a period of eight and a half hours with an overall temperature decrease of $0.4C^{\circ}$. The instruments were scanned every eight hours for a further four days to record any relaxation phenomena.

9.7.1 Longitudinal deformation

The overall mean longitudinal deformation was -0.3×10^{-3} ins at full pressure. The results of the previous transducer stability test would indicate that the cavity was in a state of plane strain.

9.7.2 Diametral deformation

The mean diametral deformation is shown plotted against time in Fig. 59. The pressure reduction during the third day of pressurisation is clearly reflected in the reduction of deformation seen in the full

plateau. This graph of deformation against time indicates linear elastic behaviour in both the loading and unloading phases of the experiment, with a suggestion of creep occurring during the ten days at full pressure. A linear regression of the deformation at full pressure gives an increase in deformation of 1.3×10^{-8} in/min which may be compared with the 8.1×10^{-8} in/min recorded during the three day 200 psi test. Both these values must be considered in the light of the 0.4×10^{-8} in/min. recorded in the transducer stability tests once the cause, if any, of the transducer drift is identified.

The value of μ, defined in Equation (50), for this test was calculated and the resulting values of Young's modulus may be seen in Table 10. It would appear from the values in Table 10 that there has been a progressive increase in the magnitude of Young's Modulus during the experimental programme. Further tests should show whether this is due to work hardening of the rock salt or due to experimental errors.

At the end of the unloading phase of this test the cavity was left with a deformation of 0.52×10^{-3} ins. Over a period of ten hours this deformation gradually relaxed into a permanent set of approximately 0.25×10^{-3} ins. This relaxation curve may be seen in Fig. 59.

9.7.3 Radial deformation

A graph of the radial deformation plotted against time is shown in Fig. 60. The deformation shown in this graph is the mean displacement of the nine anchors at each of the four points under consideration, 9", 2', 4', 10' from the cavity surface. The displacement is plotted relative to the cavity centreline.

From Figs. 59 & 60 it can be seen that there is a radial deformation of approximately 1.03×10^{-3} in at the cavity surface with

a deformation, relative to the cavity centreline, of 0.25×10^{-3} at Anchor No. 4 (nine inches into the rock). This would suggest that most of the cavity deformation is contained by the first few inches of rock. The movement of Anchor No. 1 (ten feet into the rock), when converted into strain, confirms the expected pattern of strain diminishing to zero at points remote from the cavity.

It would appear from Fig. 60 that Anchors No. 1, 2 and 3 undergo a negative deformation upon the return of the cavity to atmospheric pressure. When viewed in the light of a deformation measurement accuracy of $\pm 0.075 \times 10^{-3}$ in., with a standard deviation of 0.04×10^{-3} in., the low negative deformation loses its significance.

FIG. 49 100 p.s.i. TEST

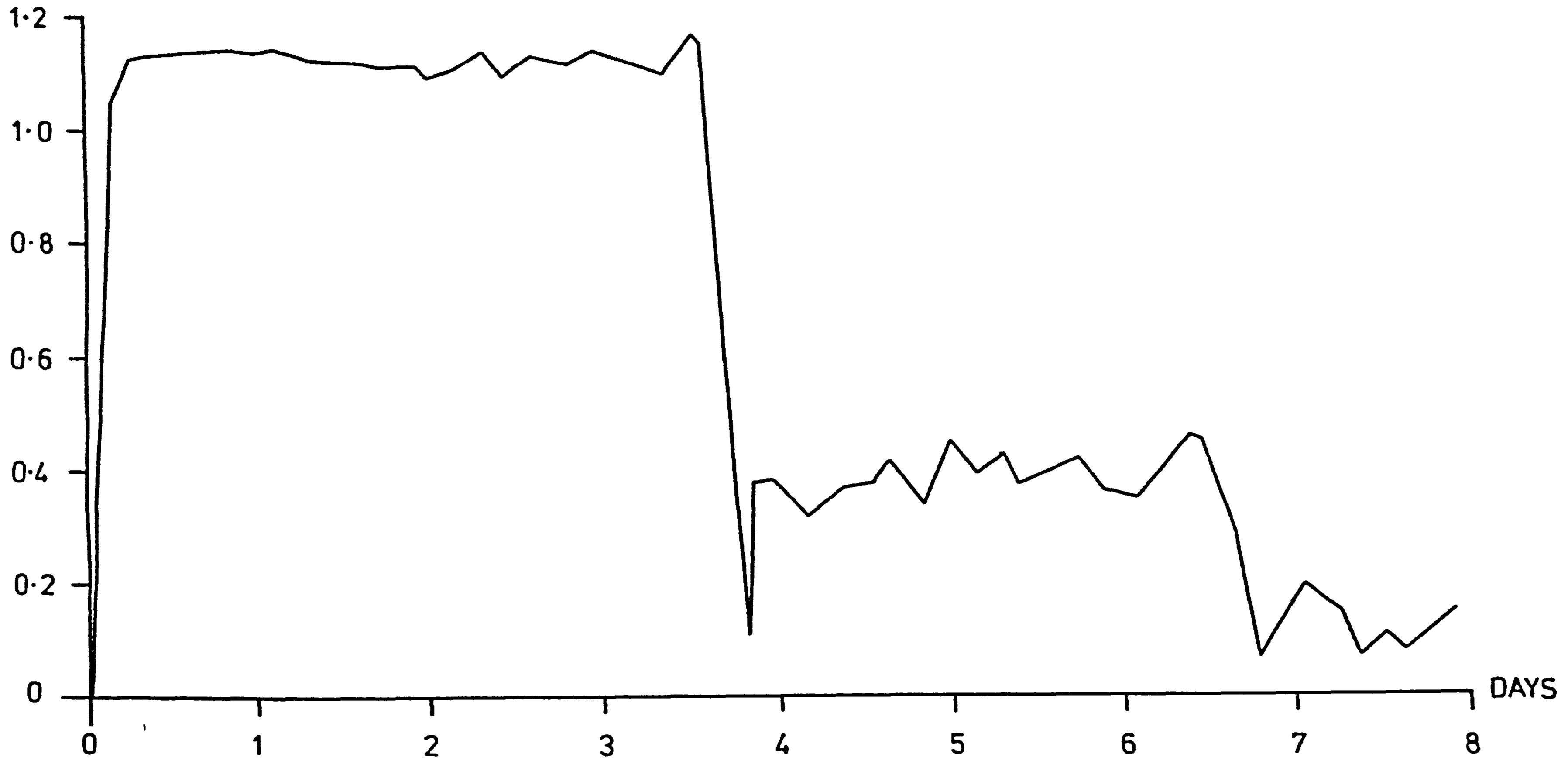

FIG. 50 DIAMETRAL DEFORMATION / CAVITY PRESSURE
(100 p.s.i. TEST)

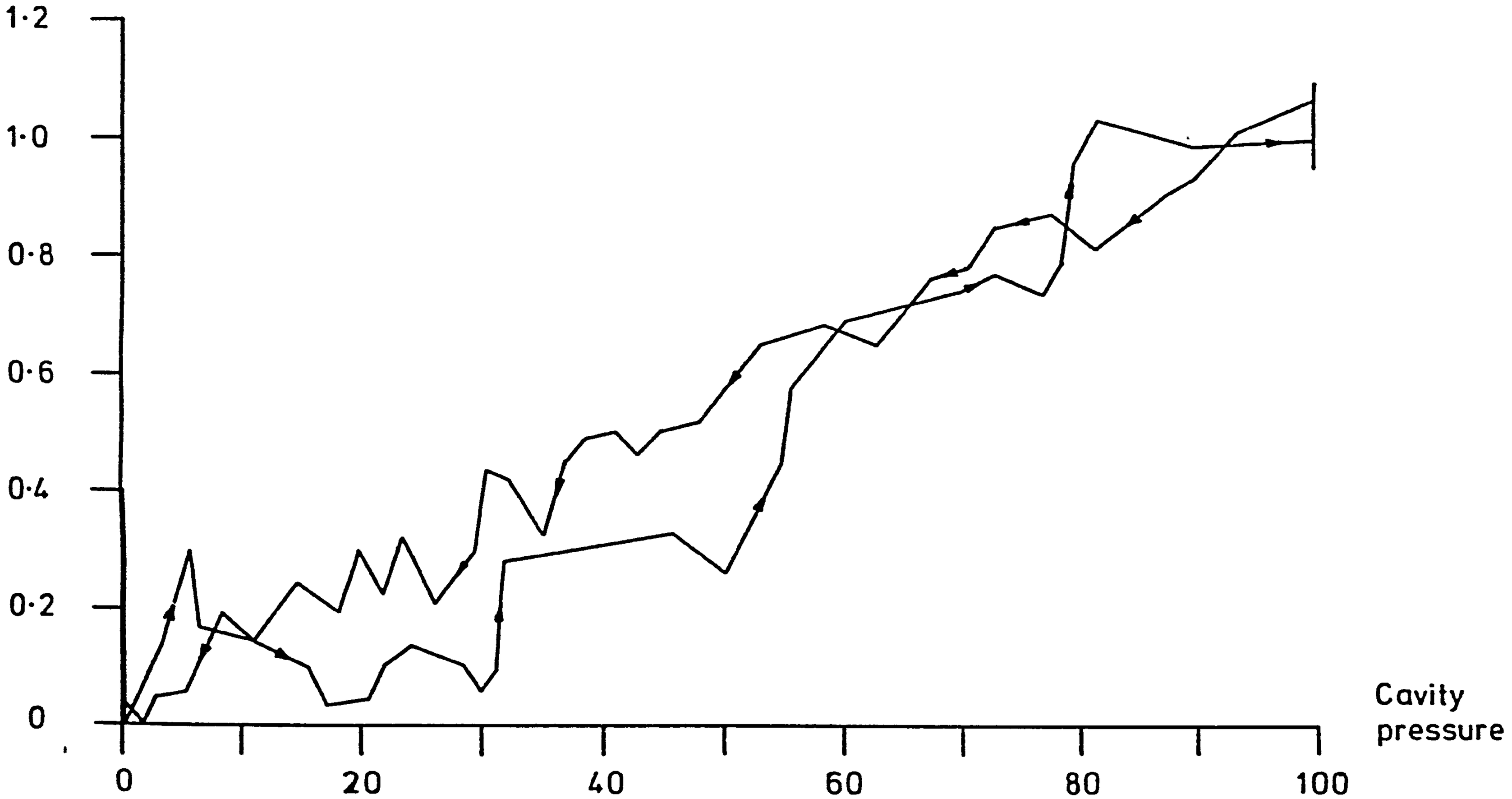

FIG. 51 DISPLACEMENT OF ANCHOR No.1 IN BOREHOLE C.V. RELATIVE TO THE CAVITY SURFACE

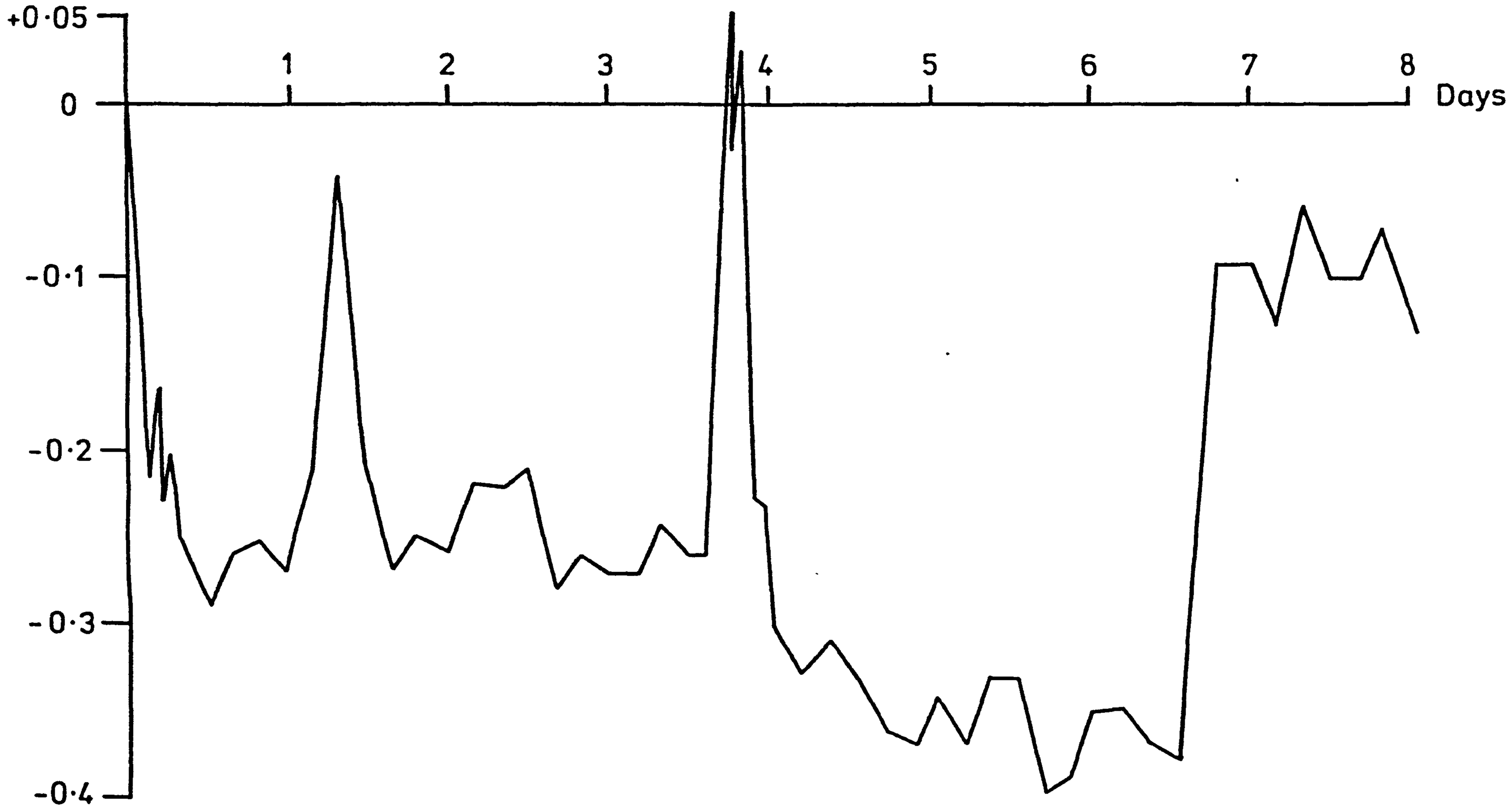

FIG. 52 MEAN DIAMETRAL DEFORMATION (+10 C° TEST)

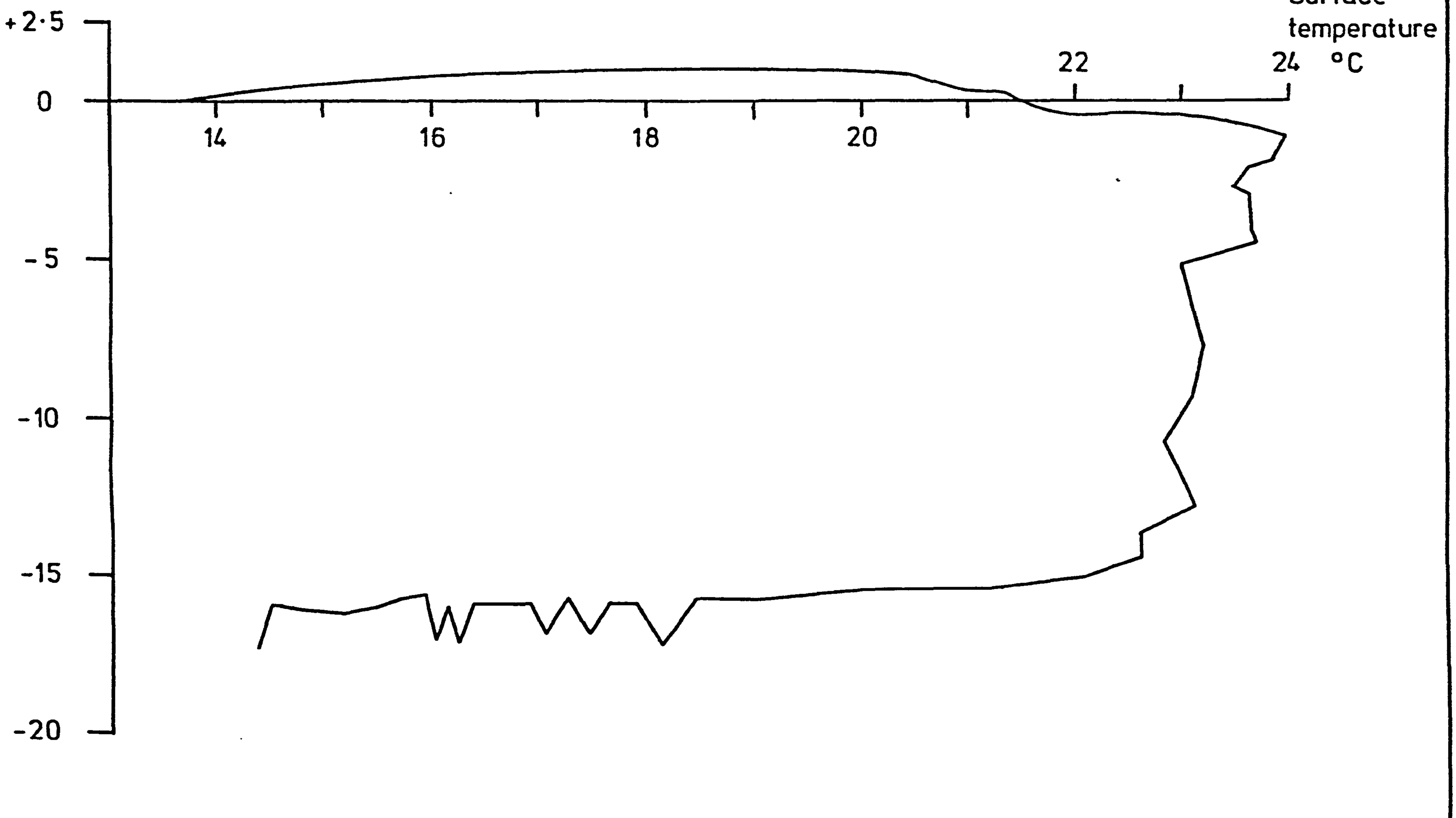

FIG. 53 DEVELOPMENT OF MEAN DIAMETRAL DEFORMATION AND CAVITY SURFACE TEMPERATURE

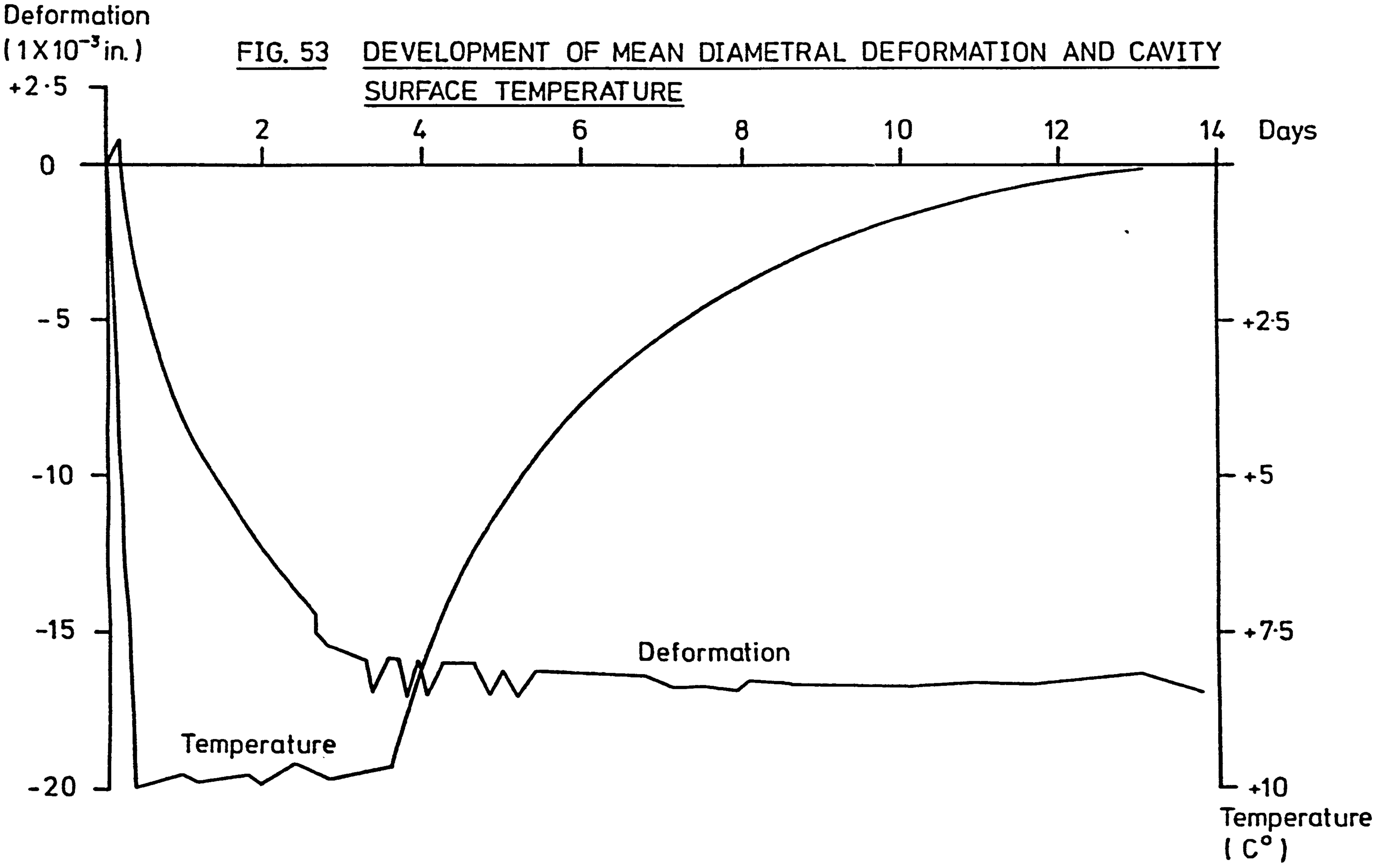

FIG. 54 DEVELOPMENT OF RADIAL DEFORMATION OF BOREHOLE B.V.

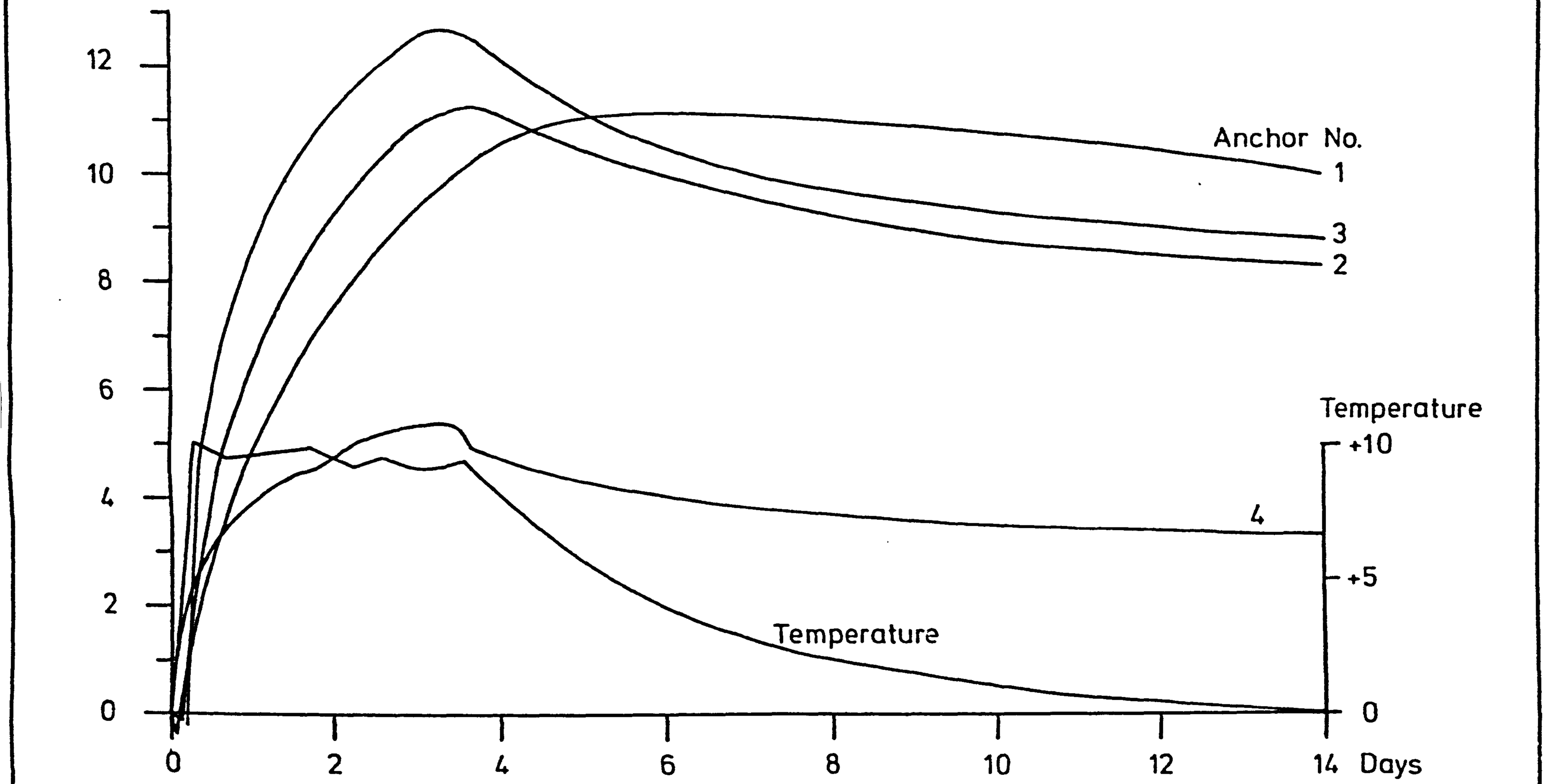

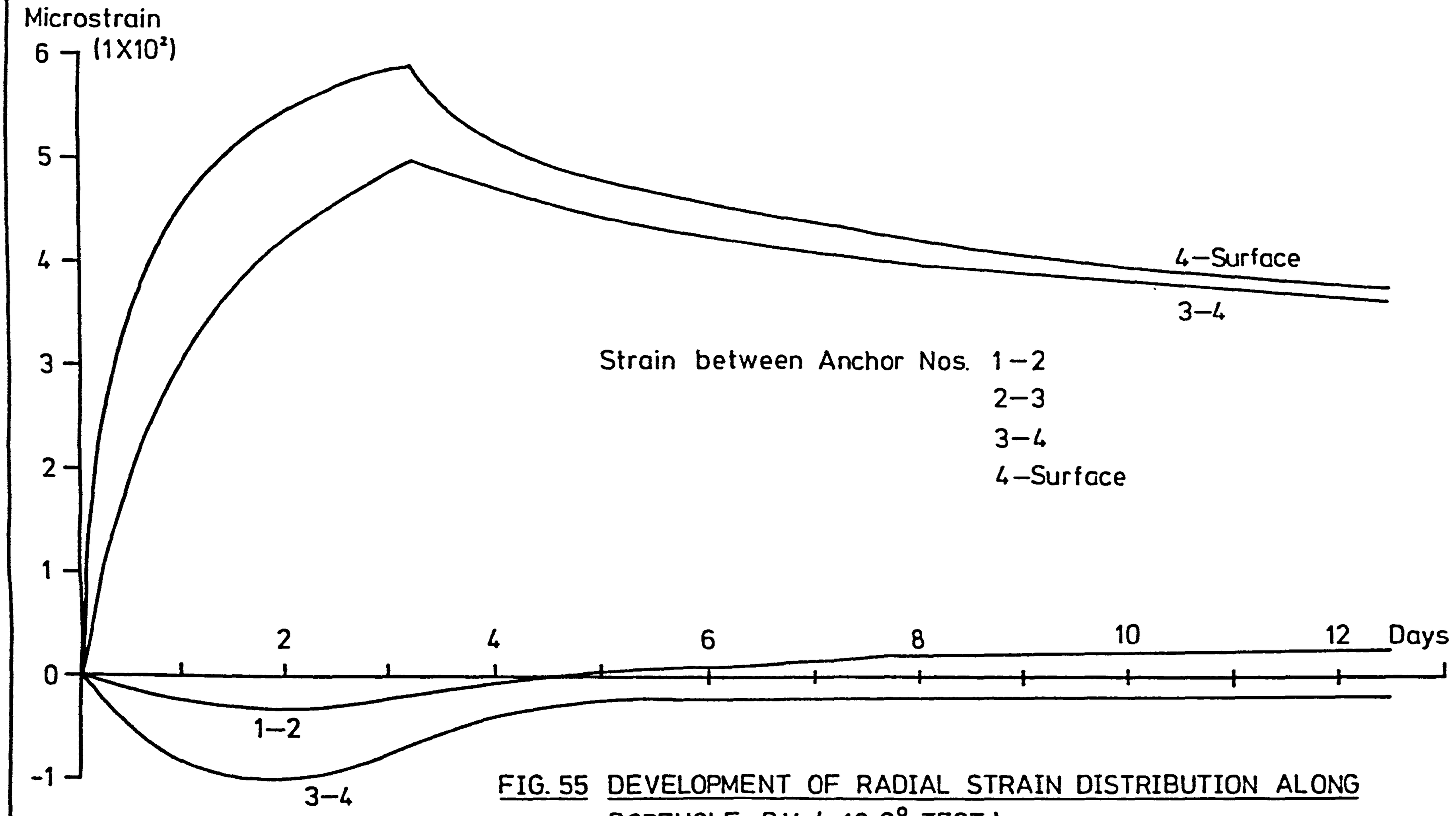

FIG. 55 DEVELOPMENT OF RADIAL STRAIN DISTRIBUTION ALONG BOREHOLE B.V. (+10 C° TEST)

FIG. 56 MEAN DIAMETRAL DEFORMATION / CAVITY PRESSURE

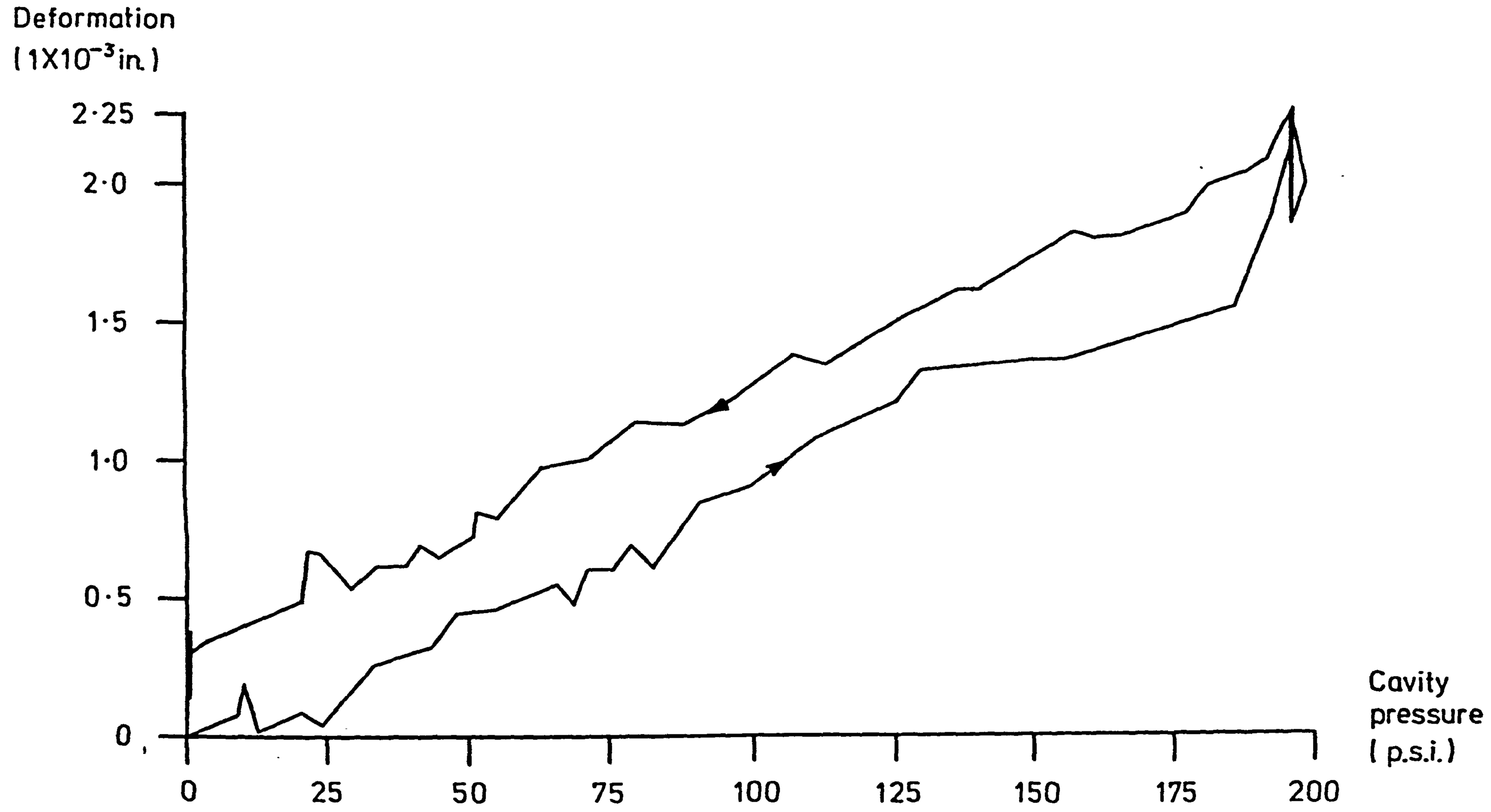

FIG. 57 MEAN DIAMETRAL DEFORMATION (200 p.s.i. TEST)

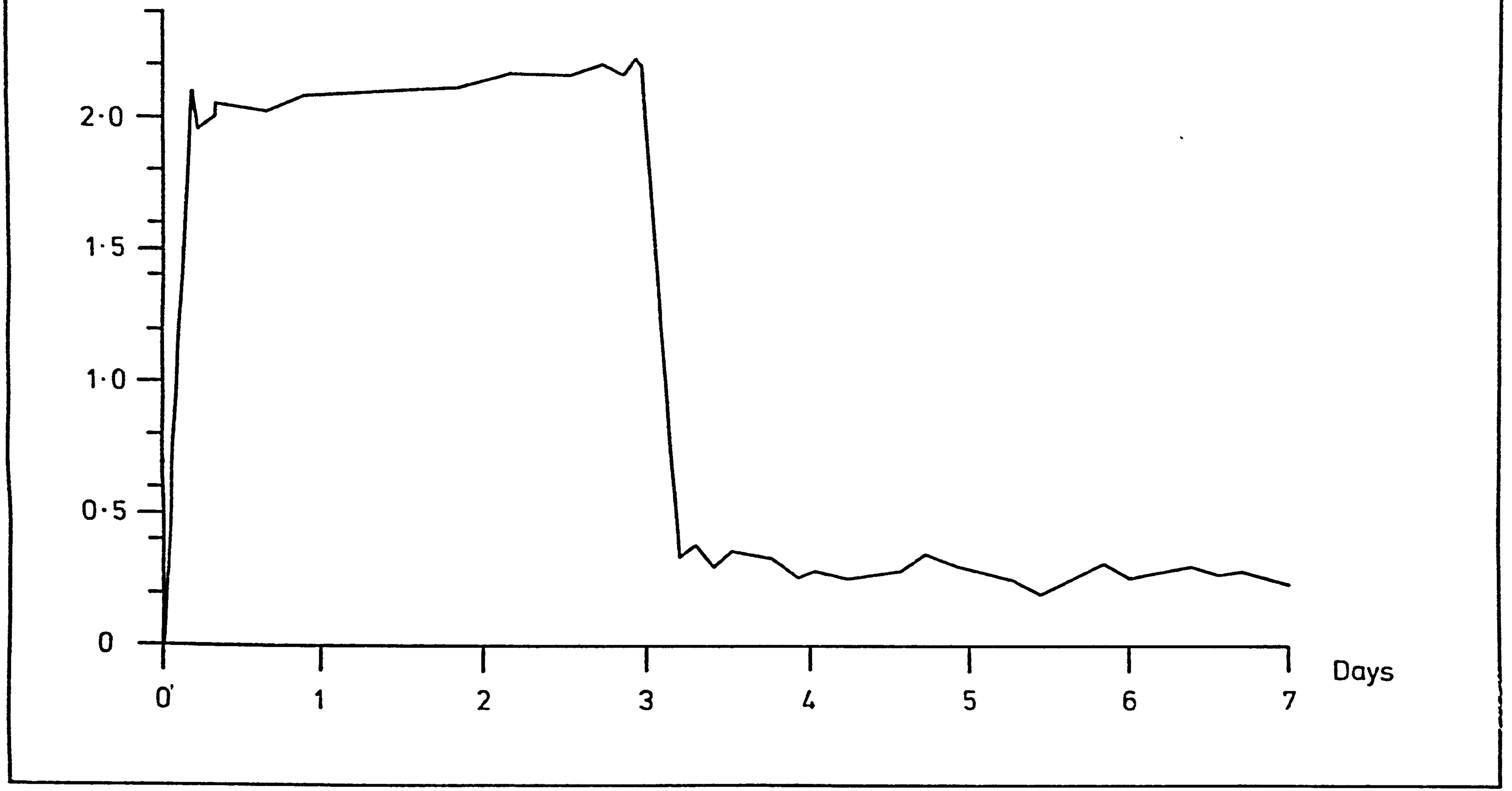

FIG. 58 TRANSDUCER STABILITY TEST

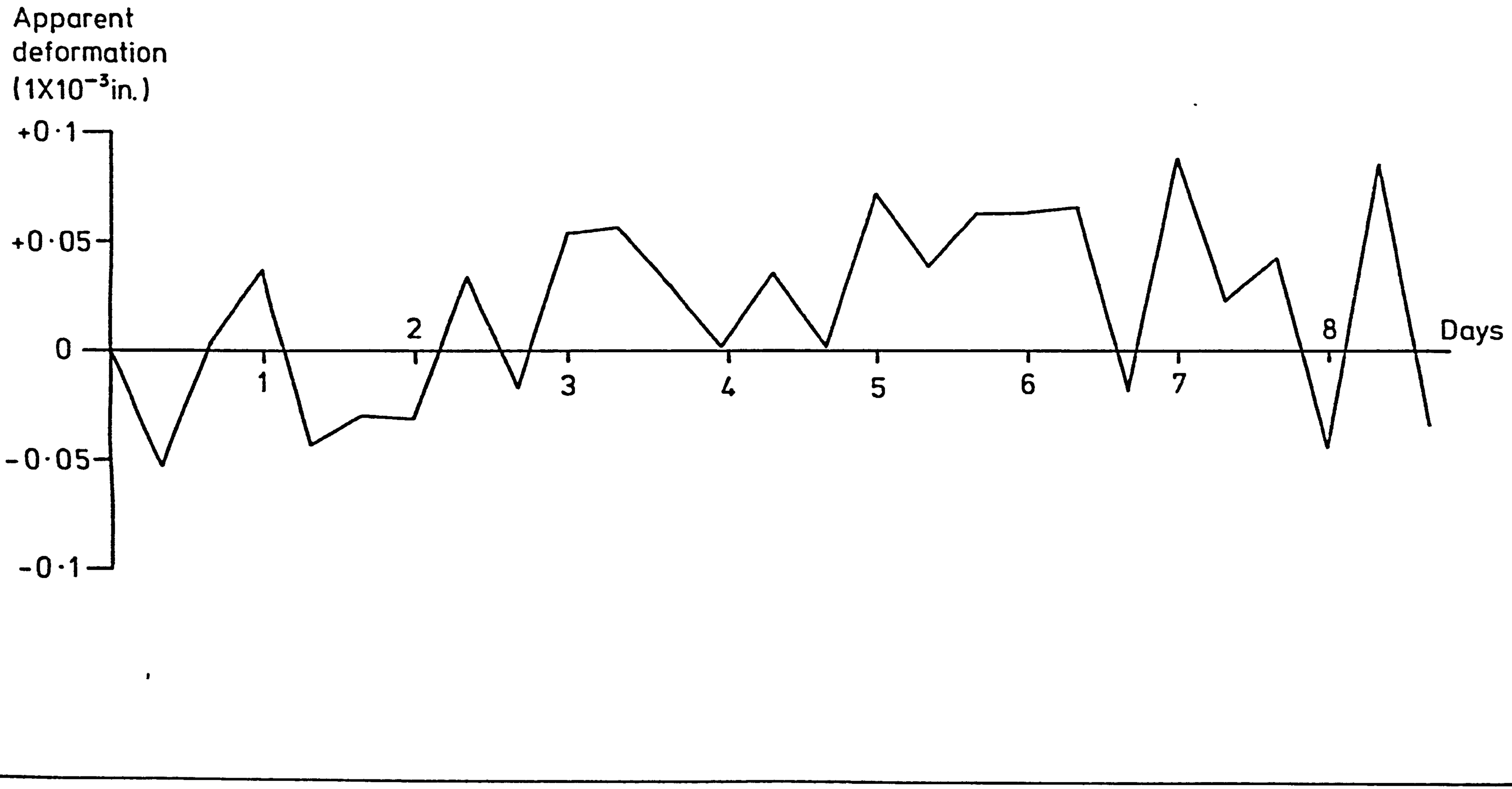

FIG. 59 MEAN DIAMETRAL DEFORMATION (EXTENDED 200 p.s.i. TEST)

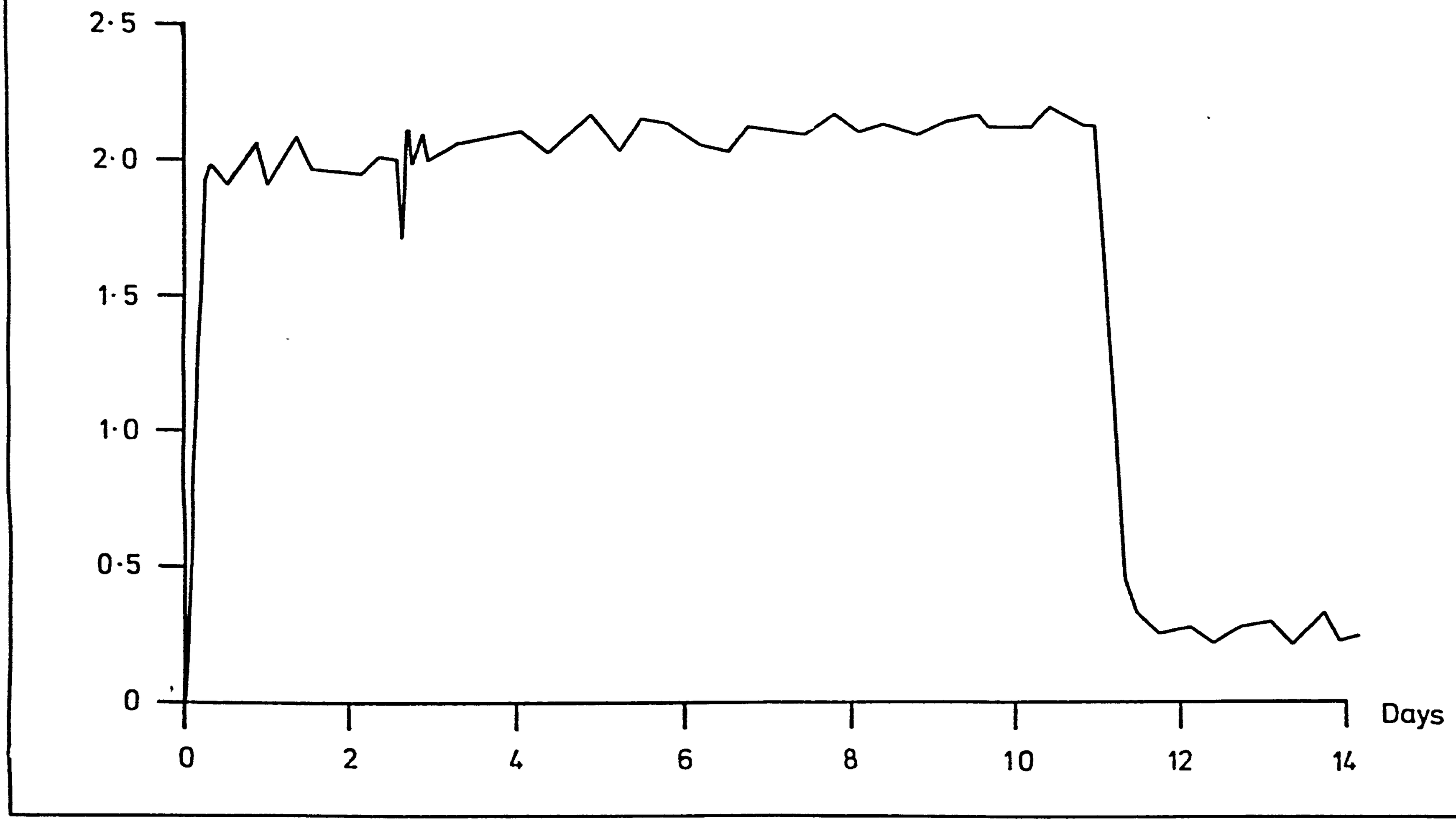

FIG. 60 DEVELOPMENT OF MEAN RADIAL DEFORMATION

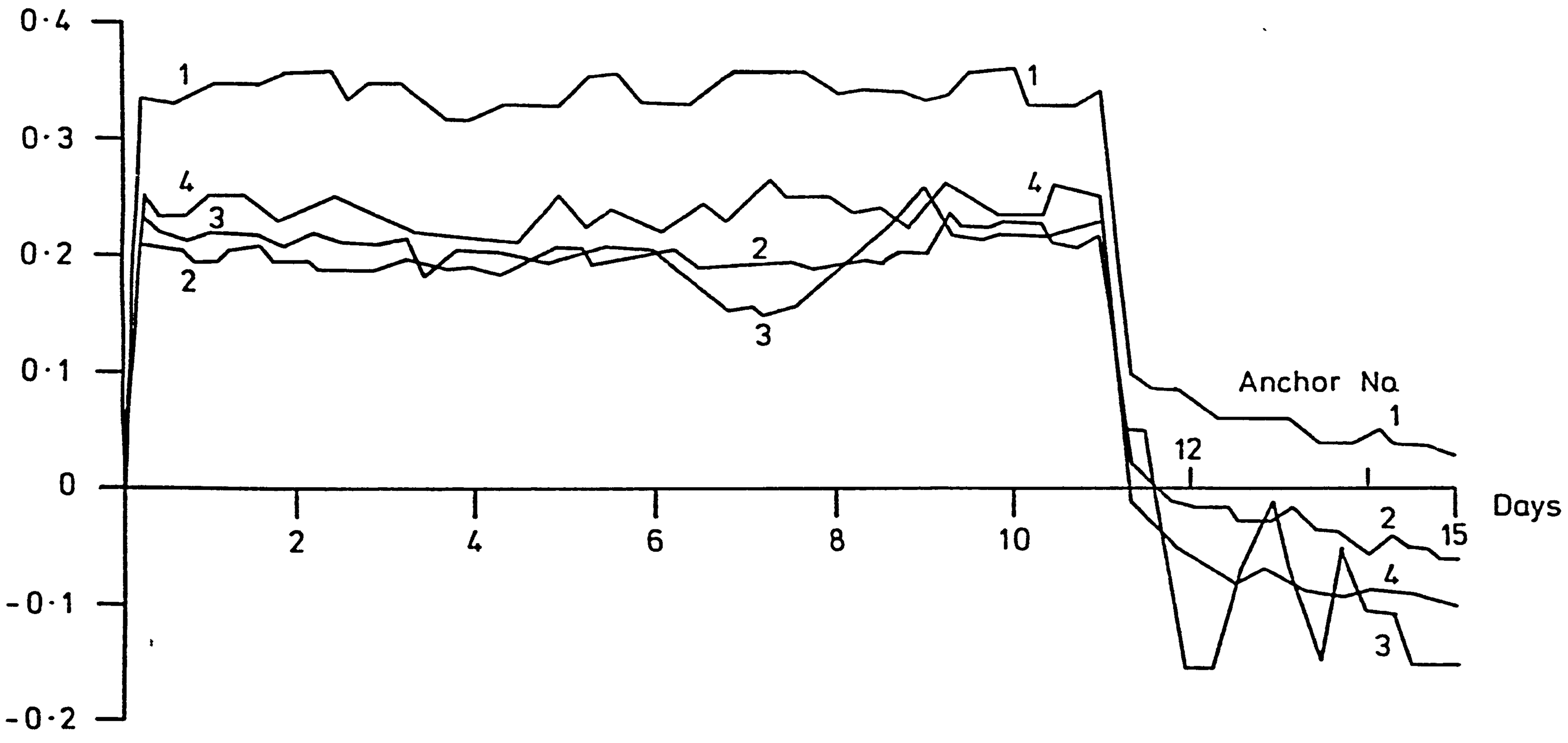

CHAPTER 10

CONCLUSIONS.

CHAPTER 10

10.0 CONCLUSIONS

The research project, designed to investigate the rock mechanics problems of utilising brined salt cavities for underground gas storage, originated five years ago and will continue for at least one more year. This thesis has briefly traced the history of the project to date and considered in more detail the engineering and instrumentation problems inherent in such an ambitious experiment. Finally, the thesis has discussed the results of the preliminary tests of the experimental programme and has attempted a qualitative explanation of the recorded rock behaviour.

10.1 The Experimental Installation

It cannot be said that any one problem encountered in this experiment proved a major difficulty; the overriding difficulty was one of finding solutions to the many and varied minor problems. The history of these minor problems began with the construction of the first access room with the interception of a brine feeder requiring a new access room to be mined, thus delaying the project for three months.

Minor problems continued to occur during the construction of the experimental cavity and were largely due to the over-optimism of the sub-contractors and suppliers in their equipment, products and technical abilities. Once the cavities had been excavated and installation work begun, the problems became centred around the technical difficulties inherent in any complex large scale instrumentation and data recording system.

10.1.1 The instrumentation scheme.

The temperature measurement system proved upon installation to be

wildly inaccurate. The cause of the inaccuracy was only partially traced and as a result the thermistors had to be recalibrated in situ. The in situ recalibration left the temperature measurement system with an overall accuracy of approximately $\pm 0.15C^{\circ}$.

The initial instability of the transducers used for deformation measurements was eventually traced to the manner in which the d.c. - a.c. converter took its load from the supply lines. This problem was solved by connecting 1000 uF capacitors across the supply terminals of each transducer. With the type of transducer and recording equipment used an accuracy of ± 25 microinches should have been possible but an analysis of steady-state transducer readings indicated a mean accuracy of $\pm 0.075 \times 10^{-3}$ inches.

The pressure transducer connected to both data logger and chart recorder caused electrical interaction between the two recording instruments. Simultaneous operation of the two recording instruments produced erratic pressure readings. The problem was solved by installing a separate transducer for each recording instrument, with the transducer connected to the data logger having an accuracy of ± 0.5 psi.

10.1.2 Ancillary equipment

The compressed air system presented very few difficulties, with the problems of cavity leakage and compressor overheating being quickly solved. The pressure control valve controlled the cavity air pressure to within ± 2 psi.

The heater/chiller proved to be a very difficult piece of equipment to commission. After many tests and trial runs it was discovered that it was incapable of counteracting rapid temperature variations and consequently it was only used to generate and maintain temperature differences. The heater/chiller could control temperature differences to an accuracy of $\pm 0.2C^{\circ}$.

The remaining ancillary equipment, discussed in Chapter 7, did not present any serious problems and functioned to design specifications.

10.2 Preliminary results

The results discussed in Chapter 9 are from the first few tests of Phase I of the experimental programme, and due to instrumentation teething troubles and lack of time, detailed quantitative analysis was not possible.

Chapter 9 described the results from three types of test:-

(i) Pressure tests
(ii) Temperature test
(iii) Transducer stability test

The most startling piece of information to come from the pressure tests was that the in situ value of Young's Modulus was at least twice the value obtained from laboratory tests. This fact has great relevance to rock stress determination based on strain measurement and to mine design work in general. Analysis of the time-dependent deformation observed in the 200 psi tests would eventually yield the visco-elastic constants of the mathematical model.

The results of the $+10C^{\circ}$ test were not conclusive due to the poorly sited temperature-compensating thermistors taped onto the diametral and longitudinal extensometers. This test however, did appear to confirm the zero rock surface movement prediction of the linear elastic and linear visco-elastic models.

The transducer stability test indicated an accuracy of $\pm 0.075 \times 10^{-3}$ inches with the possibility of a small upward trend

requiring statistical analysis for clarification.

10.3 Future work

This thesis has described the design, implementation and initial results of a long term research project. Future research on this project will be of two forms; the in situ experimental work will be continued and a quantitative analysis of past and future results will be attempted.

Section 9.1 describes the limitations of long range planning of the in situ experimental work, but bearing in mind these limitations a provisional experimental programme has been proposed. These proposals, found in Appendix A, put forward a series of tests ranging through simple pressure and temperature tests to tests involving both pressure and temperature together, culminating in tests of a cyclical nature.

The analysis of the results of the experimental programme has, at the time of writing, only just begun. The first few tests have indicated that a statistical treatment of the results will be necessary before any data derived from the tests can be used to compare and develop mathematical models. Ultimately this data will be of direct use in predicting the long term stability of brined salt cavities used for high pressure gas storage.

APPENDIX A

SCHEDULE OF PROPOSED IN SITU EXPERIMENTS

PHASE I (Continued)

Pressure (p.s.i.)	Temperature (°C from ambient)	Remarks
0	0 to -5 to 0	Rapid test
0	0 to -5 to 0	Temperature decrease maintained for 12 hours
0 to 100 to 0	0	Test carried out with diametral extensometers BR & BL interchanged to investigate erratic behaviour of BR
0	0	Cavity left under ambient conditions for three weeks to obtain steady state readings for statistical purposes Readings taken every four hours

PHASE II

0 to 200 to 0	0 to +2 to 0	Cavity maintained at +2 for three days. On third day a pressure test is superimposed and cavity returned to ambient
0 to 200 to 0	0 to +5 to 0	As for previous test, but a higher surface temperature is imposed
0 to 100 to 0	0 to -2 to 0	Cavity maintained at -2 for three days, and a pressure test superimposed on the third day

Pressure (psi)	Temperature (°C from ambient)	Remarks
0	0 to +15 to 0	Rapid test
0 to 100 to 0	0	For comparison with the results from previous 100 psi tests

PHASE III

0	0 to +5 to -5 to 0	Repeated rapidly five times at a low air pressure
0 to 200 to 0	0 to +5 to -5 to 0	Pressure cycled at such a rate that T = +5 when P = 200 and T = -5 when P = 0. Continued for 5 days.
0	0 to -10 to 0	Rapid test
0 to 100 to 0	0 to -10 to 0	Held at -10 for twelve hours, returned to ambient & quickly followed by the pressure test
0 to 200 to 0	0 to +10 to -10 to 0	Cycled for five days at such a rate that T = +10 when P = 200 and T = -5 when P=0.

REFERENCES

1. Clarke, D.J.; Cribb, G.S.; Walters, W.J. — The Philosophy of Gas Storage. J.Inst. Gas Engrs., 11, 748-772, 1971

2. Copp, D.L. — Gas transmission and distribution. Walter King, Ltd., London, 1967.

3. Jones, H — Storage of Gas Underground in Aquifers. Proc. Inst. Civ. Engrs., 26, 317-330, 1963.

4. Johnson, C.J. — Gas Reservoirs in British Porous Rock Structures. J. Inst. Gas Engrs, 2 (3), 159, 1962.

5. Evans, B.M. — Design and Construction of Underground Storage Units for Gaseous and Liquid Products. J. Inst. Gas Engrs., 4, 151-182,1964.

6. Crowther, E — Pressure Storage of Town Gas in a Prepared Underground Cavity. Trans. Inst. Gas Engrs., 109, 179-215, 1959-60.

7. Remson, D.R.; Dommerso, B.; Jessen, F.W. — Techniques for Developing Predermined Shaped Cavities in Solution Mining. 2nd Symp. on Salt, 2, 297-310, Northern Ohio Geol. Soc. 1966.

8. Budavari, S. — The application of Mathematical Models to Rock Mechanics Problems. Ph.D. Thesis, University of Newcastle upon Tyne, 1968.

9. Timoshenko, S. — Theory of Elasticity. McGraw-Hill Book Co., 1951.

10. Nowacki, W. — Thermoelasticity. Pergamon Press, 1962.

11. Obert, L. Duvall, W.I. — Rock mechanics and the design of structures in rock. John Wiley & Sons, Inc., 1967.

12. Potts, E.L.J. — An investigation into the design of room and pillar workings in rock salt. The Mining Engineer, No. 49, Oct. 1964.

13. Forster, J. — Stability investigation in the mining of evaporites. Ph.D. Thesis, University of Newcastle upon Tyne, 1967.

14. Hedley, D.G.F. — Deformation and failure characteristics of rock salt and potash. Ph.D. Thesis, University of Newcastle upon Tyne, 1965.

15. Carslaw, H.S. Jaeger, J.C. — Conduction of heat in solids. Oxford University Press, 1947.

16. Thompson, T.W. — Ph.D. Thesis, University of Newcastle upon Tyne, 1973.

17. Brookes, A.M.P. — Basic instrumentation for engineers and physicists. Pergamon Press, London, 1968.

18. Volotkovsky, S., Poltava, L., Bimko, V., Podolsky, V. — Automatic control components for mining. MIR Publishers, Moscow, 1968.

19. — Temperature. Its measurement and control in science and industry. American Institute of Physics, Vol. 2, Chapman & Hall, London 1955

19a Friedberg, S.A. — "Semi conductors as thermometers"

19b. Hoge, H.J. — "Temperature measurement in engineering"

20 — YSI Precision thermistors. Yellow Springs Instrument Co., Ohio, U.S.A.

21. Symposium on the measurement and control of temperature in science and industry. American Institute of Physics. Reinhold, New York, 1941.

21a Mueller, E.F. "Precision resistance thermometry"

21b Roeser, W.F. "Thermoelectric thermometers"

22 Hole, V.H.R. Design of circuitry for the use of thermistors in temperature measurement. Electronic Components, 25th Feb., 1972.

23 Thompson M. Personal communication.